Vascularization and osteogenesis in bone physiological processes influenced by bio-active molecules and scaffolds

Dissertation

in fulfilment of the requirements for the degree of “Dr. rer. nat.”

of the Faculty of Mathematics and Natural Sciences

at Kiel University

submitted by

Fanlu Wang

Kiel, 2020

First examiner: Prof. Dr. Susanne Alban

Second examiner: Prof. Dr. Sabine Fuchs

Date of the oral examination: 31, March, 2020

Abstract

In bone tissue engineering, bioactive molecules which modulate bone growth and biocompatible biomaterials, which often provide biomimetic properties, are combined with progenitor or stem cells involved in bone physiological processes. This tissue replacement approach provides a new therapeutic strategy for bone repair and regeneration especially for larger bone defects which often occur after trauma or bone tumor resection for instance. In this context, the aim of this thesis is to investigate the detailed biological functions of new bioactive molecules. Further the thesis is focused on hydrogels used for instance as delivery systems of such bioactive factors or cells, aiming to develop the basis for new clinical applications in bone pre-vascularization and regeneration.

First, this thesis assesses the impact of fucoidan extracts, a group of marine origin bioactive molecules, on the formation of vascular structures in co-culture models relevant for bone repair and in osteosarcoma. Human mesenchymal stem cells (MSCs) which can differentiate to the bone forming osteoblastic cells, respectively the osteosarcoma cell line MG63 and outgrowth endothelial cells (OECs) which possess a high potential of angiogenesis, were used to create co-culture models relevant for bone regeneration or osteosarcoma. Here the aim was to study the angiogenic and osteogenic regulatory effects of fucoidan in the co-cultures as functional units. In both types of co-culture models, crude fucoidan extracts significantly reduced angiogenesis which was associated with a decrease of angiogenic factors on the protein level, thus suggesting an impairing effect of this type of fucoidan on angiogenesis in co-cultures via binding and reducing the levels of free angiogenic factors VEGF and SDF-1 in the system.

In the next part of this thesis, the physiological molecule vitamin D_3 (calcitriol) was studied in terms of its potential to modulate the inflammatory or immunological response in a bone regeneration respectively infection co-culture model stimulated with LPS. Bone infections after the application of implant materials for instance are associated with severe clinical consequences. Vitamin D_3 revealed a beneficial effect on angiogenic activity in co-cultures, as well as a positive effect on osteogenic activity. Here, especially the mineralization in the late osteogenic process was enhanced. However, although no significant impact on the inflammatory response was observed, Vitamin D_3 induced an increase in the gene expression of the antimicrobial peptide LL-37 in MSC, thus indicating a potential beneficial influence on the immune defense in the bone in case of infection to be further refined.

Last, the thesis examines bio-functionalized hydrogels for bone regeneration and tissue engineering. In this part, hydrogels consisting of mineralized silk fibroin fibers and UV-inducible gel-components induced excellent MSCs adherence along the bio-functionalized silk fiber component and a significant upregulation of VEGF expression level, thereby indicating a high potential of this injectable composite biomaterial for bone regeneration and vascularization.

Overall, bioactive compounds and bio-functional scaffolds investigated in this thesis showed the ability to modulate angiogenesis on the cellular and molecular level, to trigger the immune defense or to serve as injectable bone materials guiding the performance of osteogenic cells via their biomimetic properties. Nevertheless, further research will be necessary to employ these approaches in a clinical setting for bone repair and regeneration.

Key words: OEC, MSC, co-culture, Angiogenesis, Osteogenesis, VEGF, Fucoidan, Vitamin D_3, tissue engineering, biomaterials.

Zusammenfassung

Im Rahmen des Knochen „Tissue Engineerings“ werden sowohl bioaktive Moleküle, die das Knochenwachstum modulieren, als auch biokompatible Biomaterialien, die oft biomimetische Eigenschaften aufweisen, mit Vorläufer- oder Stammzellen, die an den physiologischen Prozessen des Knochens beteiligt sind, kombiniert. Dieser Ansatz des Gewebeersatzes bietet neue therapeutische Strategien für die Knochenheilung und Regeneration speziell bei größeren Knochendefekten, die z.B. nach Trauma oder auch nach Knochentumoren auftreten. In diesem Zusammenhang untersucht die vorliegende Arbeit zunächst die biologische Wirkung neuer bioaktiver Moleküle. Darüber hinaus zielt die Arbeit auf die Untersuchung von Hydrogelen die u.a. als „delivery Systeme“ für bioaktive Moleküle oder therapeutischen Zellen dienen können, um so Grundlagen für deren klinische Anwendung bei der Knochen-(Prä)Vaskularisation und Regeneration zu schaffen.

Zunächst setzt sich diese Arbeit mit dem Einfluss von Fucoidan Extrakten, einer Gruppe von bioaktiven Molekülen marinen Ursprungs, auf die Bildung von Gefäßstrukturen, die für die Knochenvaskularisation während der Knochenreparatur und bei Osteosarkomen relevant sind, auseinander.

Es wurden daher Kokulturmodelle entwickelt, bestehend aus menschlichen mesenchymalen Stammzellen (MSCs), die in knochenbildende osteoblastische Zellen differenzieren, bzw. aus der Osteosarkom-Zelllinie MG63 und „outgrowth endothelial cells“ -Endothelzellen (OECs), welche ein hohes Angiogenese-Potenzial aufweisen, um die Prozesse der Knochenregeneration bzw. im Osteosarkom darzustellen. Das Ziel dieses Ansatzes war die angiogene und osteogene Wirkung von Fucoidanen in diesen Kokulturmodellen als funktionelle Einheit zu untersuchen. In beiden Gruppen der Kokulturen wurde die Angiogenese durch das „crude“ Fucoidan signifikant reduziert. Diese Reduktion war assoziiert mit der Abnahme angiogener Faktore auf der Proteinebene, so dass die Beeinträchtigung der Angiogenese in Kokulturen sehr wahrscheinlich durch die Bindung von Fucoidan an freie angiogene Faktoren wie VEGF und SDF-1 im System erklärt werden kann.

Im nächsten Teil der Arbeit wurde das physiologische Molekül Vitamin D_3 (Kalzitriol) bezüglich der entzündungs- und immunmodullatorischen Eigenschaften im Knochenregenerations- bzw. Infektions-Kokulturmodell nach LPS Stimulation untersucht. Knocheninfektionen, die z.B. bei Knochenimplantaten auftreten können, haben schwerwiegende klinische Konsequenzen für den Patienten. VD_3 zeigte einen positiven Effekt auf die Gefäßbildung und die osteogene Differenzierung im Kokulturmodel. In diesem Zusammenhang wurde durch VD_3 speziell die Mineralisierung in der späten Phase der osteogenen Differenzierung verbessert. Obwohl kein signifikanter Einfluss von VD_3 auf die Entzündungsmediatoren nach Infektion nachweisbar war, wurde durch VD_3 das antimikrobielle Peptid LL-37 in MSC induziert und damit ein positiver Einfluss von VD_3 auf die Immunabwehr im Knochen

bei der Infektion nachgewiesen, welche jedoch genauer definiert werden muss.

Im letzten Teil untersuchte diese Arbeit bio-funktionalisierte Hydrogele hinsichtlich ihres Potenzials für die Knochenregeneration im „Tissue Engineering“. In diesem Teil zeigten Hydrogele basierend auf mineralisierten Seidenfibroinfasern und UV induzierbaren Gelkomponenten eine hervorragende Adhäsion von MSC entlang der biofunktionalisierten Seidenfibroin-Komponenten. Außerdem wurde eine signifikant erhöhte Expression von VEGF festgestellt, so dass diese injizierbaren Komposit Biomaterialien ein hohes Potenzial für die Knochenregeneration aufweisen.

Zusammenfassend zeigten die in dieser Arbeit untersuchten bioaktiven Substanzen und biofunktionalen Materialien die Fähigkeit die Angiogenese auf molekularer und zellulärer Ebene zu beeinflussen, die Immunantwort zu induzieren oder als injizierbare Knochenmaterialien zu fungieren bzw. das Verhalten von Knochenzellen über deren biomimetische Eigenschaften zu beeinflussen. Dennoch sind weitere Studien notwendig, um solche Grundlagenansätze zukünftig in der Knochenheilung oder Regeneration auch klinisch einsetzen zu können.

Schlüsselwörter: OEC, MSC, Kokultur, Angiogenese, Osteogenese, VEGF, Fucoidan, Vitamin D_3, Tissue Engineering, Biomaterialien.

List of Abbreviations

Abbreviation	Full name
ALP	Alkaline phosphatase
AM	Acrylamide
Angpt-1	Angiopoietin-1
Angpt-2	Angiopoietin-2
BP	bisphosphonate
BSA	Bovine serum albumin
°C	Celsius (aka centigrade)
C3	Complement 3
CAC	Circulating angiogenic cell
CaP	Calcium phosphate
CD	Cluster of differentiation
CFU-EC	Colony forming unit-endothelial cell
CLSM	Confocal laser scanning microscope
Col	Collagen
CPC	Cetylpyridinium chloride
DMEM	Dulbecco's Modified Eagle's Medium
DMSO	Dimethyl sulfoxide
DNA	Deoxyribonucleic acid
EC	Endothelial cell
ECFC	Endothelial colony forming unit cell
ECM	Extracellular matrix
EDTA	Ethylenediaminetetraacetic acid
EGF	Epidermal growth factor
EGM-2	Endothelial cell growth medium-2
Elisa	Enzyme-Linked ImmunoSorbent Assay
EPC	Endothelial progenitor cell
FGF	Fibroblast growth factor
g	gravity (centrifugation)
h	hour
H_2SO_4	Sulfuric acid

HA	Hyaluronic acid
HEPES	4-(2-hydroxyethyl)-1-piperazineethanesulfonic acid
ICAM	intercellular adhesion molecule
IKVAV	Ile-Lys-Val-Ala-Val
IL-6	Interleukin-6
ISO	International Organization for Standardization
LAL	Limulus Amebocyte Lysate
LPS	Lipopolysaccharide
µg	microgram
µL	microliter
mg	milligram
min	minute
mL	milliliter
mmSF	mineralized micro silk fibroin
MSC	Mesenchymal stem cell
mSF	micro silk fibroin
NaCl	Sodium chloride
$NaHCO_3$	Sodium Hydrogen Carbonate
NaOH	Sodium hydroxide
nM	nanomolar
PBS	Phosphate buffered saline
PCL	Polycaprolactone
PCR	Polymerase chain reaction
PEG	Polyethylene glycol
Pen/Strep	penicillin/streptomycin
pHEMA	Poly (hydroxyethyl methacrylate)
PLGA	Poly (lactic-co-glycolic acid)
pOB	primary osteoblast
PVA	Poly (vinyl alcohol)
RGD	Arg-Gly-Asp
RNA	Ribonucleic acid
ROI	region of interest
RPL13a	Ribosomal Protein L13a

RUNX2	Runt-related transcription factor 2
s	second
SDF-1	Stromal cell-derived factor-1
SF	Silk fibroin
TBS	Tris Buffered Saline
TE	Tris-EDTA
TLR4	Toll-like receptor 4
TRACP5	Tartrate-resistant acid phosphatase 5
TRITC	Tetramethylrhodamine
UV	Ultra violet
VCAM	Vascular cell adhesion molecule
VD_3	1α, 25-dihydroxyvitamin D_3
VEGF	Vascular endothelial growth factor
VEGFR	Vascular endothelial growth factor receptor
vwf	von Willebrand factor

List of content

1. Introduction

As a highly vascularized tissue, bone possesses extraordinary self-healing capacity and undergoes a continuous remodeling process, therefore bone defects can be completely healed and new bones can be formed after injury [1]. However, massive bone loss and fractures caused by pathological or traumatic events still need surgical treatment to assist bone formation. Bone grafting, the traditional and widely applied therapeutic strategy of bone repair, still faces several challenges due to ischemia, rejection, infection, limited sources of donors and immune responses in recipients [2, 3]. Thus, the emergence of pre-vascularized bone constructs in the context of bone tissue engineering provides advanced alternatives for conventional bone defect transplantation. There are three components in bone tissue engineering: stem cells/progenitor cells for bone formation and vascularization; biological factors to accelerate cell adhesion, proliferation, migration and differentiation; and the biomaterials/scaffolds which provide a physical and biological environment to the cells [4].

Blood vessels play an important role in bone formation and repair due to their functions of delivering blood cells and nutrients. The past studies have shown that vascularization and osteogenesis in bone are two coupled physiological processes [5]. At the cellular level, molecular crosstalk exists between endothelial cells and bone forming osteoblastic cells [6]. In this context, endothelial progenitor cells, which contribute to the formation of new blood vessels, and osteogenic cells have been employed in co-culture systems, where the promotive effect on both angiogenic and osteogenic activities has been found [7, 8]. Furthermore, the co-culture models also provide an *in vitro* platform to study the mechanisms of osteogenesis and vascularization in bone physiological and pathological processes, as well as the reciprocal reactions between various cell types at both cellular and molecular levels.

Besides the biochemical regulators such as the well-known growth factors and component proteins involved in the bone physiological processes, recent studies have

discovered some additional bio-functional compounds which have been shown to influence vascularization and bone formation. Fucoidan, an extracted component from brown algae, is supposed to possess a number of bioactivities including its impact on angiogenesis which is of interest in our study [9]. Moreover, this thesis also investigated physiological molecules such as vitamin D_3 (1α, 25-dihydroxyvitamin D_3) to assess its influence on the pro-inflammatory response in the co-culture model of bone regeneration.

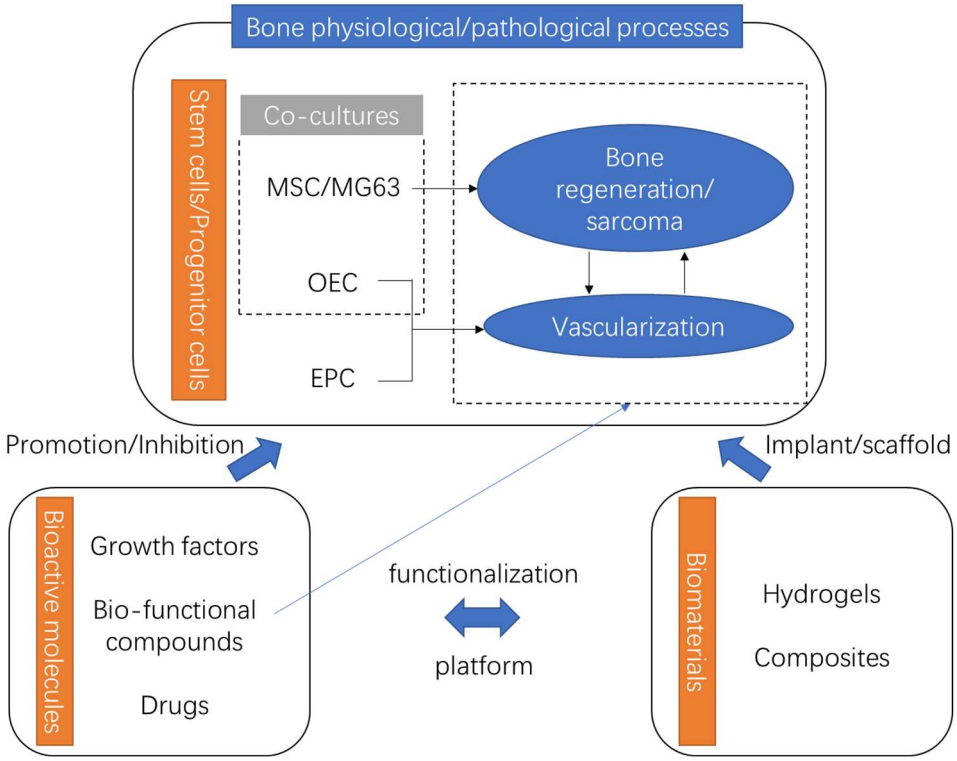

Figure 1.1 General strategies of bone regeneration and vascularization.

In addition, biomaterials and scaffolds are also needed in a delivery system for bioactive components and molecules to establish the physical and biochemical environment for cells, thereby developing efficient pre-vascularization for bone repair and regeneration in bone constructs.

In the up-coming part of introduction, the relevant background with more details and mechanisms will be presented.

1.1 Background

1.1.1 Bone

Bones, according to their shape and serving place, are classified to long bones, short bones, flat bones and irregular bones. They are composed of two types of structures: cortical bone (or compact bone) has low porosity and mainly constructs the outer hard layer of long bones; cancellous bone (or trabecular bone) with 50-90% porosity exists in flat and cuboidal bones, as well as the heads of long bones [10]. Bone contributes to the calcium homeostasis [11] in addition to other physiological functions such as the structural and mechanical support of the body and the protection of inner organs. It is built up by different types of cells, organic extracellular matrix (ECM) and inorganic depositions. Bone cells include osteocytes, osteoblasts, osteoclasts and osteoprogenitor cells. Osteocytes are mature osteoblasts which maintain bone structures; Osteoblasts produce ECM components and participate in bone formation and osteoclasts are bone dissolving cells. The organic matrix of bone consists of collagen, proteoglycans, fibronectin, osteocalcin and phospholipids; the inorganic part of bone is comprised with mineralized calcium (hydroxyapatite), citrate, carbonate and water which makes up approximately 10% of the weight of bone [12, 13].

Different from other tissues, bone possesses an incredible capability to repair, heal and regenerate itself from fractures, pathological defects and trauma without forming scar [14]. Bone develops through two mechanisms or their combination which reflect the evolutionary history [15]: One is called endochondral ossification, in which cartilage tissue forms first before calcification occurs. This cartilage matrix provides stable mechanical properties and is then replaced by hard bone tissue. In the other mechanism, intramembraneous ossification, mesenchymal precursor cells proliferate and differentiate directly into bone tissue without forming the cartilage matrix. The bone repair process could be sorted into several phases including early inflammation, followed by the recruitment of mesenchymal precursor cells which differentiate into osteoblasts and form new bone [16]. The osteoclasts together with osteoblasts are

involved in the following remodeling phase which achieves to resorb damaged or old bone and at the same location form new bone. Bone remodeling occurs continuously throughout the whole lifetime to replace and repair the old bone and adjust the bone in accordance with loading change without changing the bone size. In contrast, bone modelling in which osteoclasts resorb bone and osteoblasts form new bone at different sites results in the change of bone size and shape, and mainly happens before skeletal maturity or in bone healing [17].

1.1.2 Bone tissue engineering

Bone self-healing may fail when a bone defect is too massive. In clinical practice, bone grafts are transplanted to promote bone formation and to provide mechanical support. There are 3 categories of bone grafts based on the source of material: autografts, allografts and xenografts. Autografts are transplanted from a different site of the same individual, while allografts and xenografts are harvested from different individuals of the same species or different species respectively. The autografts are used to repair bone defects as the gold standard but are limited by the mass of available healthy bone tissue. Allografts and xenografts also have both advantages and disadvantages in clinical practice. Both grafts overcome the limitations in terms of available bone tissue, exclude the need of additional surgery and thus limit the associated site pain of patients [18]. However, both substitutes introduce the risk of disease transmission and immunologic reactions [2, 19]. Therefore, new strategies of tissue engineering have emerged to open up new therapeutic options in this area.

Tissue engineering was defined as an interdisciplinary research field that aims to develop biological substitutes to restore, maintain, or improve tissue function based on the principles of engineering and life science by Langer and Vacanti [20]. In this definition, first appropriately engineered biomaterials are needed to provide the structure for cell attachment, cellular activities and tissue development. Second, signaling molecules (growth factors), biomechanical and micro/nano structural properties which relate to the cell behavior and promote the formation of tissues should

be considered in the system. Third, a considerable amount of stem cells or progenitor cells are required. [4]

In bone tissue engineering, biomaterials are designed and chosen according to the bone physiological environment and the main functions of bone structure. Therefore, the material composition, mechanical properties and architectures such as porosity, surface features and interconnectivity are crucial for bone biomaterials and should be considered in their design and development in order to attain the optimal effect to support and promote bone growth and regeneration. Different categories of materials are applied in bone replacement including metals, ceramics and polymers.

To improve efficiency and to accelerate bone formation, biomaterials in bone engineering are usually combined with bioactive molecules, such as growth factors, and bioactive compounds. The bioactive molecules and growth factor can be integrated into the systems in multiple ways, including directly adding them, using controlled release strategies or covalent binding approaches [21, 22].

At the early bone healing stage, the recruitment of surrounding host cells could be impaired or delayed specifically in large bone defects, thus scaffolds preloaded with progenitor cells have been employed to improve efficiency and accelerate bone formation. In the following parts, the widely used stem cells derived from bone marrow for osteogenesis and blood derived progenitor cells for forming new blood vessels will be introduced in details.

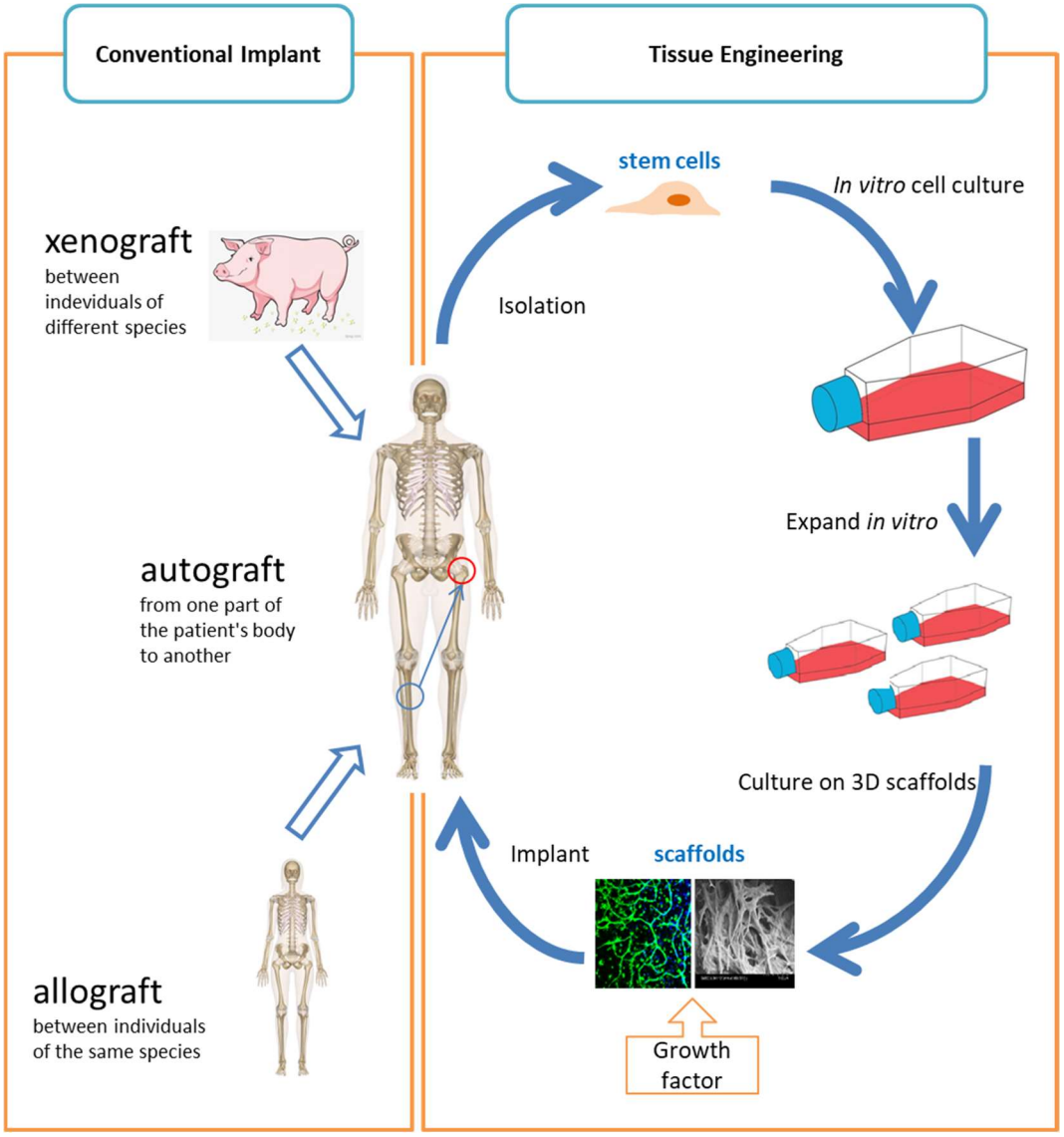

Figure 1.2 Scheme of bone grafting and principle of bone tissue engineering. (The images of skeletons, animal and culture flask are from online resources; The fluorescent and SEM images of cells in scaffolds are from the work of Sun et al. [23])

1.1.3 Mesenchymal stem cells (MSCs) and MSCs in bone regeneration

The human mesenchymal stem cells (MSCs) are known as tissue-specific progenitor cells with a certain capacity of differentiation and the potential as cell source in tissue engineering [24]. MSCs were first isolated and expanded from bone marrow [25] and demonstrated pluripotent differentiation capacities and self-renewal [26]. In addition, MSCs have been found in many other tissues and sources including adipose, peripheral blood and some non-skeletal tissues [27-29]. The bone marrow derived MSCs are isolated from cancellous bones and separated from hematopoietic cells by their plastic

surface adherence and cultured at a high density for further expansion and passaging *in vitro*. These MSCs are characterized with the surface markers STRO-1, CD29, CD73, CD90 and CD146 lacking expression of CD34, CD45, CD14 markers [30, 31], however, there is no MSC-specific marker discovered so far. The bone marrow derived MSCs can be induced to differentiate to osteoblasts *in vitro* by adding a variety of factors, for example, a mixture of dexamethasone, calcitriol, ascorbic acid and β-glycerophosphate for osteogenic lineage differentiation [32]. Therefore, in bone tissue engineering the bone marrow derived MSCs are often pre-differentiated to form bone in combination with osteoinductive bone biomaterials to realize a fast and effective bone healing for severe and critical sized bone defects and traumatic lesions in clinical practice [33].

1.1.4 Neovascularization: vasculogenesis and angiogenesis

The network of blood vessels, transporting oxygen and nutrients and at the same time removing waste of metabolic activities, plays an essential role in maintaining normal physiological processes, tissue regeneration and wound healing. Blood vessels form and develop mainly through 2 mechanisms: vasculogenesis and angiogenesis. In angiogenesis, new vascular structures are formed from pre-existing networks [34]. Vasculogenesis, in contrast, is the *de novo* formation of blood vessels mediated by stem cells. Both mechanisms contribute to the early development to establish the whole vascular system of the body and support new tissue growth. The neovascularization in adults mainly relies on angiogenesis to expand the vasculature in damaged tissues and wounds, while vasculogenesis has also been observed in specific pathological conditions [35, 36] and seems to contribute to tissue regeneration as well.

The wall of blood vessels consists of the inner (*Tunica intima*), the intermediate (*Tunica media*) and the outer (*Tunica adventitia*) layer. The inner layer is formed by endothelial cells supported by a subendothelial layer; The middle layer is where the smooth muscle cells are located; And the outer layer consists of connective tissue. The angiogenesis starts with the sprouting of existing blood vessels initiated by specific proteases which degrade and remove collagen and other components in the ECM. Thus, endothelial cells

are able to migrate and proliferate along the sprouting direction followed by the lumen formation to accomplish the primary new vessel structures [37]. In contrast, vasculogenesis requires the differentiation and assembly of endothelial progenitor cells to form new blood vessels at that site [38, 39]. The newly formed vessels in both processes are afterwards stabilized and matured via the recruitment of pericytes and deposition of extracellular matrix [40].

Sprouting is the key step in angiogenesis and the regulators are essential to activate the process. The vascular endothelial growth factor (VEGF) is the most investigated growth factor promoting angiogenesis and vasculogenesis [41]. VEGF family consists of VEGF-A, VEGF-B, VEGF-C, VEGF-D and VEGF-E members, with molecular weights ranging from 34 to 45 kDa [42]. There are a lot of isoforms, of which the VEGF121 and VEGF165 are the majorities. The differences in chemical structure amongst these isoforms enable different biochemical effects and various affinities to VEGF receptors and heparin sulfate [43]. VEGF binds to the receptor VEGFR-1 and VEGFR-2 which are both expressed by endothelial cells [44]. Previous studies have indicated that VEGF regulates angiogenesis by activating the sprouting and promoting the adhesion, migration and survival of endothelial cells [45]. In addition, VEGF plays a key role in mobilizing the endothelial progenitor cells from bone marrow [46]. Besides VEGF, angiopoietin-1 (Angpt-1) and angiopoietin-2 (Angpt-2) are both angiogenic factors of interest. Angpt-1 and -2 are both ligands for the Tie-2 receptor on endothelial cells. Angpt-1 promotes pericyte adhesion, enhances vessel stability and tightens endothelial junctions [47, 48]. Angpt-2, as a natural antagonist for Angpt-1, blocks Angpt-1 from activating Tie-2. It destabilizes blood vessels and promotes angiogenesis in cooperation with VEGF via stimulating vascular sprouting [49].

Angiogenesis in a pathological process, for instance, in tumor growth undergoes similar mechanisms and shares the same regulators or physiological process [50]. As a prominent regulator of angiogenesis, VEGF obviously plays a key role in tumor growth as well. Previous experiments have confirmed that tumors cannot develop under the

condition of inadequate blood vessel system [51]. Therefore, VEGF-targeted inhibitors have been developed, aiming at suppressing or cutting off the angiogenesis process in order to control tumor growth [52].

1.1.5 Endothelial progenitor cells (EPCs) and outgrowth endothelial cells (OECs)

Twenty years ago, cells which are defined as circulating endothelial progenitor cells (CEPCs) were discovered and isolated in adults, thereby updating the knowledge of postnatal vasculogenesis [53]. It has been found that these endothelial progenitor cells (EPCs) contribute to neovascularization *in vivo*, differentiate to endothelial cells and incorporate in the new forming blood vessels. They are characterized by CD34, CD133 which are typical hematopoietic stem cell surface markers and endothelial surface marker VEGFR2, which is often used in combination with CD34 and/or CD133 to acquire an enriched population of EPCs [53-55]. At the same time, many other markers have been investigated to characterize the EPCs including CD45, CD105, CD106, CD117, CD144, acetylated low-density lipoprotein uptake and aldehyde dehydrogenase activity [56]. Numerous studies have shown that CEPCs are derived from bone marrow [57, 58] and mobilized into the peripheral circulation mediated by VEGF [46, 59] and other stimulators such as Angpt-1 [60] and SDF-1 [61, 62] under ischemic conditions. Based on preclinical research of the biological function and role of EPCs in neovascularization, they were applied to the sites of ischemia or vascular diseases in the form of cellular injection and surface capture [63]. Due to the overlapped hematopoietic and endothelial surface markers which are used to characterize the EPCs, there are still difficulties in isolating the “true” endothelial progenitors [64]. The EPCs characterized with CD34, CD133 and VEGFR2 are heterogeneous populations of cells where each subpopulation plays various roles in neovascularization and re-endothelialization [65, 66]. These cells may not differentiate to endothelial cells or form blood vessel structures *in vitro* but contribute to the neovascularization via secreting cytokines and growth factors to help construct new blood vessels [67, 68]. Nowadays

EPCs have been successfully applied in the field of tissue engineering to enhance angiogenesis in implants [69, 70].

The isolation of EPCs from peripheral blood or bone marrow is performed by plastic adherent cultures of mononuclear cells or magnetic activated cell sorting based on various surface markers [53, 54]. In this study, we isolated mononuclear cells from the buffy coat of human peripheral blood by biocoll gradient centrifugation. These cells were seeded on collagen type I coated plastic surfaces and cultured in endothelial growth medium supplemented with growth factors including VEGF, hFGF, hEGF and serum. Within 5-7 days, the adherent cells on the plastic surface after removal of nonadherent ones were defined as early EPCs in our work. Within 2-4 weeks after isolation, colonies of cobblestone-like cells appeared at the peripheral area of the culture wells, and these cells were named as outgrowth endothelial cells (OECs, in other works also described as EOCs, late EPCs and ECFCs).

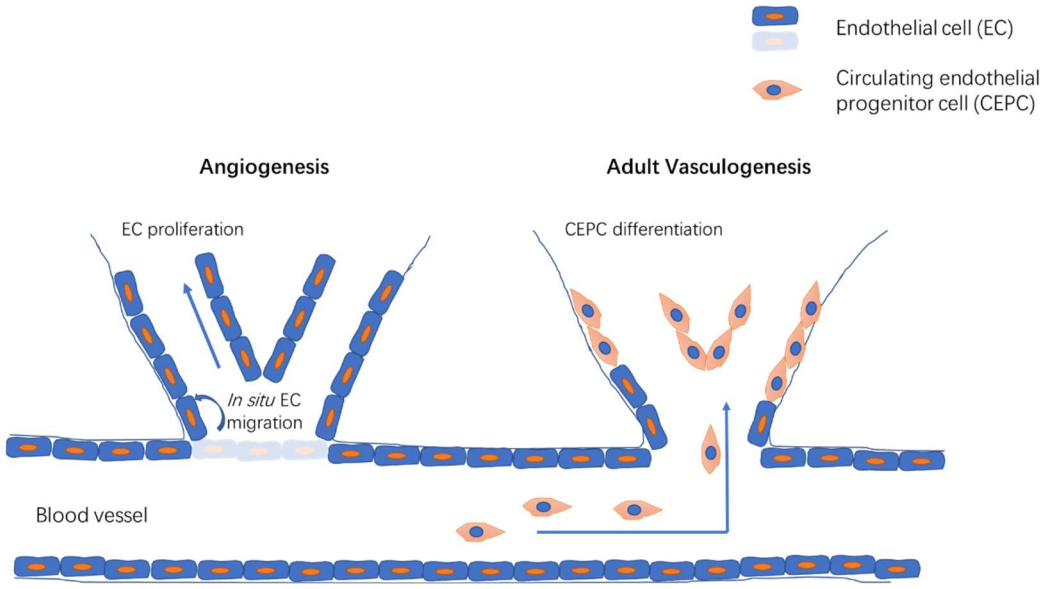

Figure 1.3 The neovascularization scheme in adult modified from Sales et al. [71]

It has been found that OECs are a small but homogenous subpopulation of peripheral blood isolated mononuclear cells with a low frequency of appearance. Different from early EPCs which contribute to new vessels through paracrine manners, OECs form tubular capillary structures and physically participate in vessel formation [72, 73].

Therefore, in terms of *de novo* vessel forming function, OECs are more likely to be the true endothelial progenitors. Both early EPCs and OECs have been applied in the ischemic conditions or tissue engineering scaffolds to promote the neovascularization for their synergic collaboration. On the other hand, both types of cells release the matrix metalloproteinases to facilitate sprouting *in vivo* [74]. To efficiently meet the needs of tissue engineering and clinical applications, an enriched population of OECs is required. It has been found that the number of circulating EPCs relates to some physiological and pathological factors, for instance, estrogens and physical condition [75, 76]. In addition, the protocol modification of OEC isolation has been shown to enable higher numbers of OECs obtained from individual donors [77].

Description as	**Early endothelial progenitor cells (EPCs)**	**Outgrowth endothelial cells (OECs)**
Other descriptions	EPC, EC, CFU-EC, CAC, AT, AC, early outgrowth, CE-EPC, CMMC, early EPC	EPC, EC, CFU-EC, EOC, BOEC, EPDC, EC-like, late EPC, late endothelial out-growth
Morphology	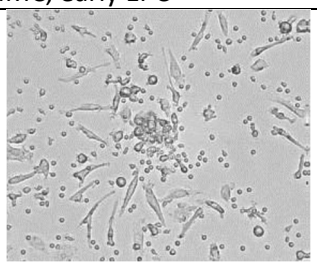 Spindle like	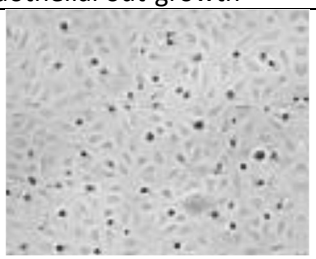 Cobble-stone like
Appearance	7 days after isolation	2-3 weeks after isolation
Surface markers	CD45+, CD34+, CD14+, CD133+, CD31+, Flt-1+, vWF+, eNos+, VE-Cadherin+, KDR+, CD36+, Tie-2+, CD146-	CD34+, CD31+, Flt-1+, vWF+, eNos+, VE-Cadherin+, KDR+, CD36+, Tie-2+, CD146+, Caveolin-1, CD45-, CD14-, CD133-
Proliferation *in vitro*	low	high
Potential of angiogenesis *in vitro*	No angiogenic structures formed on Matrigel	Angiogenic structures formed on Matrigel
Potential of angiogenesis *in vivo*	Support angiogenesis via paracrine way	Participate in angiogenesis

Table 1.1 Table of early EPCs and OECs, adapted from Fuchs et al. [78].

The early EPCs grow fast in the first 2 weeks in culture but gradually die whereas the OECs at the beginning grow at a low speed but possess a good proliferative potential. OECs express many endothelial surface markers like CD31, VE-Cadherin, e-NOS, von Willebrand factor (vwf), but not the hematopoietic markers CD14 or CD45. Although early EPCs share some endothelial markers with OECs, they do not have endothelial functional features and keep hematopoietic markers which correlate to their hematopoietic origin [73] (Table 1). The analysis of markers on circulating EPCs points out OECs may derive from a CD34+, CD45- subpopulation [79]. Nevertheless, the distinct origin remains unclear for OECs due to the lack of suitable markers to separate the OECs derived from their precursors from other endothelial cells which actually constitute the majority of circulating endothelial cells in blood [80].

1.1.6 Angiogenesis in bone tissue engineering

The vasculature not only plays a crucial role in maintaining functions and homeostasis of bone but also participates in bone development and repair [5]. Hence, the abnormality or insufficiency of blood vessels can provoke bone disease or failure of bone implant [81-83]. The angiogenesis and osteogenesis processes are closely related and interact with each other via a series of mediators such as BMP-2 and VEGF in bone healing [84-86]. The knowledge of signaling mechanism in these collaborating processes brings effective strategies for bone tissue engineering, such as incorporating bioactive factors in bone constructs to induce cellular activities for bone formation [87].

1.1.7 Co-culture models

The co-culture models are usually employed to study vascularization and osteogenesis, especially the relationships and interactions between different cell types involved in these processes. This cellular strategy to co-seed the angiogenic and osteogenic precursors has also been used to efficiently achieve pre-vascularized bone formation in engineered 3D constructs.

In our co-culture models, the osteogenic induced MSCs were used due to their self-renewal potential, strong proliferative ability and better time and cost efficiency in terms of cell culture process. The outgrowth endothelial cells, co-implanted to the osteogenic cells, were applied to promote vascularization in the bone regenerative model. A variety of studies have demonstrated the formation of vascular structures by co-implantation of endothelial cells with osteogenic cells *in vivo* and *in vitro* [7, 8, 88-90].

Endothelial cells assemble into tubular capillary-like structures when co-cultured with osteoblastic cells which produce the ECM component collagen type I, as well as angiogenic factors such as Angiopoitin-1 and VEGF to regulate angiogenesis and promote the viability of ECs [91-93]. Collagen provides a binding site for endothelial cells to attach and perform their angiogenic activities stimulated by the angiogenic factors. In addition, recent studies have shown that angiogenesis *in vitro* is highly influenced by the differentiation state of osteogenic cells in co-culture systems [94, 95], seeding density, the origin of endothelial cells [96] and culture conditions [97].

In turn, endothelial cells have been found to produce the bone morphogenetic proteins which promote differentiation of MSC towards osteoblasts [98]. The co-existence of endothelial cells also promotes the osteogenic potential in co-cultures with an increase in alkaline phosphatase (ALP) activity, deposition of collagen type I and bone formation [90, 98, 99]. In a previous report, MSCs were found to differentiate to pericytes which stabilized the vascular structures formed by ECs [88]. Overall, the co-culture of endothelial and osteogenic cells results in the bi-directional functions on up-regulating both angiogenic and osteogenic processes through the reciprocal cellular interaction and information exchange without the requirement of additional stimuli [100].

In summary, the co-culture system provides a platform where different cell types closely communicate via signaling molecules in an intimate manner to mimic the physiological and pathological environment *in vivo*. The strategy to combine two or

more cells types is a good tool to study the underlying mechanisms of cell-cell interactions and cellular response to the chemicals or external stimuli. An in-depth understanding of cellular pathways and mechanisms in bone homeostasis and repair is vital to identifying accurate targets for bone regeneration and treatment of bone diseases. Furthermore, the co-cultures of blood vessel forming cells resulting in functional vascular structures in bone constructs could significantly improve the survival and integration of implants in hosts [101].

1.1.8 Bio-functional compounds in this study

1.1.8.1 Fucoidan and its bio-functions

The sulfated polysaccharides extracted from sea weeds have drawn growing attention for several reasons, for instance, their marine origin, potential applications as scaffolding material in drug delivery and their attributed biological activities [102]. As a member of this family, fucoidan, the extract from brown algae, has been discovered to possess anti-viral [103, 104], anti-tumor [105, 106], anti-oxidant [107], anti-inflammatory [108] and anti-coagulant [109] properties based on a large numbers of studies *in vitro* and *in vivo*. It is believed that the bioactivities of fucoidan are tightly related to its chemical structure and composition, including molecular weight, sulfation degree, molecular geometry and sugar composition [102, 110, 111]. Nevertheless, the heterogeneity of its chemical structure which largely depends on the source species, extracting method and even harvesting season has brought difficulties to the study on the relationship between bioactivities and specific structures of individual fucoidan [110, 112]. One major aspect of this study focuses on the influence of fucoidan on angiogenesis. The report of opposite effects of fucoidan on angiogenesis associated with molecular weight again demonstrated the impact of chemical structure on biological activities [113]. The commercial fucoidan from *fucus vesiculosus* known as a crude extract is widely used in biomedical research and its chemical structure has been assessed [114]. It has been identified a mixture of polysaccharides with a wide spectrum of molecular weight and chemical structures in this product [115]. This

fucoidan extract has been found an anti-angiogenic effect on retinal pigment epithelial cell line via suppressing the secretion and expression of VEGF [116]. The results indicate the application potential of fucoidan in controlling tumor progression. In a recent study, the fucoidan *f. vesiculosus* has been functionalized to produce a hydrogel scaffold for cell loading and drug delivery, showing its potential in biomedical applications [117].

1.1.8.2 Vitamin D_3 and its functions in bone formation and infection

Besides fucoidan, the physiological compound vitamin D_3 is also of interest in our study. Vitamin D_3 has been well known for its essential role in bone mineralization and calcium regulation [118]. It is produced in the skin from the precursor 7-dehydrocholesterol under the ultraviolet B radiation [119]. After being delivered to the liver, Vitamin D_3 is converted to 25-hydroxycholecalciferol (25(OH)D) via 25-hydroxylation in the presence of enzyme and undergoes a further hydroxylation at 1-α position in kidney to form the bioactive form of Vitamin D_3: 1,25-dihydroxyvitamin D_3 ($1,25(OH)_2D_3$ or calcitriol) [120, 121]. Numerous studies have demonstrated the effects of VD_3 on osteogenic differentiation and bone remodeling process, which implies its indispensable clinical application in bone healing and repair process [122-124]. Bone healing starts from an inflammatory stage. VD_3 has been reported to affect the inflammatory cytokines IL-1 and IL-6 in serum, as well as on their expression levels *in vitro* [125-127]. VD_3 modulates osteoblast proliferation, production of collagen type I, the major component protein in bone extracellular matrix, and bone mineralization regulator osteocalcin in osteoblasts [122]. In addition, VD_3 has been reported to impact osteoclastogenesis and bone resorption mediated by osteoclasts [128, 129]. An upregulated level of VEGF has been detected in osteoblastic cells induced by VD_3, indicating its effect on vascularization in bone [130]. Although many results of cellular and molecular effects of VD_3 still remain various and inconsistent due to the difference between cell culture and experimental models, early studies help researchers identify more biological functions of VD_3 in bone physiological processes. Clinical cases

reported the changes of vitamin D_3 level in serum after recent bone fractures or surgery, suggesting the involvement of VD_3 in bone healing and skeletal homeostasis [131]. Furthermore, VD_3 has been reported to influence the immune response and show anti-inflammatory effects in recent studies [132-135]. It can induce the production of anti-microbial peptide cathelicidin (LL-37) in monocytes/macrophages in order to defend against pathogenic compounds, such as LPS (Lipopolysaccharide) [136].

1.1.9 Bone biomaterials

1.1.9.1 Review of biomaterials in bone tissue engineering

As described above, biomaterials - another key element in bone tissue engineering, have been developed for bone repair and regeneration with different kinds of materials or their combinations. Metallic biomaterials possess good compressive strength; thus, they are often used in load-bearing applications. For instance, titanium is widely used in bone plates and screws or a part thereof for its excellent mechanical properties and compatibility to fix the bone and bear loads during the healing process [137]. Ceramic biomaterials are developed from bone inorganic component calcium phosphate; they, together with bio-glasses with good osteoinductive properties are often used for replacement and fillings in bone fractures [138, 139]. The natural bone ceramic hydroxyapatite has also been applied in coating and filling, and combined with scaffolds for its merits of good stability, biocompatibility and osteoinductivity to induce new bone formation [140, 141]. In addition, the porous structure and micro/nano surface of bone biomaterials also possess osteoinductive properties to mediate bone formation [142]. Polymer biomaterials could be categorized into synthetic and natural macromolecules. They are more flexible in fabrication as well as biochemical and compositional modification to obtain excellent mechanical properties, bioactivities and controlled biodegradability [143, 144]. In most cases, bone substitutes need to provide mechanical stability before being replaced by new bone. Thus, biodegradable and bioresorbable biomaterials have been developed. The magnesium bone fixation plates and screws, for example, degrade by oxidation, lose their mechanical properties and are

finally resolved by the surrounding newly formed bone after a period of time [145]. The polymer or bio-ceramics based resorbable bone materials degrade via a cell-mediated enzymatic reaction or change of chemistry [146, 147].

The primary requirement for biomaterials in bone tissue engineering is biocompatibility which is defined as the ability to support normal cellular activities without inducing local or systematic toxicity in the hosts [148]. The ideal biomaterials in bone tissue engineering enable bone cell attachment, proliferation, differentiation and bone formation on their surfaces, which is defined as osteoconduction, or instruct bone formation at an ectopic site, termed as osteoinduction [149, 150]. On the contrary, implants that release cytotoxic chemicals or byproducts of cell-material interactions can cause a local or systematic problem, such as death of tissue or carcinogenicity to the hosts [151, 152]. In clinical practice, the foreign body reactions could be triggered immediately right after the implantation, thus provoking an acute inflammatory response [153, 154]. The bio-functionality and integration of implants are determined by the magnitude and duration of the tissue response [155]. Immediately after implantation, proteins in blood and body fluids adsorb to the surface of biomaterial, thus recruiting macrophages to form a layer of foreign body cells, which are then covered with an outer zone of layered fibroblasts and connective tissue [153, 156]. It is believed that this process makes the implant biocompatible to the host and is associated with the surface roughness and chemical nature of the biomaterials [157]. In the case of long-term use, the wear particles, corrosion or degraded products from bulk biomaterials can cause chronic inflammation, leading to implant failure and disintegration [158, 159]. Thus, the assessment of *in vitro* cytotoxicity, long term reproductive toxicity, carcinogenicity, blood interaction, irritation, local effect, degradation, and *in vivo* testing is of importance for biomaterials before they are applied in clinical devices according to the ISO technical standard.

In addition to the material itself, the architecture of biomaterials and scaffolds also plays an important role in regulating bone formation. The work of Sicchieri et al. [160]

described the impact of pore size of PLGA-CaP composite scaffolds on the osteoblastic response of cells. In this work, 470-590 μm pore size (in the range of 470-1200 μm) of the scaffolds was found to increase vessel number and bone formation. Whereas, the results from Hollister's group with polycaprolactone (PCL) scaffolds showed the insignificant influence of pore size ranging from 350 to 880 μm on bone formation in an *in vivo* bone regeneration model [161]. It seems the optimal pore size for bone growth and development alters with the materials used and their manner of application. Studies have demonstrated the critical size of pores for bone TE starts around 200 μm which gives enough space for nutrition infusion, ingrowth of bone tissue and vascularization in the scaffolds [162, 163].

Increasing the pore size sometimes leads to the compromised mechanical properties of scaffolds; however, these two aspects should be engineered in a balanced way to acquire the best enhancement of bone growth in and around the scaffolds with sufficient duration and strength of the implants. The mechanical properties of scaffolds also influence the cell behaviors such as migration and differentiation by the mechano-transduction process to convert external mechanical information into internal biochemical signals through the cooperation and interaction of extracellular components, transcellular molecules and the cell skeleton [164, 165]. The work of Engler's group indicated that stiffness regulated differentiation of MSCs on the polyacrylamide hydrogels with tunable elasticity [166]. It has also been shown that the angiogenic response in endothelial cells is associated with the stiffness of the collagen matrix [167]. Different cells are adapted to their living microenvironment *in vivo* and communicate with the surrounding cells, tissues and the matrix. The stiffness of tissues varies in a huge range from 1 kPa in the soft brain tissue to more than 20 GPa Young's modules in the hard cortical bone tissue [168, 169]. Thus, the design of the components and architecture of bone biomaterials should take into account the original surrounding environment of cells and tissues.

Last but not least, the bioresorbability and the micro/nano structure of the topography should also be evaluated in terms of the efficacy and impact on cellular activities in various systems [170, 171]. In all, bone biomaterials, instead of serving as simply scaffolds for cellular activities and tissue growth, have been developed with more bio-functions adapted to specific applications, such as regulating cell activity and delivering bioactive molecules. The current design of bone biomaterials employs new material technology and deep understandings of bone formation to mimic the native environment of bone tissue in various aspects with the aim of successful bone repair and regeneration.

1.1.9.2 Hydrogels and modification in bone tissue engineering

Hydrogels, as a form of polymer biomaterials, can be fabricated using hydrophilic macromolecule networks formed by chemical covalent bonds, physical interactions or entanglement. In hydrogels, a large amount of water is retained. Depending on the source of the polymers, hydrogels can be sorted into synthetic and natural materials. In bone tissue engineering, synthetic polymers, such as poly ethylene glycol (PEG) and poly vinyl alcohol (PVA), are often used as scaffolds and delivery systems in the form of a hydrogel [172-174]. PEG, for instance, could be conjugated with the pedant peptide RGD (ArgGlyAsp) to enable cellular adhesion [175], and modified with cell cleavable peptides for biodegradable properties [176]; the mechanical properties of PEG could be tailored by changing the molecular weight, concentration or crosslinking density of the polymer [177]. The natural macromolecules, especially the ECM components, with intrinsic cellular affinity provide another choice of matrices for bone regenerative medicine. These natural materials, such as collagen, chitosan, fibrin, alginate, hyaluronic acid, silk fibroin and gelatin are modified or hybridized with synthetic polymers to obtain tunable high strength, thermostability and bioactive functions [178, 179]. Collagen type I, as the major organic component of bone ECM has been widely applied as a matrix to provide both physical support for cell-matrix interactions and biochemical cues to regulate cell activities [180, 181]. Collagen has a complex structure

of fibrils which are constituted with parallelly assembled macromolecular helices [182]. In addition to the drawbacks of variation and high cost of large batch production, the full length ECM macromolecules with low solubility have no advantages in biochemical modification [183]. Instead, gelatin - the hydrolyzed product of collagen, overcomes these difficulties and inherits the cell adhesive motifs and biodegradable sites from collagen. Modified gelatin has been reported to provide tunable mechanical properties related to the macromolecule concentration, functionalization degree and crosslinking density [184, 185]. Functionalized gelatin and its synthetic hybrid hydrogels have been successfully introduced in tissue engineering as scaffolds for cell encapsulation to achieve sustained viability and proliferation of endothelial cells, and formation of vascular networks *in vivo* [186, 187]. Recently, an engineered collagen mimetic hydrogel which was constructed with triple helical protein functionalized with RGD sequence peptides and biodegradable crosslinkers has been demonstrated for its potential in chondrogenesis, enabling the strategy to create a complex dynamic ECM like construct with multiple functional peptides for tissue regeneration [188].

As biomaterials, hydrogels possess several advantages. For instance, the high water content of hydrogels provides a cell-friendly environment with excellent biocompatibility. The development of injectable hydrogels with smart molecules allowing *in situ* gelation has brought a new strategy to bone tissue engineering, overcoming the difficulties of highly invasive surgical approaches and the dissymmetric shape of bone defects. With this strategy, the water soluble monomers with initiators or solutions of *in situ* hydrogel-forming macromolecules are injected to sites which are difficult to access. The gelation process is usually controlled by a change in the physiological conditions such as temperature, pH value or physiologic fluid and external aids, for example, UV light [189, 190]. Moreover, incorporating bioactive ligands or ECM functional peptides to matrix components in hydrogel biomaterials may achieve a better efficacy in tissue regeneration. The IKVAV (Ile-Lys-Val-Ala-Val) peptide, one of the bioactive peptide sequences of ECM protein laminin, is believed to

enhance the endothelial cell attachment, migration and angiogenic process [191]. The work from Nakamura's group presented the pro-angiogenic effect of their artificial extracellular matrix (ECM) proteins containing the IKVAV sequence in collagen gels *in vitro* [192] and on atelocollagen membranes *in vivo* [193], suggesting the strategy to combine functional components of ECM into biomaterials in tissue engineering.

1.2 Aim of the study

The main purpose of this thesis is to characterize the specific effects of bio-functional molecules and develop biomaterials in the context of bone tissue engineering. In this thesis, the primary outgrowth endothelial cells derived from peripheral blood which can contribute to angiogenesis and form the capillary-like structures *in vitro* were co-cultured with osteogenic cells to establish a bone vascularization model. The marine origin bioactive compound fucoidan was studied in the co-cultures and separately in mono-cultures of OECs, MSC and bone sarcoma cell line MG63 for its regulatory effect on angiogenesis. In addition, the co-cultures and correlating mono-cultures were further applied to study the angiogenesis/osteogenesis in bone inflammation induced by LPS and assess the impact of vitamin D_3 in this process. Last, the OECs and osteogenic MSCs were encapsulated in functionalized collagen hydrogels and silk fiber composite hydrogels to assess their potential as pre-vascularized constructs or osteogenic promotive scaffolds in the context of vascularization in bone regenerative medicine. The main experimental setups are depicted in the flow chart (Figure 1.4) and the specific tasks include:

- Apply fucoidan extract to bone regenerative and tumor models to quantitatively analyze its bio-functions on vascularization in bone physiological and pathological processes at both cell and molecular levels, and to a uveal melanoma co-culture model, at a relatively safe dose in terms of endotoxicity and cytotoxicity on each of the cell types.
- Evaluate the angiogenic activity under an inflammatory response induced by LPS in a bone regenerative model and study the function of vitamin D_3 in this model by means of quantitative experimental tools.
- Develop the mechanically stable and bio-functional injectable collagen hydrogels aiming to promote vascularization for fast regenerative effects and determine cell activities at the cellular and molecular levels.

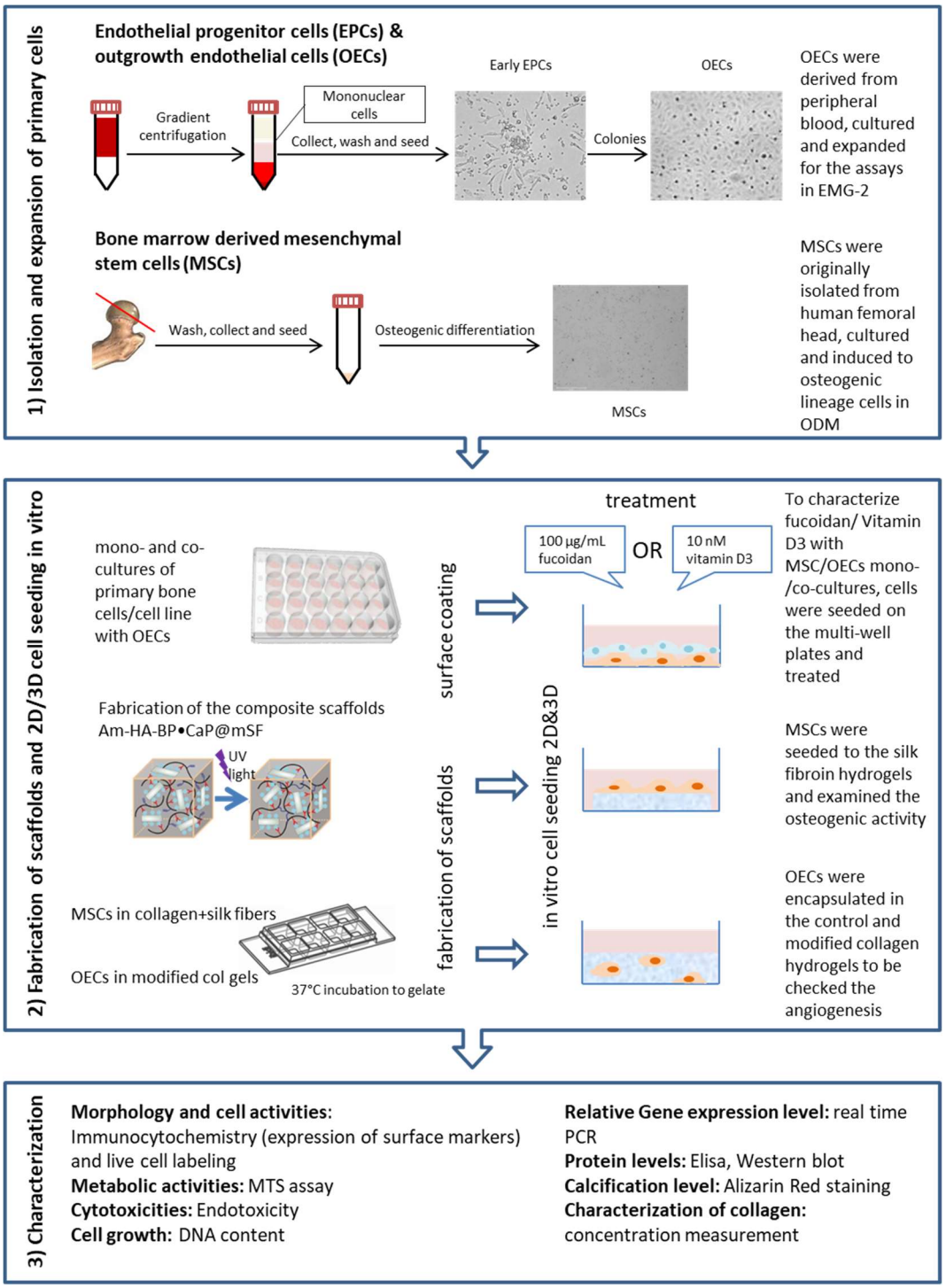

Figure 1.4 The flow chart.

- Evaluate the bone regenerative properties of the silk fiber composite hydrogels *in vitro* especially the cellular response to the bioactive component involved in the scaffolds.

2. Materials and Methods

2.1 Materials

2.1.1 Instruments

Instrument	Model	Manufacturer
Beakers	DURAN	SCHOTT, Mitterteich, Germany
CASY	CASY TT	OLS, Bremen, Germany
Centrifuge	Biofuge primo R	Heraeus, Hanau, Germany
	Multifuge 3 S-R	Heraeus, Hanau, Germany
Confocal laser scanning microscope	LSM 510 Meta	Zeiss, Oberkochen, Germany
Cryo 1°C Freezing Container	NALGENE® Mr. Frosty	Thermo Scientific, USA
Cryotank	Locator 4 plus	Thermo Scientific, Marietta OH, USA
Electrophoresis Power Supply	PowerEase 500	Invitrogen, Eugene, USA
Epi-fluorescent microscope	Evos FL Auto 2	Life Technologies, Grand Island, USA
Fluorescent Microplate reader	Spectra FLUORA plus	TECAN, Maennedorf, Switzerland
Fridge (4°C)	profi line	LIEBEHERR, Austria
Freezer (-20°C)	Premium Nofrost	LIEBEHERR, Austria
	comfort	
Freezer (-80°C)	HERA freeze	Heraeus, Hanau, Germany
Fumehood	Köttermann	Köttermann, Uetze, Germany
GraphPad Prism 5	GraphPad software	GraphPad Software, Inc., La Jolla, CA, USA
ImageJ	NIH ImageJ	National Institutes of Health

Incubator	BBD6220, HERA cell 240	Thermo Scientific, Langenselbold, Germany
Magnetic stirrer	RH basic 2	IKA, Staufen, Germany
	VARIOMAG® MONO	Thermo Scientific, Langenselbold, Germany
Laminar flow bench	HERA safe	Heraeus, Hanau, Germany
Light microscope	Axiovert 25	Zeiss, Oberkochen, Germany
Lyophilizer	CoolSafe ScanVac	LaboGene™, Allerød, Denmark
Microcentrifuge	3722L	Fisher Scientific, USA
	220VAC	Carl ROTH, Germany
Microplate reader	Apollo LB 911	Berthold Technologies, Bad Wildbad, Germany
Western blot electrophoresis chamber	Mini Gel Tank	Invitrogen, Eugene, USA
	Mini Blot Module	
Nanodrop	Nano Drop 2000	Thermo Fisher, Erlangen, Germany
Orbital shaker	swip	Edmund Bühler, Germany
pH meter	Inolab, pH 7110	WTW, Weilheim, Germany
Pipettes 2-10µL, 10-100µL, 100-1000µL multichannel pipette 30-300µL Repeater pipette	Research plus Research 300 Multipette® plus	Eppendorf, Hamburg, Germany
Pipette aid	pipetus	HIRSCHMANN LABORGERÄTE
Real-time PCR cycler	Rotor-Gene Q	Qiagen, Hilden, Germany
Roller mixer	SRT9	Stuart, Staffordshire, UK
Smart fluorescent cell analyzer	JuLI	NANOENTEK Inc.
Sonicator	MSE	MSE, London, UK

Surgical kit, spatulas, tweezers	/	Carl ROTH, Germany
Thermoblock	Thermomixer comfort	Eppendorf, Hamburg, Germany
Vacuum pump	AC500	HLC, Bovenden, Germany
Vacuum aid	Vacu boy	Integra Biosciences, Fernwald, Germany
Vortex	VORTEX-GENIE 2	Scientific Industries, Bohemia, NY, USA
Waterbath	1004	GFL, Burgwedel, Germany
Weighing machine	BP211D	Sartorius, Göttingen, Germany

2.1.2 Consumables

Consumables	**Manufacturer**
24-well-plates lid, sterile	TPP, Trasadingen, Switzerland
48-well-plates lid, sterile	falcon, corning NY, USA
96-well-plates lid, sterile	Sarstedt, Nümbrecht, Germany
96-well-plates, F, Trans	greiner bio-one, Frickenhausen, Germany
96-well-plates, Med binding (Elisa)	greiner bio-one, Frickenhausen, Germany
Foil paper	Universal, Düsseldorf, Germany
Cell scrapers	Sarstedt, Nümbrecht, Germany
Cell Strainers 40µm Nylon	Falcon, Durham, USA
Centrifuge Tubes (15mL, 50mL)	Sarstedt, Nümbrecht, Germany
Combitips Advanced®	Eppendorf, Hamburg, Germany
CryoPure Tube 1.8mL	Sarstedt, Nümbrecht, Germany
DispenserTips, Ritips®	Ritter, Schwabmünchen, Germany
Filter 0.2µm non-pyrogenic	Sarstedt, Nümbrecht, Germany
High performance chemi-luminescence films	GE healthcare, little Chalfont, UK
Microtubes (500µL, 1.5mL, 2mL)	Sarstedt, Nümbrecht, Germany
Needles 20G×1 ½", Sterican®	B.BRAUN, Melsungen, Germany

NovexTM WedgeWellTM 4-20% Tris-Glycine Gel	invitrogen, Carlsbad, USA
µ slide 8 well ibidi	ibidi, Martinsried, Germany
Pasteur pipettes	Assistant, Germany
pH-indicator paper pH1-14	Merck, Darmstadt, Germany
Pipette tips (10, 200, 1000µL)	Sarstedt, Nümbrecht, Germany
PVDF membrane	millipore, Bedford, USA
Rotor-Gene Strip Tubes & Caps	STARLAB, Hamburg, Germany
Serological Pipettes (5mL, 12mL and 25mL)	Sarstedt, Nümbrecht, Germany
Slide-A-Lyzer® 3.5K Dialysis Cassettes	Thermo scientific, Rockford IL, USA
Syringe (5mL, 10mL, 20mL)	BD, Madrid, Spain
Tissue culture flasks vent. Cap (T25, T75, T175)	Sarstedt, Nümbrecht, Germany
Thermanox plastic coverslips	Thermo scientific, Rochester NY, USA

2.1.3 Buffers and solutions

Buffer	**Composition**
buffy-coat buffer	2 mM EDTA, 0.5% FBS in PBS
Collagen gelating reconstitution buffer 10×	2.205 w/v% $NaHCO_3$, 0.04 M HEPES, 0.16 M NaOH aqueous solution
Electrophoresis buffer (Tris-Glycine SDS buffer)	50 mM Tris, 192 mM Glycin, 0.1% SDS, pH 8.0
RIPA buffer	150 mM NaCl, 1% NP-40, 0.5% sodium deoxycholate, 0.1% SDS, 50 mM Tris, pH 8.0
Tris Buffered Saline (TBS buffer)	20 mM Tris, 140 mM NaCl, pH 7.6
TBS/T buffer	1% Tween® 20 in TBS buffer
Tissue buffer	15% FBS, 1% Fungizone, 1% Cyproby and 1% pen/strep in Medium 199 GlutaMAX™
Transfer buffer	20% methanol in Tris-Glycine SDS buffer

2.1.4 Chemicals and reagents

Name	Manufacturer
1α,25-Dihydroxyvitamin D_3	Sigma-Aldrich, St. Louis, MO, USA
Alizarin Red S Stain Solution	millipore, Billerica, USA
Accutase®	Biowest, Nuaillé, France
Acetic acid	Merck, Darmstadt, Germany
Ascorbate-2-phosphate	Sigma-Aldrich, St. Louis, MO, USA
β-Glycerophosphate	Sigma-Aldrich, St. Louis, MO, USA
Biocoll	Biochrom, Berlin, Germany
Bovine serum albumin (BSA)	millipore, Kankakee, USA
Calcein AM fluorescent dye	BD Biosciences, Bedford, USA
Cell Tracker	Invitrogen, Eugene, USA
Collagen type I (rat tail)	Corning, Bedford, MA, USA
Cetylpyridinium chloride (CPC)	Roth, Karlsruhe, Germany
Cyproby	FRESENIUS KABI, bad Homburg, Germany
Dexamethasone	Sigma-Aldrich, St. Louis, MO, USA
Dimethyl sulfoxide (DMSO)	Sigma-Aldrich, St. Louis, MO, USA
Ethylenediaminetetraacetic acid (EDTA)	SERVA, Heidelberg, Germany
Ethanol	Merck, Darmstadt, Germany
Fetal bovine serum (FBS)	Sigma, Taufkirchen, Germany
Fibronectin	Millipore, Temecula, CA, USA
Fluoromount Aqueous Mounting Medium	Sigma-Aldrich, St. Louis, MO, USA
Fucoidan from *fucus vesiculosus*	Sigma-Aldrich, Taufkirchen, Germany
Fungizone	Biozol, Eching, Germany
Glycin	Merck, Darmstadt, Germany
Halt™ Protease Inhibitor Cocktail (100×)	Thermo scientific, Rockford, IL, USA
HEPES	Sigma-Aldrich, St. Louis, MO, USA
Hoechst	Sigma-Aldrich, Taufkirchen, Germany
IKVAV peptide	Biosyntan, Berlin, Germany
Isopropanol	Merck, Darmstadt, Germany

LDS Sample buffer (4×)	Thermo scientific, Rockford, IL, USA
L-Glutamine (100×)	Gibco, Darmstadt, Germany
Lipopolysaccharides (LPS) from E coli	Sigma, Deisenhofen, Germany
Medium 199 GlutaMAX™ Medium 199 10×	Gibco, Darmstadt, Germany Sigma-Aldrich, St. Louis, MO, USA
Methanol	Carl Roth, Karlsruhe, Germany
NP-40	Roche, Indianapolis, IN, USA
Nuclease-free water	Ambion, Carlsbad, CA, USA
Paraformaldehyde solution in PBS 4%	Affymetrix, Cleveland, USA
Phalloidin-TRITC	Sigma-Aldrich, St. Louis, MO, USA
penicillin/ streptomycin (Pen/Strep)	Biochrom, Berlin, Germany
Phosphate buffered saline (PBS) 10×	Gibco, Darmstadt, Germany
Phosphatase Inhibitor Cocktail (100×)	Cell signaling technology, Leiden, Netherland
Precision Plus protein™ WesternC™ standards	BIO-RAD, Hercules, USA
Precision Protein™ StrepTactin-HRP Conjugate	BIO-RAD, Hercules, USA
SDS	Sigma-Aldrich, St. Louis, MO, USA
skimmed milk	BIO-RAD, Hercules, USA
Sodium Chloride (NaCl)	J.T.Baker, Deventer, Netherland
Sodium deoxycholate	Sigma-Aldrich, St. Louis, MO, USA
Sodium Hydroxide (NaOH)	Merck, Darmstadt, Germany
Sodium Hydrogen Carbonate ($NaHCO_3$)	Merck, Darmstadt, Germany
Sulfuric acid (H_2SO_4)	Roth, Karlsruhe, Germany
SYBR® Select Master Mix	Applied biosystems, Austin, USA
Triton® X-100	Sigma-Aldrich, Taufkirchen, Germany
Tris	Carl Roth, Karlsruhe, Germay
TRIzol® Reagent	Ambion, Carlsbad, CA, USA
Trypsin/EDTA (10×)	Biochrom, Berlin, Germany
Tween® 20	Roth, Karlsruhe, Germany
Vascular endothelial growth factor-165	Biomol, Hamburg, Germany
Water Ampuwa®	FRESENIUS KABI, bad Homburg, Germany

2.1.5 Cell culture medium

Medium	Supplement
Endothelial growth medium-2	Endothelial basal medium-2 (EBM-2) 500 mL (Lonza Walkersville, MD, USA) +Supplements: 10 mL FBS, 0.2 mL Hydrocortisone, 2 mL hFGF, 0.5 mL VEGF, 0.5 mL IGF-1, 0.5 mL ascorbic acid, 0.5 mL hEGF, 0.5 mL Heparin +Extra 25mL fetal bovine serum (FBS) +1% penicillin/ streptomycin (Pen/Strep)
MSC growth medium	Dulbecco's Medium Essential Medium (DMEM)/Ham F-12 (Biochrom, Berlin, Germany) +20% fetal bovine serum (FBS) +1% Pen/Strep
MG63 growth medium	Dulbecco's MEM (Biochrom, Berlin, Germany) +10% FBS +1% Pen/Strep +1% L-Glutamine
Osteogenic differentiation medium (ODM)	DMEM/Ham's F-12 (Biochrom, Berlin, Germany) +0,1 µM dexamethasone +10 mM β-glycerol phosphate +50 µM ascorbate-2-phosphate +10% FBS +1% Pen/Strep
Growth medium for melanoma cell lines	RPMI 1640 medium (Gibco®/Life Technologies, Germany) +10% FBS +1% Pen/Strep

2.1.6 Antibodies

Primary antibody	Source	Dilution	Manufacturer
Immunocytochemistry			
Anti-human CD31	Mouse	1:50	Dako, Glostrup, Denmark
Anti-human VE-Cadherin	Goat	1:50	R&D, Minneapolis, USA
Anti-human LL-37	Mouse	1:50	Abcam, Cambridge, UK
Anti-human CXCR4	Mouse	1:50	R&D, Minneapolis, USA
Western blot			
Anti-human cathelicidin	Rabbit	1:1000	Abcam, Cambridge, UK
Secondary antibody	**Source**	**Dilution**	**Manufacturer**
Immunocytochemistry			
Alexa488 anti mouse	Rabbit	1:1000	Invitrogen, Oregon, USA
Alexa488 anti goat	donkey	1:1000	Invitrogen, Oregon, USA
Alexa555 anti goat	donkey	1:1000	Invitrogen, Oregon, USA
Alexa555 anti mouse	donkey	1:1000	Invitrogen, Oregon, USA
Western blot			
lgG-HRP anti rabbit	Goat	1:5000	Santa Cruz biotechnology, Santa Cruz, USA

2.1.7 Kits

Kits	Manufacturer
CellTiter 96® AQueous One Solution Cell Proliferation Assay	Promega, Madison, USA
DuoSet® ELISA Development kit	R&D, Minneapolis, MN, USA
EndoLISA®	Hyglos, Germany
high capacity RNA-to cDNA Kit	Applied Biosystems, Carlsbad, CA, USA
Human LL-37 ELISA kit	Hycult Biotech, Uden, Netherlands
LAL Chromogenic Endotoxin Quantitation Kit	Pierce, Rockford IL, USA
peqGOLD DNase Digest Kit	VWR peqlab, Erlangen, Germany
peqGOLD Total RNA Kit	VWR peqlab, Erlangen, Germany

Pierce® BCA protein Assay	Thermo Fisher Scientific, Pierce Rockford, IL, USA
Pierce ECL Western Blotting Substrate	Thermo, Rockford, USA
Quant-iT PicoGreen dsDNA assay kit	molecular probes, Oregon, USA
QuickZyme Soluble Collagen Assay	QuickZyme Biosciences, Leiden, Netherlands
RNA-to cDNA Kit	Applied Biosystems, Carlsbad, CA, USA

2.1.8 Primers

Gene name	Primer assay name	Catalogue No.
ALP	Hs_ALPL_1_SG QuantiTect Primer Assay	QT00012957
Angiopoietin-1	Hs_ANGPT1_1_SG QuantiTect Primer Assay	QT00046865
Angiopoietin-2	Hs_ANGPT2_1_SG QuantiTect Primer Assay	QT00100947
C3	Hs_C3_1_SG QuantiTect Primer Assay	QT00089698
Cathepsin K	Hs_CTSK_1_SG QuantiTect Primer Assay	QT00093856
CD68	Hs_CD68_1_SG QuantiTect Primer Assay	QT00037184
CD163	Hs_CD163_1_SG QuantiTect Primer Assay	QT00074641
CD206	Hs_MRC1_1_SG QuantiTect Primer Assay	QT00012810
CXCR4	Hs_CXCR4_2_SG QuantiTect Primer Assay	QT02311841
Osteocalcin	Hs_BGLAP_1_SG QuantiTect Primer Assay	QT00232771
Collagen-1	Hs_COL1A1_1_SG QuantiTect Primer Assay	QT00037793
ICAM	Hs_ICAM1_1_SG QuantiTect Primer Assay	QT00074900
IL-6	Hs_IL6_1_SG QuantiTect Primer Assay	QT00083720
Integrin β1	Hs_ITGB1_1_SG QuantiTect Primer Assay	QT00068124
LL-37	Hs_CAMP_1_SG QuantiTect Primer Assay	QT00010458
SDF-1	Hs_CXCL12_1_SG QuantiTect Primer Assay	QT00087591
TLR4	Hs_TLR4_2_SG QuantiTect Primer Assay	QT01670123
TRACP5	Hs_ACP5_1_SG QuantiTect Primer Assay	QT00199801
VCAM	Hs_VCAM1_1_SG QuantiTect Primer Assay	QT00018347
VE-Cadherin	Hs_CDH5_1_SG QuantiTect Primer Assay	QT00013244
VEGF	Hs_VEGFA_2_SG QuantiTech Primer Assay	QT01036861

vwf	Hs_VWF_1_SG QuantiTect Primer Assay	QT00051975
RPL13A	Hs_RPL13A_1_SG QuantiTect Primer Assay	QT00089915
RUNX2	Hs_RUNX2_1_SG QuantiTect Primer Assay	QT00020517
Gene name	Sequence	Annealing temperature
CD 31	for 5'- CCGGATCTATGACTCAGGGACCAT-3' rev 5'-GGATGGCCTCTTTCTTGTCCAG-3'	55 °C

2.2 Methods

2.2.1 Isolation and culture of MSCs

Human mesenchymal stem cells (MSCs) which are loosely attached to cancellous bone structures were isolated from human femoral heads. Cells were first collected by washing the bone fragments in tissue buffer (including anti-bacterial and anti-fungal substances) and subsequently buffy coat buffer (2.2.3) several times. Cells in washing solutions were centrifuged at 400 g for 10 min and resuspended in phosphate buffered saline (PBS) in a new sterile falcon tube. The cell suspension was filtrated through cell strainers (40 μm) to remove the left-over fine bone debris and tissues after washing. After centrifugation at 400 g for 5 min, cells were resuspended in Dulbecco's Medium Essential Medium (DMEM)/Ham F-12 supplemented with 20% fetal bovine serum (FBS) and 1% penicillin/ streptomycin (Pen/Strep) and seeded at a density of 2×10^6 cells/cm^2 in collagen type I (around 3 mg/mL stock concentration, 1:100 diluted in PBS, incubated for 1h at 37°C) coated flasks. The non-adherent cells were removed by changing medium 24 h after isolation. MSCs were expanded by subcultures in growth medium supplemented with 10% FBS to obtain a relatively large population. Cells at passage 2 were further cultivated in osteogenic differentiation medium (ODM) for 2 weeks to induce osteogenic lineage cells.

2.2.2 Isolation and expansion of OECs

Human outgrowth endothelial cells (OECs) are isolated, derived and cultured from human peripheral blood. First, the human peripheral blood was 1:2 diluted with buffy coat buffer which comprises of 2 mM ethylendiaminetetraacetate (EDTA) to prevent cell clots. The diluted blood was gently placed on 15 mL biocoll in falcon tubes followed by density gradient centrifugation at 400 g for 35 min without brake. The whitish layer of mononuclear cells was aspirated (The layers from top to bottom: a plasma layer, the interphase of mononuclear cells, a layer of biocoll-opaque, granulocytes and erythrocytes on the bottom) and washed several times respectively

with buffy coat buffer and PBS. Cells were resuspended in endothelial cell growth medium-2 (EGM-2) with supplements from the kit, 5% FBS and 1% Pen/Strep, and seeded in collagen type I coated 24-well-plates at a density of 2.6×10^6 cells/cm^2. After 7 days, cells (early EPCs) were subcultured to new collagen type I coated 24-well-plates at a density of 2.6×10^5 cells/cm^2. The cobblestone-like outgrowth endothelial cell (OEC) colonies were observed within 2-3 weeks mainly in the peripheral areas of the wells. OECs were cultured and expanded in a relatively wide span of passage numbers with stable cell phenotypes and homogenous population in fibronectin coated flasks.

2.2.3 Cell culture

In this thesis, all cell types were split at a ratio of 1:2 after reaching 80-90% confluence and cultured in a humid atmosphere supplied with 5% CO_2 at 37°C. Fresh culture medium was applied every other day.

The osteogenic differentiated MSCs in the experiments were maintained in ODM and applied to the assays at passage 2 to 4; OECs were cultured and expanded in EGM-2 for the experiments up to passage 12. Osteosarcoma cell line MG63 was cultivated in Dulbecco's MEM supplemented with 10% FBS, 1% L-Glutamine and 1% Pen/Strep. MG63 cells with different passage numbers between 15 and 23 were used in mono-cultures and co-cultures with OECs. The primary uveal melanoma cell line 92.1 and metastatic melanoma cell line OMM2.3 were maintained in their growth medium (RPMI supplemented with 10% FBS and 1% Pen/Strep).

2.2.4 Cell seeding for mono-/co-cultures

2.2.4.1 Bone regeneration/tumor models

Both mono- and co-cultures were employed to study the effect of bio-functional molecules. For OEC, MSC and MG63 mono-cultures, cells were seeded in fibronectin coated 24 well-plates at a density of 40000 cells/cm^2 (or 96-well-plates for MTS assay). For co-cultures, MSCs and MG63 were seeded as described above, and then OECs were

added at the same density on the next day. The mono-cultures were cultivated in respective cell growth medium and the co-cultures in EGM-2.

2.2.4.2 Uveal melanoma models

To evaluate angiogenesis in uveal melanoma models, OECs were co-cultured respectively with the primary uveal melanoma cell line 92.1 and metastatic melanoma cell line OMM2.3. The melanoma cells (92.1/OMM2.3) were seeded onto fibronectin coated Thermanox coverslips in 24-well-plates at a density of 50000 cells/cm^2 (100000 cells/well). On the next day, OECs were added at a density of 50000 cells/cm^2 to the respective uveal melanoma cell line. The co-cultures were maintained in EGM-2 with the addition of 100 µg/mL fucoidan for 7 days or cultivated in medium as control.

2.2.5 Bio-functional compound treatment of mono- and co-cultures

The fucoidan crude extract from Sigma was solubilized in ultrapure water to prepare the aqueous stock solution at a concentration of 10 mg/mL and sterilized by aseptic filtration for the subsequent biological characterization.

MTS assay was performed to study the metabolic activity of individual cell type in response to fucoidan dose. In this assay, fucoidan of different concentrations (from 0 to 500 µg/mL) was applied to OEC, MSC and MG63 mono-cultures in 96-well-plates (100 µL/well).

According to the MTS result, 1 mL medium supplemented with 100 µg/mL fucoidan was applied to each well of mono-/co-cultures one day after seeding the cells, or cells were grown in medium as controls for the experiments performed in 24-well-plates to assess the cellular, angiogenic and osteogenic activities. Medium and fucoidan treatment were freshly prepared and changed every 3 days.

To study the function of Vitamin D_3 in the bone regenerative model, OEC/MSC mono- and co-cultures in 24-well-plates were treated with 10 nM Vitamin D_3 in 1 mL medium/well on the next day of cell seeding. Medium change was performed every 2

days. On the 5th day of Vitamin D_3 treatment, LPS (100 ng/mL) was added and incubated for 48 h.

2.2.6 Functionalized collagen hydrogel

2.2.6.1 Collagen hydrogel modification

The collagen molecules were modified with or without IKVAV peptides through disulfide bond formation in the presence of the mild oxidizing agent DMSO [194]. Compared with the conventional manners which require basic or neutral pH and a long duration, this method can be performed in mild acidic pH at an efficient reaction rate.

The collagen type I (rat tail) solution (in 0.02 M acetic acid) was diluted (1:5) in 0.5 M HEPES and adjusted to pH 6.0 (by 1 M NaOH). The IKVAV peptide (reconstituted to 5 mg/mL in sterile distilled water) or equivalent volume of water as modified control was applied to the diluted collagen solution at a ratio of 650 µg peptide/ 6 mg collagen with continuous stirring. The solutions were incubated at 4°C for 3 min after adding 20%v/v DMSO to cool down after DMSO dissolution. The aqueous mixtures were allowed to react for 24 h at room temperature with stirring. The modified collagen solutions with and without IKVAV peptides were dialyzed against deionized water for 24 h in pre-hydrated Slide-A-Lyzer® 3.5K Dialysis Cassettes with regular water changes. The IKVAV and control modified (without the addition of IKVAV) solutions were collected in 50 mL falcons and frozen at -80°C for at least 2 h for the following 48 h lyophilization. The freeze-dried collagen was dissolved in sterile filtered 0.02 M acetic acid to the initial volume of collagen solution before modification. Before use, the concentration of collagen in both modified collagen solutions were determined and stored at 4°C.

2.2.6.2 Determination of collagen concentration

The triple helical structure and specific amino acid content of collagen bring difficulties to its characterization of concentration. In this experiment, it was found the QuickZyme

Soluble Collagen Assay based on Sirius Red dye binding to collagen is a suitable method to determine the collagen concentration in the samples.

The stock collagen type I solution (Corning) and both modified collagen solutions were first 1:6 diluted in 0.02 M acetic acid solution followed by a further 1:10 dilution in the dilution buffer provided in the kit. The sample dilutions and 8-points serial dilutions of the standard prepared in duplicate were pipetted (140 µL/well) to a V-shape plate. The dye Sirius Red which binds to collagen was applied (60 µL/well) to the samples and standards and incubated on ice for 10 min. The V-shape plate sitting in a flat bottom plate was centrifuged at 3000 g for 60 min at 4°C. The collagen-dye complex precipitation on the bottom of the wells was gently washed with washing solution for 3 times to remove the excess dyes and dried by placing the plate upside down on a paper towel for 5 min. The complex was resuspended in 150 µL detection solution/well for color development. 100 µL colored solution of each well was transferred to the reading microplate which was read at 540 nm to perform data analysis according to the standard curve.

2.2.6.3 Collagen hydrogel preparation

The collagen and derivative collagen solutions were adjusted to an equal concentration (C_{col}). The collagen and modified collagen stock solutions in the volume of V_{stock} (Formula 1) were diluted to a final volume (V_{col}) with 0.02 M ascetic acid up to the volume of ($0.8\times V_{col}$) and balanced with ($0.1\times V_{col}$) volume of 10×fold Medium199 followed by ($0.1\times V_{col}$) volume of collagen gelating reconstitution buffer 10× (refer to 2.2.3) for the osmolarity and pH value in the pre-gelation solutions.

$$V_{stock}=(C_{col} \times V_{col})/C_{stock}$$

Formula 1. C_{col}, V_{col} and C_{stock} present final collagen concentration of hydrogel, volume of pre-gelation collagen solution and collagen concentration of sample stock solution respectively. C_{stock} was measured with the method in 2.2.6.2.

OECs were thoroughly suspended in ice cold pre-gelation collagen solutions at a density of 1×10^6 cells/mL and quickly transferred in µ slide 8 well ibidi (for visualization) or 48-well-plates for 30 min incubation at 37°C to gelate. Afterwards, the cell laden collagen hydrogels were cultured in EGM-2 medium supplemented with 50 ng/mL vascular endothelial growth factor (VEGF).

2.2.7 Cell seeding and encapsulation for 3D tissue engineering constructs

Cell seeding on 3D hydrogels: The *in vitro* bone regenerative silk fibroin composite hydrogels Am-HA-BP·CaP@mSF and control (AM-HA-BP·mSF) were UV sterilized in a 48-well-plate and incubated with ODM at 37°C for 48 h. Osteogenic differentiated MSCs were split and seeded on the scaffolds. Each scaffold was loaded with 200000 cells in 1 mL medium, cultured in a humidified atmosphere with 5% CO_2 at 37°C and fed with fresh medium every other day.

Cell encapsulation in 3D hydrogels: Cells were transferred in a 1.5 mL microtube and centrifuged at 400 g for 5 min to form a cell pellet on the bottom. The supernatant was completely aspirated, and the cell pellet was resuspended in a pre-gelation solution at a density of 1×10^6 cells/mL and mixed thoroughly before gelation.

2.2.8 Live cell staining

2.2.8.1 Calcein AM live cell staining

Calcein AM, a cell permeant dye, stains live cells to generate strong fluorescence. To visualize MSCs on the HA based composite scaffolds, the cell laden constructs were washed with PBS and incubated with Calcein AM (5 µM in ODM) for 10 min at 37°C. The Calcein AM solution was aspirated afterwards and new growth medium was applied to the stained cells ready for visualization and imaging.

2.2.8.2 Cell Tracker staining

CellTracker™ consists of fluorescent chloromethyl derivatives which are retained in live cell membranes and could be inherited by next generations. OECs were pre-labeled with CellTracker before being encapsulated in collagen hydrogels. Briefly, cells were washed twice with EGM-2 without serum (FBS) and incubated for 30 min with CellTracker (2.5 µg/mL in serum free medium) at 37°C. Then cells were washed twice with serum free medium to remove the CellTracker and incubated for 1 h in EGM-2 with serum to re-activate the metabolism before being seeded.

2.2.9 Determination of endotoxicity

The endotoxin content of fucoidan extract was initially detected with LAL chromogenic quantification assay according to manufacturer's protocol. All materials used in this assay including pipette tips, microtubes and 96-well-plates were endotoxin free (pyrogen free). The fucoidan sample (diluted in endotoxin free water to 100 µg/mL) and standards were prepared in triplicate and placed 50 µL per well into a pre-equilibrated 96-well-plate. Then LAL reagent (50 µL/well) was added. After 10 min incubation at 37°C, the substrate solution was added and incubated for 6 min followed by the addition of the stop solution (25% acetic acid). The plate was read at 405 nm with the microplate reader. The endotoxin content of the fucoidan sample at working concentration (100 µg/mL) was determined with the formulated standard curve.

EndoLISA® kit was used to further examine the endotoxin content of fucoidan sample, as the endotoxicity determined by LAL assay could be interfered with some matrix substances in the crude extract. The fucoidan sample (diluted to 100 µg/mL) and 10-fold serial standards were prepared in duplicate and applied to the pre-treated LPS specific phage binding plate, then binding buffer was added for subsequent overnight (18 h) mixing (450 rpm) at 37°C. After 3 times wash to remove the matrix substances, assay reagent was applied for the enzymatic reaction activated by endotoxin binding. The fluorescence generated by the reaction after 90 min was read at 380/445 nm of

excitation/emission wavelength and the relative fluorescence unit was calculated. The endotoxin content of the fucoidan sample was calculated from the logarithm (endotoxin concentration) which was determined by a linear fitting equation of the logarithmic standard curve.

2.2.10 MTS cell metabolic activity assay

The metabolic activity of cells was determined with CellTiter 96® AQueous One Solution Cell Proliferation Assay in which the soluble colored formazan product was produced associated with cell metabolic enzymes. MSC, MG63 or OECs respectively were seeded on 96-well-plates at a density of 40000 cells/cm^2. Cells were treated with 100 µL/well medium with different concentrations of fucoidan as described in 2.2.5. To characterize cell metabolic activity, the medium was replaced by MTS solution (1:6 diluted in medium, 120 µL/well) and the plates were incubated at 37°C for 2 h. The absorbance at 490 nm was measured in a microplate reader. The cell metabolic activities in percentage were calculated as the mean value normalized to control group (100%) after subtracting the absorbance of the blanks.

2.2.11 Immunofluorescence staining for visualization

The co-cultures on 24-well-plate were grown on Thermanox coverslips coated with fibronectin for immunostaining. Cells were fixed with 4% paraformaldehyde in PBS, washed 3 times for 5 min with PBS and then permeabilized by 10 min incubation with 0.5% Triton ®X-100. Then cells were incubated with primary antibodies which were diluted in PBS with 1% bovine serum albumin (BSA) for 1.5 h. After washing with PBS (3 times, 5 min) to remove excess primary antibodies, cells were incubated with the secondary antibodies which were diluted in 1% BSA in PBS for 30 min followed by 5-10 min incubation with Hoechst (1 mg/mL stock, 1:500 diluted in PBS). The MSCs on silk fibroin composite hydrogels were stained with F-actin binding toxin phalloidin-TRITC (0.5 mg/mL stock, 1:100 diluted in PBS) for 30 min before Hoechst. The co-culture samples on Thermanox coverslips were mounted with Fluoromount

Aqueous Mounting Medium and cell laden scaffolds were kept in PBS at 4°C before visualization.

2.2.12 Quantification of DNA content

The potential influence of bioactive molecules or specific hydrogels on cell growth was evaluated by DNA assessment. To prepare DNA samples, cells were collected as described below from the cultures in a 1.5 mL microtube for each condition. In the study of fucoidan with bone regenerative and tumor models, cells were seeded into the 24-well-plates and cultivated in the medium with addition of fucoidan. Cells in these cultures were incubated with Trypsin/EDTA for 10 min and detached from the wells with the aid of cell scrapers. For the study of angiogenesis in modified collagen gels, OECs were encapsulated and cultivated in the gels. These cell-laden collagen gels were incubated in 60°C water bath for 10 min and solubilized, thus the OECs were released in the solutions and collected for DNA quantification [195].

Cell pellets were obtained from the cell suspensions after centrifugation for 5 min at 2000 g and resuspended in 1 mL deionized water for each sample. Cell membrane was destroyed by three times freeze-thaw cycles and twice 15 s sonication. The double-stranded DNA content released in the aqueous solution was examined with Quant-iT PicoGreen dsDNA assay kit which includes the fluorescent nucleic acid stain. Each sample or standard was prepared in triplicate. DNA amount was determined by fluorescence using a microplate reader at 485/535 nm of excitation/emission wavelength according to a standard curve.

2.2.13 Gene expression analysis

2.2.13.1 Preparation of cell lysate

<u>The mono- and co-cultures in 24-well-plates:</u>

In the study of bioactive molecules with the bone regenerative/tumor models, cells were seeded in 24-well-plates and cultivated in various conditions. To lyse the cells, 500 µL cell lysis buffer provided in the total RNA kit was applied to each condition.

The cell-laden 3D hydrogels:

Cells in collagen hydrogels or on the silk fibroin composite hydrogels were lysed by TRIzol Reagent. The cell-laden collagen gels of each condition were collected in 1 mL TRIzol in a 2 mL microtube. After three times freeze-thaw cycles, gels were solubilized in the TRIzol lysate by pipetting up and down through a 20 G needle. 200 µL chloroform was added to the lysate and vigorously mixed. After 12000 g centrifugation for 15 min at 4°C, the upper aqueous part was collected to perform the total RNA isolation.

For the silk fibroin composite hydrogel seeded with MSCs was washed twice with PBS and transferred into a 2 mL microtube with 300 µL TRIzol. After 3× freeze-thaw circles, the TRIzol lysate of each type of hydrogels was collected into a new microtube and vigorously mixed with 200 µL chloroform. After 12000 g centrifugation for 15 min at 5°C, the aqueous part was collected for the total RNA isolation.

2.2.13.2 Total RNA isolation

The total RNA was isolated according to the manufacturer's protocol of peqGOLD Total RNA Kit. First, the lysates/aqueous RNA containing solutions were transferred in DNA Removing Columns and centrifuged at 12000 rpm for 1 min to remove DNA in the samples. The flow-through lysates were loaded with equal volume of 70% ethanol and thoroughly mixed. Thereafter, the lysates were applied in PerfectBind RNA columns for the RNA to bind on the membrane, centrifuged at 10000 rpm for 1 min and washed with wash buffer I. DNase Digest was applied to the columns and incubated for 15 min to further remove DNA in the samples. After 3 times wash with wash buffer I and II, RNA was eluted in sterile RNAse-free dH_2O for the following RNA concentration measurement with a NanoDrop.

2.2.13.3 Reverse transcription

The transcription was performed with high capacity RNA-to cDNA Kit. RNA samples were denatured by 10 min incubation at 70°C. 1 µg of RNA for each sample was transferred in a 0.5 mL microtube, mixed with 10 µL of 2× RT buffer and 1 µL of 20×RT Enzyme Mix and adjusted with Nuclease-free water to a final volume of 20 µL. The reaction solutions were then incubated at 37°C allowing the RNA-cDNA reverse transcription to progress. After 1 h, the reaction was inactivated by 5 min incubation at 95°C and the complementary DNA (cDNA) samplers were filled up to 100 µL with Nuclease-free water.

2.2.13.4 Real-time qPCR (Quantitative real time polymerase chain reaction)

Real-time PCR was performed for primers as indicated in the table 2.1.8 using Ribosomal Protein L13a (RPL13a) as internal control. Quantitative real-time PCR was carried out using a total volume of 25 µL for each reaction and the SYBR® Select Master Mix, cDNA QuantiTect® Primer Assay or CD31, Nuclease-free water, and cDNA were added. The mixtures were preheated to 50°C for 20 min and 95°C for 20 min followed by 40 cycles of step 1: 95°C for 15 sec and step 2: 60°C for 60 s. The relative gene expression was calculated with ΔΔcT method. The conditions of treated cells or cells with modified scaffolds were compared to untreated or unmodified conditions which were normalized to 1 as control.

2.2.14 Protein analysis

2.2.14.1 Enzyme Linked Immunosorbent Assay (Elisa)

The sample supernatants were collected to perform ELISA for VEGF, SDF-1, angiopoietin-1, angiopoietin-2, soluble ICAM-1 and IL-6 with DuoSet ELISA Development kits according to manufacturer's protocols. The med binding 96-well-plates were coated with 100 µL capture antibodies per well and incubated at room temperature overnight. The coated plates were washed 3 times with wash buffer (0.05%

Tween® 20 in PBS) and blocked with 1% BSA in PBS (0.2 µm filtrated) for 1 h. After 3 times wash, samples and standards prepared in triplicate were added to the plates and incubated at room temperature for 2 h. The detection antibodies diluted in 1% BSA were applied to the plates after washing step and incubated for 2 h at room temperature followed by the colorimetric reaction of Streptavidin-HRP conjugates which bind to detection antibodies. The optical absorbance was detected by the microplate reader at 450 nm with a reference wavelength of 560 nm.

The LL-37 level in sample supernatants was detected with Human LL-37 ELISA kit which undergoes the same mechanism as DuoSet ELISA Development kit. In this kit, the pre-coated ready-to-use 96-well-plates have been prepared for loading samples and standards.

2.2.14.2 Protein isolation of cell lysate and quantification

Protein lysates of MSCs with and without Vitamin D_3 treatment were prepared in RIPA buffer to examine the level of LL-37 with Western Blot. MSCs were seeded in T175 flasks at a density of 40000 cell/cm^2, treated or applied fresh medium (for control group) every 2 days for 7 days. For the Vitamin D_3 treated group, 20 mL ODM with 10 nM VD_3 was applied for each treatment. On day 7, after removal of medium, cells were scraped off and collected in ice cold PBS and centrifuged at 12000 rpm for 20 min at 4°C. Each cell pellet was resuspended in 1 mL RIPA buffer supplemented with protein inhibitors (Halt^{TM} Protease Inhibitor Cocktail (100×) and Phosphatase Inhibitor Cocktail (100×), 1:100 diluted) and lysed on ice for 30 min. Samples were centrifuged at 12000 rpm for 20 min at 4°C and the supernatant was collected in a new microtube for the protein concentration determination with Pierce® BCA protein assay according to the instruction of the kit. Samples, sample dilutions and Albumin standards were prepared in triplicate and applied to a 96-well-plate. The BCA working reagent was added and incubated for 30 min at 37°C for a colorimetric reaction and detected at the wavelength of 560 nm in a microplate reader.

2.2.14.3 SDS-PAGE electrophoresis and Western blot

The protein lysates were diluted in LDS Sample buffer (4×) (1 part LDS Sample buffer (4×) with 3 parts protein lysate) and heated at 70°C for 2 minutes. Total protein extracts in equal amount (60 µg) and 5 µL size marker (Precision Plus protein™ WesternC™ standards) were loaded per lane on a NovexTM WedgeWellTM 4-20% Tris-Glycine Gel and placed in the electrophoresis chamber holder filled up with electrophoresis buffer (Tris-Glycine SDS buffer) for 1 h at 200 V. After electrophoresis, transfer buffer (20% methanol in Tris-Glycine SDS buffer) was used to transfer proteins to the PVDF membrane which was equilibrated in methanol. The membrane was blocked for 1 h at room temperature in 3% skimmed milk. The primary antibodies (anti-cathelicidin in rabbit 1:1000 in 3% skimmed milk) were applied to the membrane and incubated at 4°C overnight. After 3 times wash with TBS/T buffer, the secondary antibodies (goat-anti-rabbit IGG-HRP conjugate, 1:5000 in 3% skimmed milk) and Precision Protein™ StrepTactin-HRP Conjugate (1:10000) were applied to the membrane and incubated for 1 h at room temperature. The membrane was exposed to Pierce ECL Western Blotting Substrate and signals were detected by High performance chemi-luminescence films for further analysis.

2.2.15 Quantitative analysis of calcification with Alizarin Red staining

To quantitatively determine the calcification in MSC or MG63 mono- and co-cultures, 1 mL of Alizarin Red S Stain Solution (40 mM) was applied to the 4% PFA fixed cells in a 24-well-plate at day 14 and incubated for 30 min. Cells were washed with distilled water till the wash solution was colorless and incubated with 10% (w/v) cetylpyridinium chloride (CPC) overnight on an orbital shaker to extract the Alizarin Red dyes combined to the mineralized extracellular matrix. The Alizarin Red solutions collected from the stained cell layers and standards prepared in 10% CPC were added to a 96-well-plate and read at a wavelength of 560 nm in a microplate reader for quantitative analysis.

2.2.16 Image analysis

The angiogenic structures *in vitro* are usually quantified with the dimensional parameters of the tubular capillary-like structures including the area of OECs in angiogenic networks, the number of branching points, the number of enclosed circles and the length of identified features.

In this thesis, the angiogenic structures of the co-cultures with and without (control) addition of fucoidan were quantified with the software ImageJ 1.43 by Dr. H. Schmidt as described before [90]. Briefly, the images were segmented semi automatically and the area and length of tube-like structures were quantified. The pro-angiogenic structures of OECs in hydrogels were analyzed with the same software. In brief, the structures were subtracted with background and subsequently selected with the ROI manager (region of interest) for the measurement of total area in pixel. For MSC/OEC co-cultures with VD_3 treatment/LPS stimulation, the angiogenesis was quantified with the software AngioTool. The outline of capillary-like structures was selected and the total vessel length and number of junctions were measured.

2.2.17 Statistical analysis

All experiments mentioned above were carried out with at least 3 different donors or donor combinations. The statistical significance between different conditions or groups was assessed with paired student's t-test, one-way ANOVA or two-way ANOVA in the software Graphpad Prism 5. As it is indicated in the results, $p<0.05$ (*$p<0.05$, **$p<0.01$, ***$p<0.001$, ****$p<0.0001$) was considered as the statistically significant difference.

3. Results

Part I. Effect of bio-functional molecules in bone regenerative/tumor models

3.1 Impact of crude fucoidan extracts on angiogenesis in bone regeneration and tumor models

In various *in vitro* and *in vivo* studies, it has been demonstrated that the marine origin polysaccharide fucoidan possesses multiple biological activities. In this part, the co-culture model of outgrowth endothelial cells (OECs) with osteogenic differentiated MSCs or bone sarcoma cell line MG63 were used to assess the impact of crude fucoidan extracts on the formation of vascular structures (cell details in Table 3.1). With these models, the angiogenic activity, osteogenic activity and relevant molecules involved in both processes at the gene expression and protein levels were studied in response to the fucoidan (*f. vesiculosus*) treatment.

Cell type	Age	Gender	Passage
MSC1 (#16-4)	69	m	3
MSC2 (#16-5)	53	f	3
MSC3 (#16-6)	73	f	3
MSC4 (#15-1)	49	f	3
MSC5 (#15-4)	70	f	3
MSC6 (#15-5)	74	f	3
MSC7 (#22)	n/a	n/a	3
OEC1 (BC61)	24	f	11
OEC2 (BC74)	37	m	9
OEC3 (BC152)	34	f	8
OEC4 (BC01)	59	f	10
OEC5 (BC38)	19	f	11
OEC6 (BC67)	36	m	8
MG63	14	m	15, 17, 23

Table 3.1 List of cells and donor information in the experiments. Female (f); male (m). n/a: the donor information was not available.

3.1.1 The endotoxicity of fucoidan at working concentration

Endotoxins, such as LPS derived from the outer membrane of gram-negative bacteria, can induce acute immune reaction. As a kind of pyrogen which causes fever, endotoxin should be examined for the chemicals and materials applied in medical and

pharmaceutical fields. The endotoxin content of fucoidan (100 µg/mL) was detected to be 0.06 EU/mL according to the standard curve (Figure 3.1 a) by Limulus Amebocyte Lysate (LAL) which is derived from blood cells of the Atlantic horseshoe crab and reacts with endotoxins. Nevertheless, the endotoxicity determined with LAL assay could be disturbed by other substances in the crude fucoidan extract. Therefore, the sample was further examined with EndoLISA® kit. In this assay, endotoxin in fucoidan sample was immobilized by a recombinant bacteriophage protein which specifically binds endotoxin onto a pre-treated plate, and the matrix substances were removed by washing steps before reading the plate. In figure 3.1 b, the logarithm (endotoxin concentration) of fucoidan sample was determined with the standard curve, thus obtaining an endotoxin level of 0.003 EU/mL (<0.005 EU/mL, endotoxin free) in the fucoidan extract.

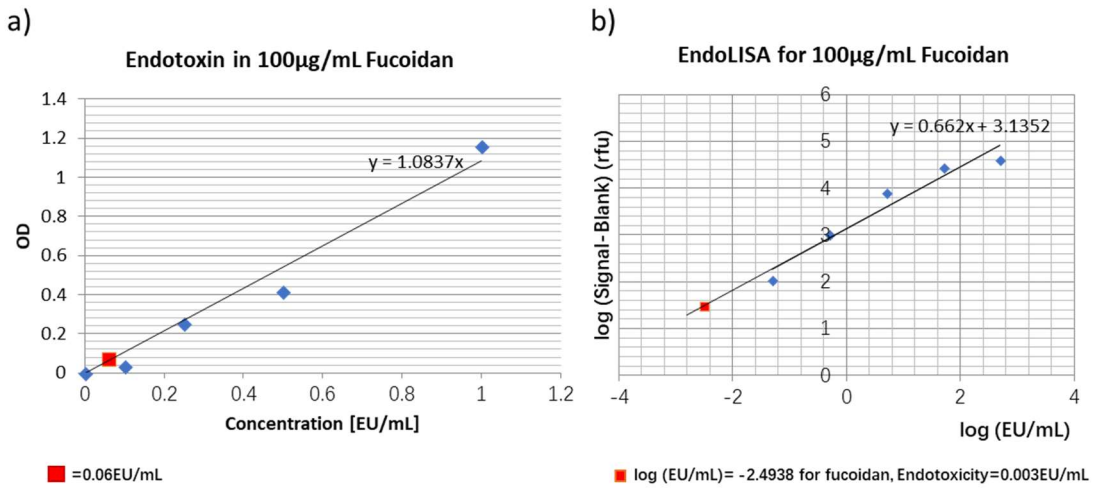

Figure 3.1 Endotoxicity of 100 µg/mL fucoidan f. vesiculosus (Sigma) determined with a) LAL chromogenic quantification assay and b) EndoLISA® kit.

3.1.2 The metabolic activity of individual cell types in response to fucoidan dose

The MTS assays were performed to examine a potential effect of fucoidan on the metabolic activities, respectively viability of MSC, MG63 and OEC in monocultures at day 10 (Figure 3.2) using different concentrations of fucoidan. MTS absorbance values are depicted as relative changes of fucoidan treated groups compared to untreated

controls (100%).

For 100 µg/mL (Figure 3.2), the metabolic activity of MSC and OECs showed only a slight but no significant reduction in fucoidan treated group compared to controls. The metabolic activity was further reduced in groups treated with higher concentrations of fucoidan. In accordance with first effects of fucoidan on OECs at a fucoidan concentration of 200 µg/mL, OECs seemed to be more sensitive compared to MSC (significant effects observed at 300 µg/mL) whereas MG63 seemed to tolerate higher concentrations of fucoidan (significant effects at 500 µg/mL). In accordance with these observations, all further experiments to assess angiogenesis as well as osteogenesis were performed with a fucoidan concentration of 100 µg/mL.

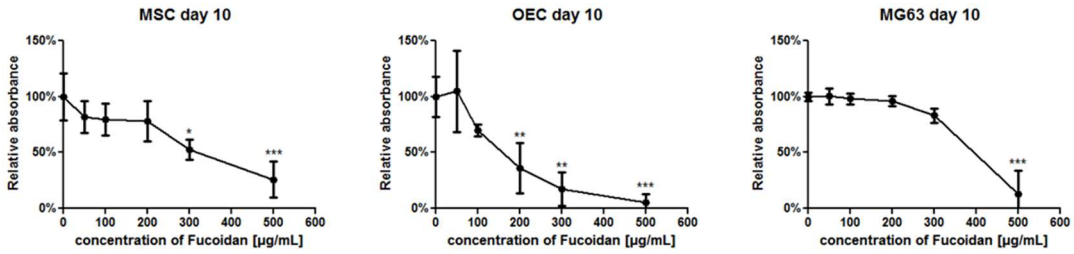

Figure 3.2 Effect of different fucoidan concentrations on the metabolic activity of OEC, MSC and MG63. Data are depicted in percent in relation to untreated groups used as controls (100%), 1-way ANOVA. p < 0.05, p** < 0.01, p*** < 0.001. n=3.*

3.1.3 Quantification of DNA content

In order to gain a deeper insight in the action of fucoidan and potential effects on cell growth, the total DNA content, as indicator for cellular proliferation, was analyzed in mono-cultures of OEC, MSC and MG63 and both groups of co-cultures using a picogreen based assay (Figure 3.3). The Total DNA content analyzed at day 10 decreased significantly for MSC monocultures but increased for mono-cultures of OEC in response to fucoidan treatment, whereas no significant difference was observed for MG63. For both co-cultures the DNA content slightly decreased in fucoidan treated groups but this trend was not statistically significant in the co-cultures.

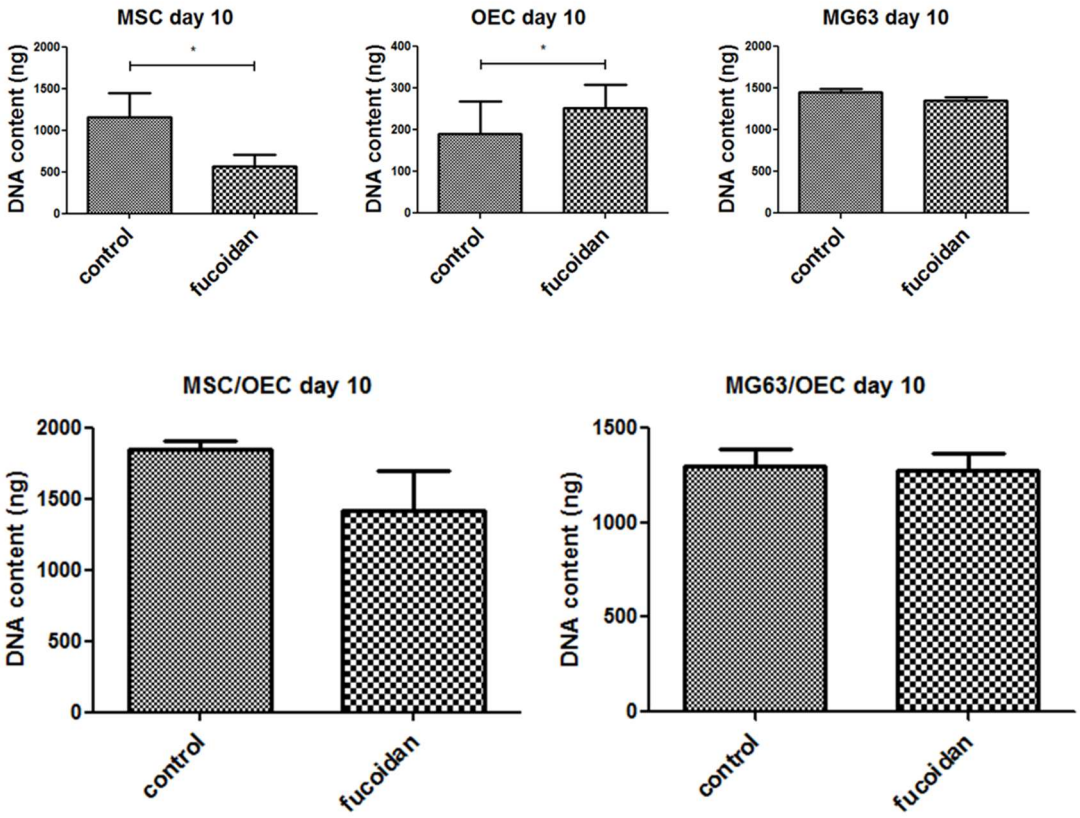

*Figure 3.3 Effect of fucoidan on cell proliferation depicted by the DNA content of MSC, OEC and MG63 mono-cultures (paired t-test) as well as MSC/OEC and MG63/OEC co-cultures (unpaired t-test). *p < 0.05. n = 3.*

3.1.4 Angiogenic structures of OECs in co-cultures and quantitative analysis

The morphology of OECs and the formation of angiogenic structures by OECs in co-cultures were visualized with confocal microscopy after immunostaining with endothelial marker VE-Cadherin (Figure 3.4 ab depicted in red) at day 10. In addition, the samples were stained for stromal-derived factor receptor CXCR4 (Figure 3.4 ab, depicted in green, nuclear counterstain with Hoechst in blue). For MSC/OEC co-cultures, OECs in the untreated control group showed elongated cell shape and were aligned into tubular structures typical for pro-angiogenic structures indicated in Figure 3.4 a. In contrast, fewer pro-angiogenic structures were observed after fucoidan treatment (100 µg/mL) and OECs remained mainly organized as monolayers with distinct cell-cell contacts as indicated by VE-Cadherin staining, although the formation of angiogenic structures was not completely blocked after fucoidan treatment.

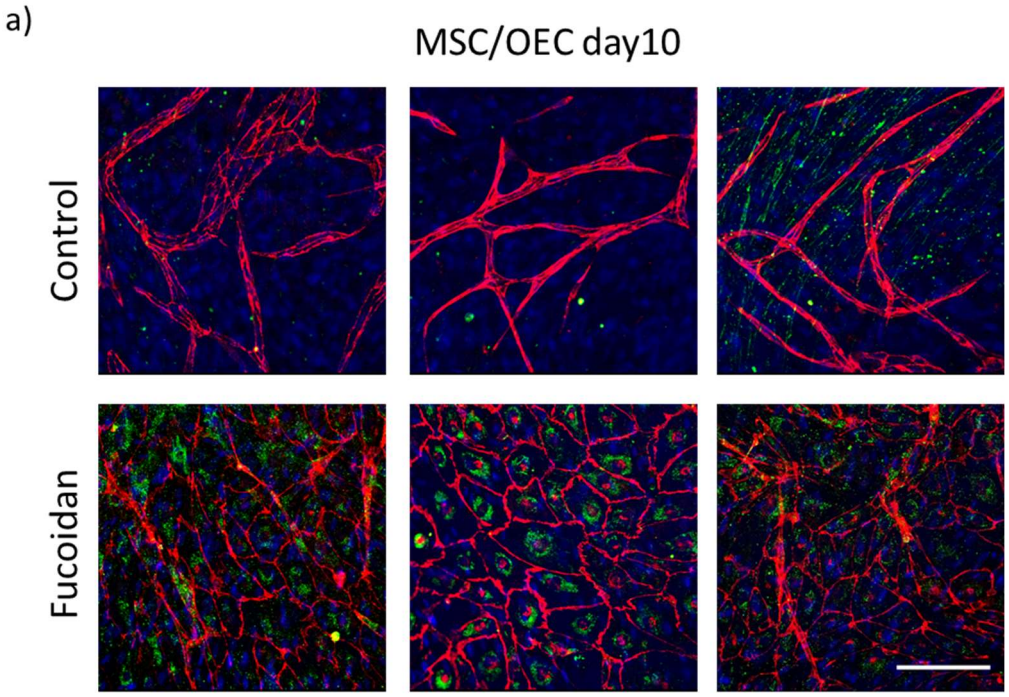
a)
MSC/OEC day10
Control
Fucoidan

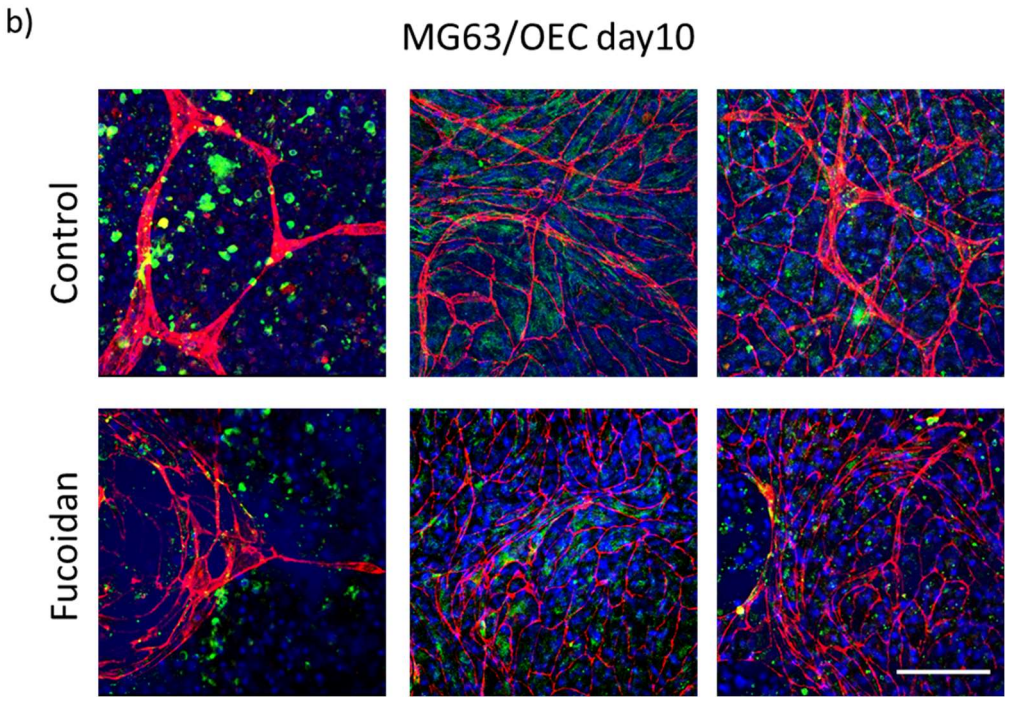
b)
MG63/OEC day10
Control
Fucoidan

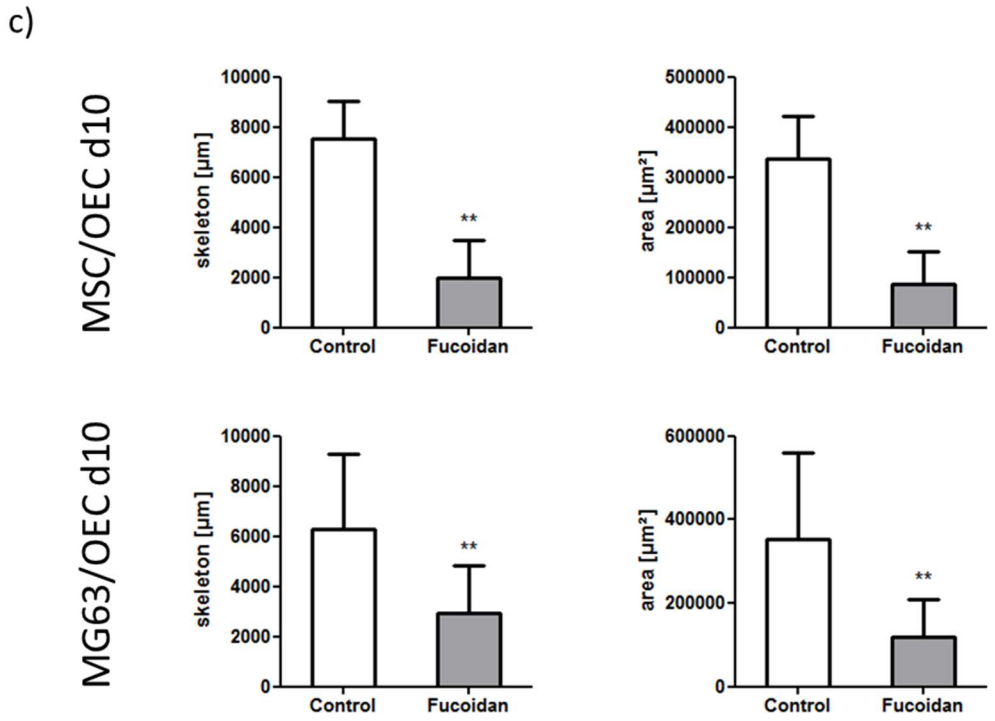

Figure 3.4 Effect of fucoidan on the morphology and pro-angiogenic structures in co-cultures. Confocal laser scanning microscopy of a) MSC/OEC and b) MG63/OEC co-cultures on day 10. VE-Cadherin is depicted in red, green channel represents staining for CXCR4 and nuclei are depicted in blue. The scale bar represents 150 µm. c) Quantitative analysis of angiogenic structures depicting the skeleton length and the area of angiogenic structures for MSC/OEC co-cultures and MG63/OEC co-cultures. The results are given as means ± S.D. and significant differences were calculated with Graph Pad Prism using an unpaired t-test ($p^* < 0.05$ and $p^{**} < 0.01$) for equal variances as verified with a variance ratio analysis (F-test, $p > 0.05$). For unequal variances (F-test, $p < 0.05$) data were analyzed using the unpaired t-test with Welch's correction. n=3.

Similar to MSC/OEC co-cultures, OECs in co-cultures with MG63 were characterized by the formation of complex angiogenic structures at day 10 in untreated control groups as shown in Figure 3.4 b. In fucoidan treated groups, only a few elongated angiogenic structures of OECs were observed mainly at the borders of OEC cell patches.

To quantify the effects of fucoidan on the formation of angiogenic structures, the quantitative image analysis as depicted in Figure 3.4 c was performed by Dr. H Schmidt. For both types of co-cultures, the addition of fucoidan to the culture medium resulted in a significant decrease in length and the area of angiogenic structures thus showing

anti-angiogenic properties of fucoidan in co-culture models relevant for normal bone physiology or osteosarcoma, respectively.

3.1.5 Quantitative assessment of gene expression of mono-/co-cultures

As a next step, the semi-quantitative real time PCR studies for mono- and co-cultures (Figure 3.5) in control and fucoidan treated groups were performed. The relative gene expression of molecules associated with bone formation and osteogenic differentiation, factors involved in control of angiogenesis and stem cell recruitment, as well as endothelial markers was analyzed.

In OECs no significant effects in the investigated genes in response to fucoidan treatment could be observed. Nevertheless, in the osteogenic cells a significant impact of fucoidan treatment was observed. This includes a significant downregulation of the molecules angiopoietin-1 (ANGPT-1) and VEGF involved in the modulation of angiogenesis by MSCs [93, 97, 196] via paracrine factors. Similar effects were also observed for the osteosarcoma cell line MG63 although the effect on VEGF was not significant for MG63. In addition, the fucoidan treatment resulted in a significant downregulation of SDF-1 in both MSC and MG63 as factors involved in the recruitment of a series of cell types [197-199]. Angiopoietin-2 (ANGPT-2), a proangiogenic factor, was tentatively downregulated in the co-cultures. In terms of effects of the fucoidan treatment on osteogenic differentiation markers, the results differed in the MSC and the osteosarcoma cell line MG63 showing significant downregulation for alkaline phosphatase (ALP) only in MSCs and significant downregulation of collagen type I in MG63. In co-cultures of MG63 and OEC again SDF-1 and its corresponding receptor CXCR4 levels were reduced in response to fucoidan, as well as collagen type I and angiopoietin-1 whereas in MSC/OEC co-cultures the trend of SDF-1 expression was opposite.

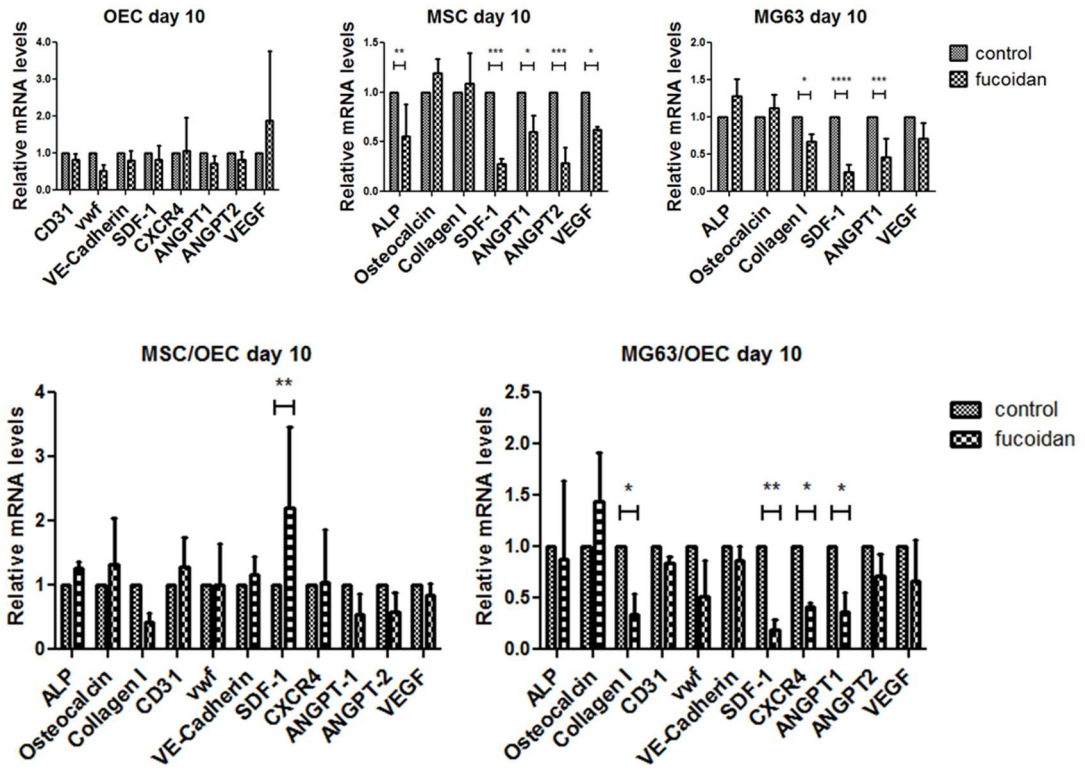

*Figure 3.5 Relative gene expression for osteogenic markers (ALP, osteocalcin, collagen I), growth factors (SDF-1, CXCR4, ANGPT-1, ANGPT-2, VEGF) and endothelial markers (CD31, vwf, VE-Cadherin) evaluated by semi-quantitative RT-PCR for mono-cultures of OEC, MSC and MG63 as well as MSC/OEC and MG63/OEC co-cultures on day 10, 2-way ANOVA. *p < 0.05, **p < 0.01, ***p <0.001 and ****p <0.0001. n = 3.*

3.1.6 Analysis of angiogenesis relevant factors in culture supernatants by Enzyme-Linked Immunosorbent Assay (ELISA)

In accordance with the results from the PCR the quantity of angiogenesis relevant factors including VEGF, ANGPT-1, ANGPT-2 and SDF-1 involved in cell recruitment and osteosarcoma progression in supernatant was measured by ELISA to gain insight on the effects of fucoidan on the protein level.

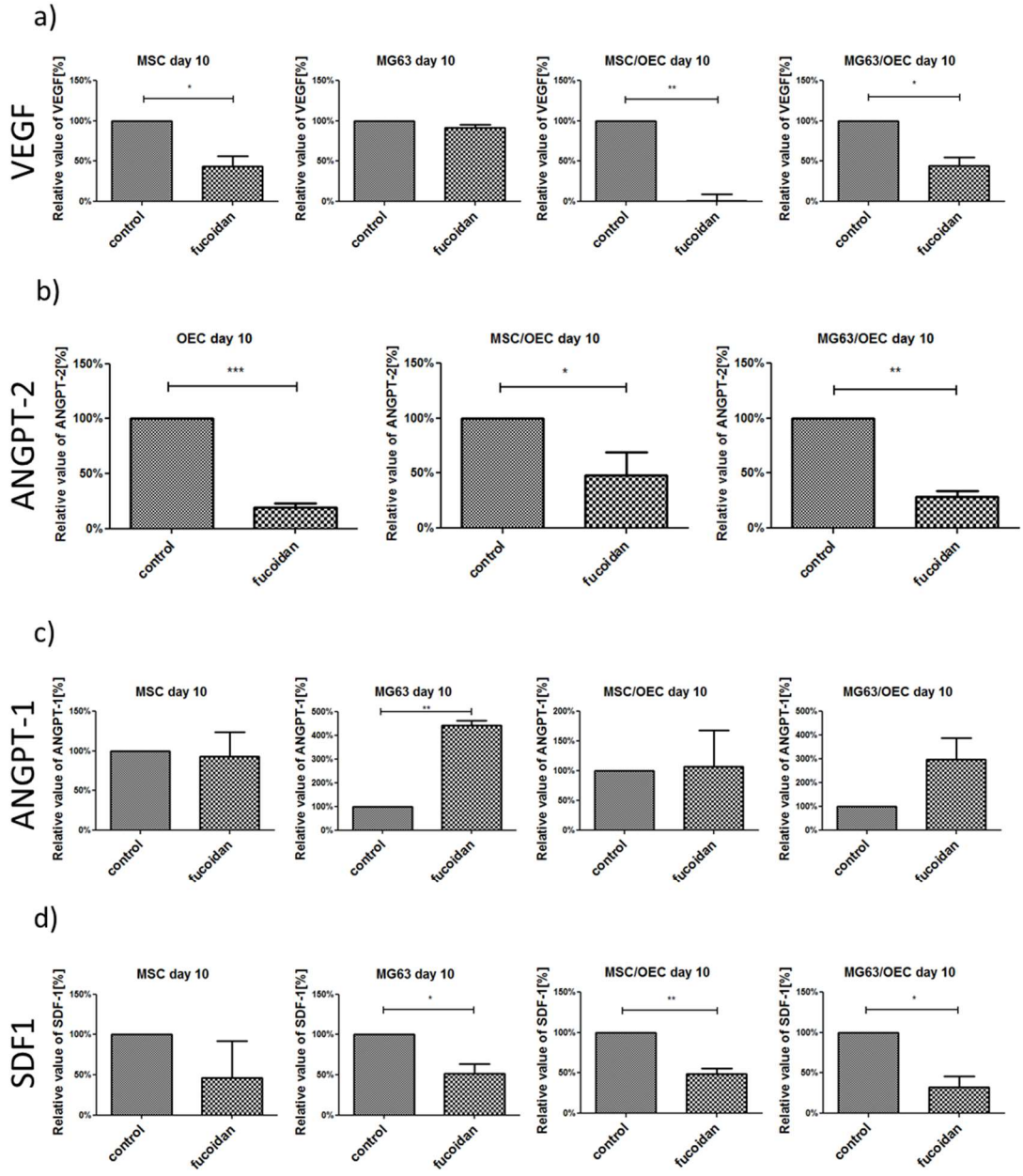

*Figure 3.6 Enzyme-linked immunosorbent assay. For a) VEGF, b) ANGPT-2, c) ANGPT-1 and d) SDF-1 in MSC, MG63 and OEC mono- and co-cultures on day 10. The ELISA data are presented in relative values of M(protein amount/DNA content) in percentage compared to the control group calculated with the formula [Msample/Mcontrol] × 100%, paired t-test. *p < 0.05, **p < 0.01, ***p < 0.001. n = 3.*

The protein levels in the supernatants were normalized to DNA content and are depicted in relative values in % to the controls (100%) in Figure 3.6. Fucoidan treatment resulted in significantly lower VEGF levels in co-cultures of MSC/OEC and MG63/OEC with similar effects observed for MSC mono-cultures (Figure 3.6 a) and tentatively for

MG63 monocultures. In addition Angiopoietin-2 a proangiogenic factor which is mainly produced by endothelial cells themselves [93] was reduced in response to fucoidan treatment in all samples (MSC and MG63: levels not detectable, data not shown). In contrast, Angiopoietin-1, which binds like the Angiopoietin-2 to the Tie-2 receptor and limits the formation of new vascular structures but leads to vascular stabilization, was increased. Finally, SDF-1 mainly associated with the recruitment of stem cells and immune cells in the bone was decreased significantly in response to fucoidan in MG63 monocultures as well as in both types of co-cultures. These reduced protein levels for VEGF, Angiopoietin-2 and SDF-1 in co-cultures in response to fucoidan are the determining factors in the physiological process of angiogenesis and cell recruitment in the co-cultures. These processes are mediated by proteins and corresponding receptor mechanisms guiding the cellular response. Potentially conflicting results on the PCR level are most probably due to compensatory upregulation of genes when the protein levels are low.

3.1.7 Quantitative Analysis of Osteogenesis

The potential effect of fucoidan on the process of bone formation was assessed by the calcification levels as depicted in Figure 3.7 on day 14 for MSC, MG63 mono- and co-cultures. The MSC mono-cultures treated with fucoidan showed a significant reduction of calcification compared to the untreated groups. Similarly, in MSC/OEC co-cultures the calcification of the fucoidan treated group was significantly lower than in the control. For MG63/OEC co-cultures and MG63 mono-cultures, a similar trend but no significant impact was observed which might be due to the tumor cell characteristics of MG63.

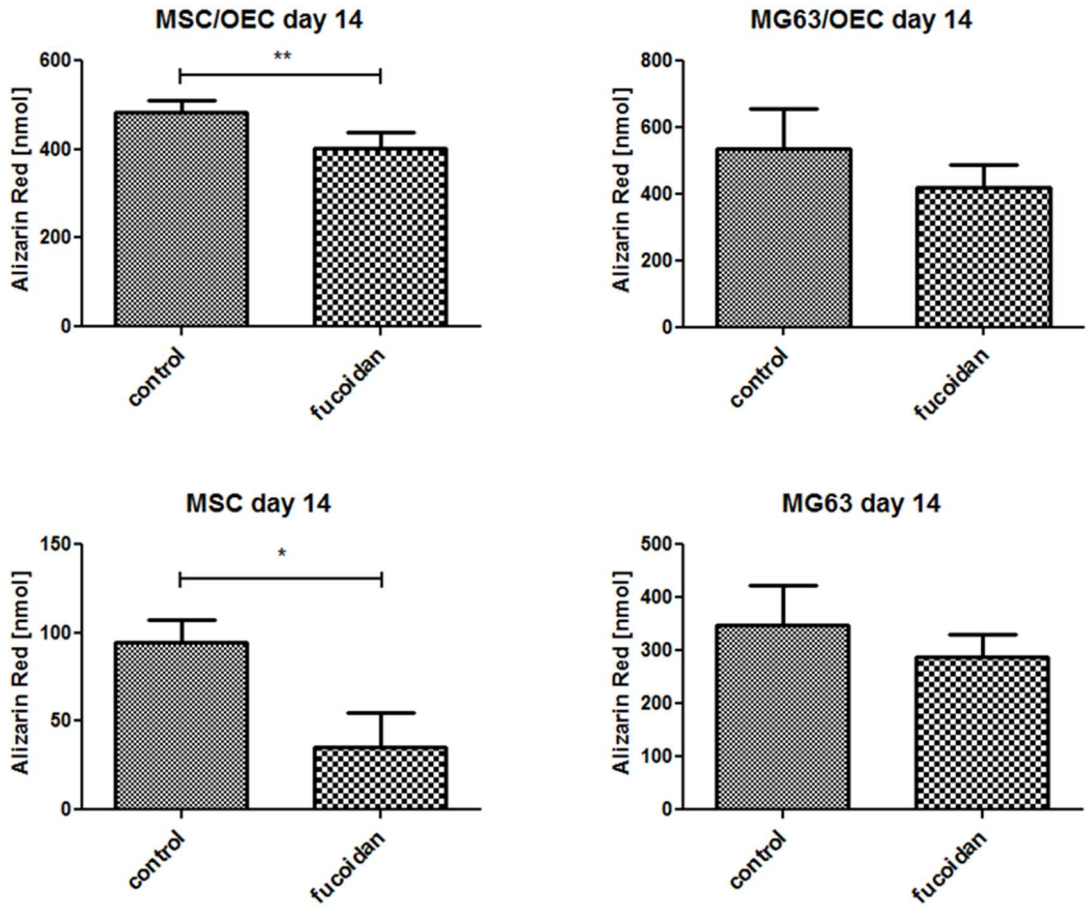

*Figure 3.7 Quantification of Calcification based on Alizarin Red in response to fucoidan for MSC, MG63 mono-cultures and co-cultures at day 14, paired t-test. *p < 0.05, **p < 0.01. n = 3.*

3.1.8 Impact of fucoidan on angiogenesis at an early time point

The effect of fucoidan on angiogenesis in the bone regenerative model was studied at an early time point as well (Figure 3.8).

On day 7, similar to MSC/OEC co-cultures on day 10, most of the OECs which were immunostained against the endothelial marker VE-Cadherin in red aligned in the tube-like pro-angiogenic networks in control, while with fucoidan treatment, OECs still remained as cell monolayers (Figure 3.8 a). In the quantitative analysis of pro-angiogenic networks in Figure 3.8 b, a significant decrease in both length and area of the pro-angiogenic networks in response to fucoidan treatment compared to control was shown, indicating the anti-angiogenic effect of fucoidan in MSC/OEC co-cultures on

day 7.

The DNA content corresponding to the cell growth for MSC/OEC co-cultures on day 7 was characterized by picogreen based reaction. Similar to the result on day 10, the DNA amount of MSC/OEC co-cultures showed a slight decrease after fucoidan treatment.

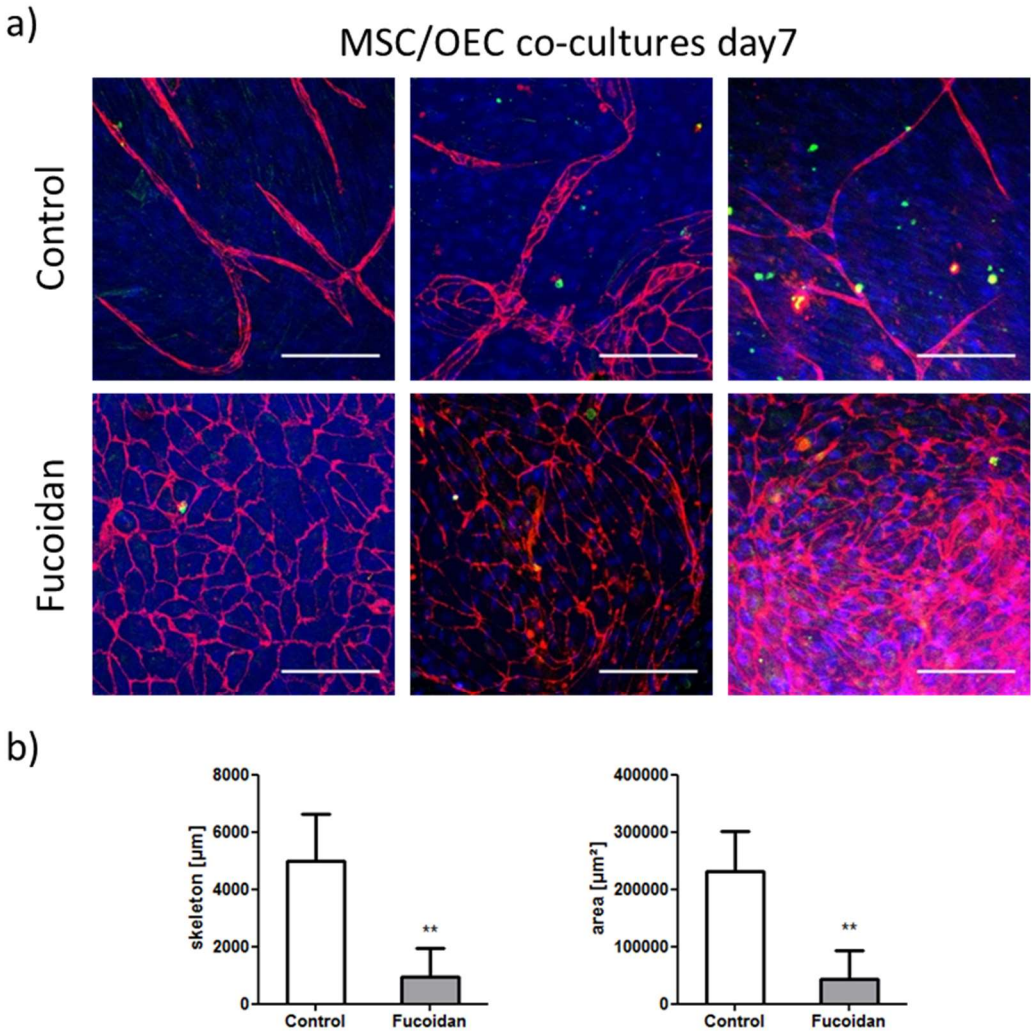

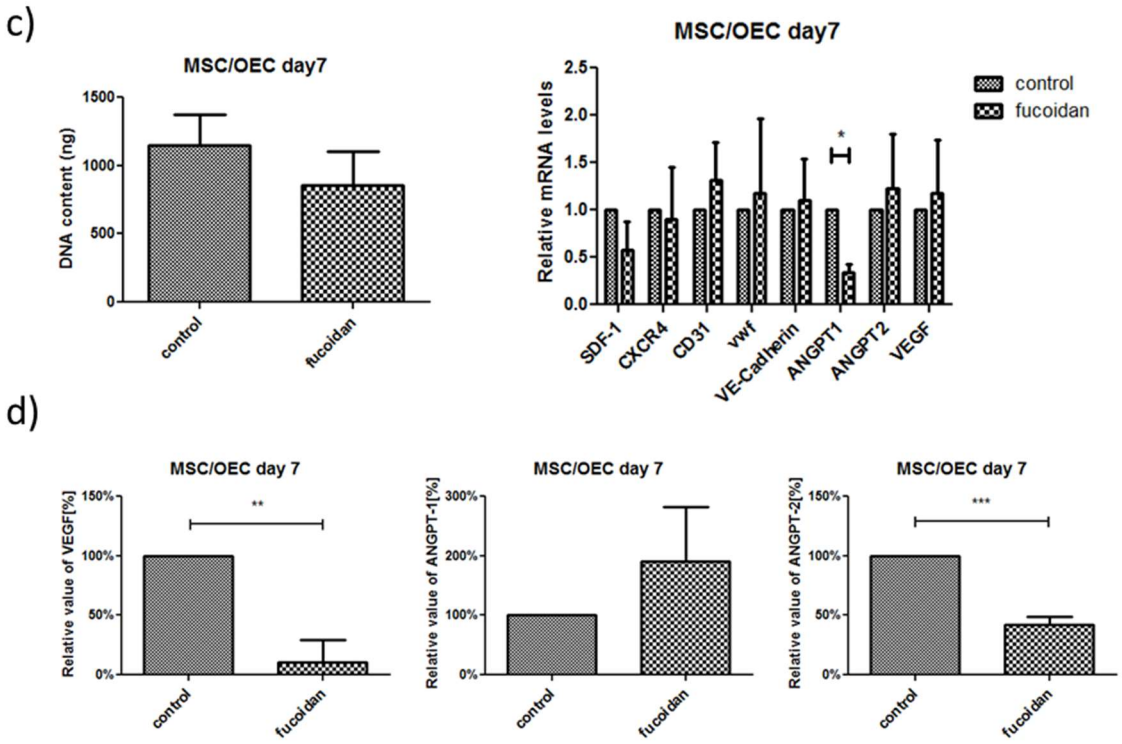

*Figure 3.8 MSC/OEC co-cultures on day 7: a) visualized by confocal laser scanning microscopy (Red: VE-Cadherin, green: CXCR4, blue: Nuclei. The scale bar represents 150 µm.); b) Quantitative analysis of length and area of pro-angiogenic structures; c) DNA content (unpaired t-test) and relative gene expression of angiogenic factors and endothelial markers (2-way ANOVA); d) ELISA for VEGF, ANGPT-1 and ANGPT-2 in the supernatant normalized to the DNA content, paired t-test. *p<0.05, **p<0.01, ***p<0.001. n≥3.*

The relative gene expression level of endothelial markers, factors in angiogenesis and cell recruitment detected by real time PCR was depicted in Figure 3.8 c for MSC/OEC co-cultures on day 7. In response to the fucoidan treatment, the proangiogenic factor angiopoietin-2 was significantly downregulated in the co-cultures.

The protein levels of angiogenic regulating factors in the supernatant of MSC/OEC co-cultures were determined with ELISA and analyzed in the same way as described in 3.1.6 for both control and fucoidan treated conditions on day 7 (Figure 3.8 d). Similar to what was observed in the co-cultures on day 10, with fucoidan treatment, the angiogenic regulator VEGF and angiopoietin-2 levels were both significantly reduced while the angiopoietin-1 level was tentatively increased without significant difference.

In this study, fucoidan significantly reduced angiogenesis in both MSC/OEC and MG63/OEC co-cultures which was associated with a decrease in the level of free angiogenic factors, VEGF and SDF-1 for instance, in the supernatant. The effect of fucoidan in MG63/OEC co-cultures suggested its potential application to impair angiogenesis in bone tumors such as osteosarcoma. Therefore, this fucoidan extract was applied to uveal melanoma cell line/OEC co-cultures to investigate its impact in the ophthalmological tumor models.

3.1.9 Impact of fucoidan on angiogenesis in ophthalmological tumor models

The crude fucoidan extract was applied to the uveal melanoma cell line/OEC co-cultures to study its impact on angiogenesis in ophthalmological tumor models. The primary uveal melanoma cell line 92.1 and metastatic melanoma cell line OMM2.3 were respectively 1:1 co-cultured with OECs at a density of 50000 cells/cm^2 for each cell type in 24-well-plates and treated with 100 µg/mL fucoidan (*f. vesiculosus*) for 7 days. The co-cultures were fixed and immunostained for the endothelial marker CD31 (in green, Figure 3.9 ab) to visualize the tubular structures of OECs. Angiogenesis, the parameters of which include the total coverage of OECs, average tubular area and length, was quantitatively analyzed in comparison to control by Dr. H. Schmidt.

For the 92.1/OEC co-cultures indicated in Figure 3.9 a, the outgrowth endothelial cells aligned in isolated small patches. In contrast, the attachment of OECs was markedly improved by fucoidan treatment, thus the larger patterns of tubular structures, which were hardly seen in control, were observed. The average tubular area and tubular length were both significantly enhanced by fucoidan treatment in this model. Nevertheless, OECs showed totally different morphology and attachment when co-cultured with metastatic cell line OMM2.3 in Figure 3.9 b. The enclosures of the tube-like pro-angiogenic structures were found on the borders of cell patches in control, whereas a few tubular structures appeared along the cell-cell contacts in OEC monolayer for the

fucoidan treated group. The average tubular area and length did not show much difference between control and fucoidan group. It seemed that fucoidan promoted the OEC attachment to the primary melanoma cell line 92.1 resulting in an increase of tubular structures compared to control. In contrast, the tubular structures formed by OECs in the co-cultures with metastatic melanoma cell line OMM2.3 did not display significant difference in response to the fucoidan treatment.

Overall, the treatment of fucoidan did not show a significant efficacy in reducing angiogenesis in the uveal melanoma cell line/OEC co-cultures as it did in MG63/OEC. In addition, there was no significant reduction in the level of VEGF detected following fucoidan treatment (details in *Dithmer et al.* in 8.3) in these models. The variety of the impact of fucoidan in these two ophthalmological tumor models indicated the distinct characteristics of melanoma cell lines at different phases. It seems that the effect of fucoidan was not only associated with the dose of application and molecular structure of the extract, but also the target cell type that OECs were seeded to for the angiogenic activity.

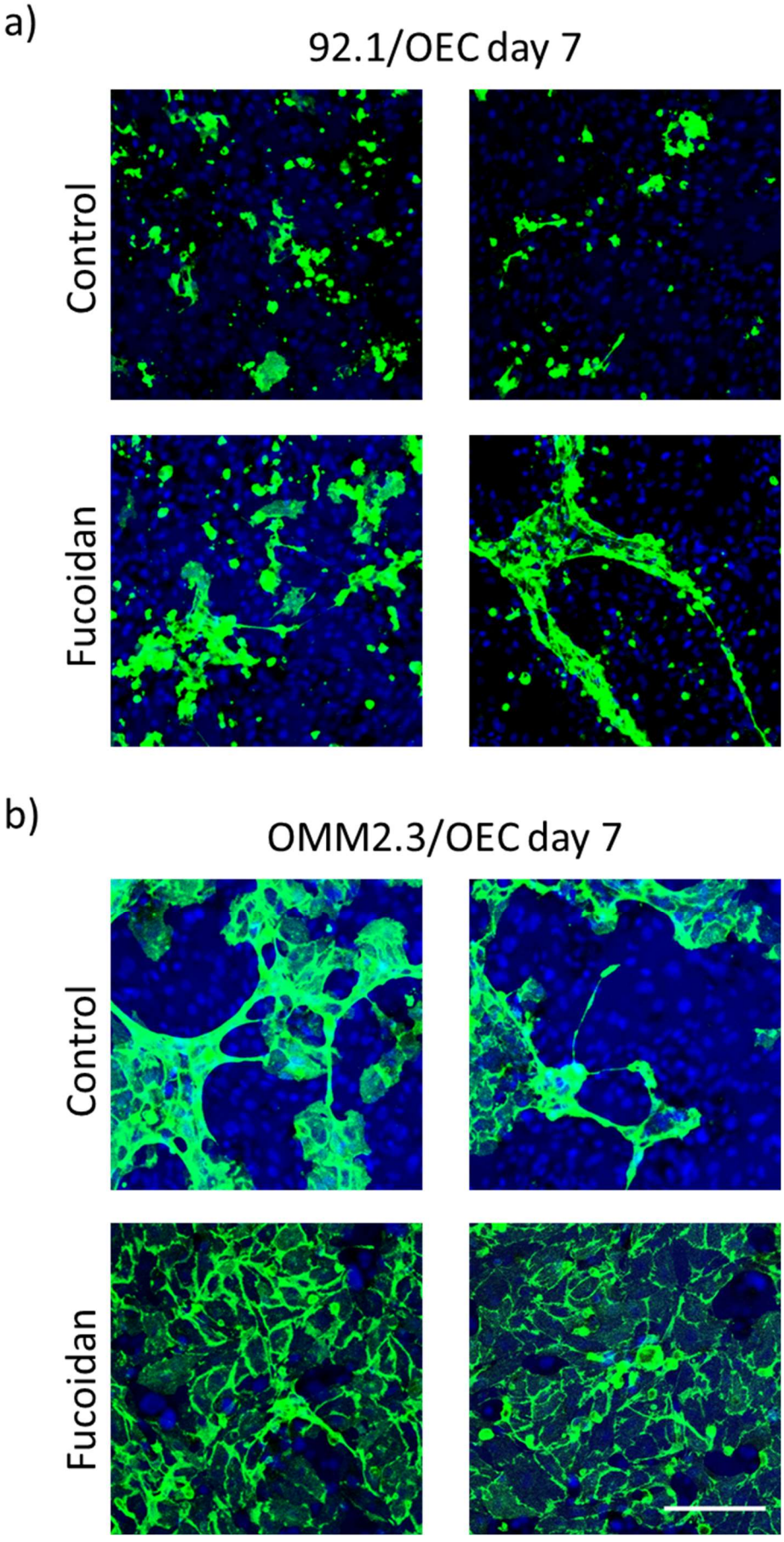
a)
92.1/OEC day 7
Control
Fucoidan
b)
OMM2.3/OEC day 7
Control
Fucoidan

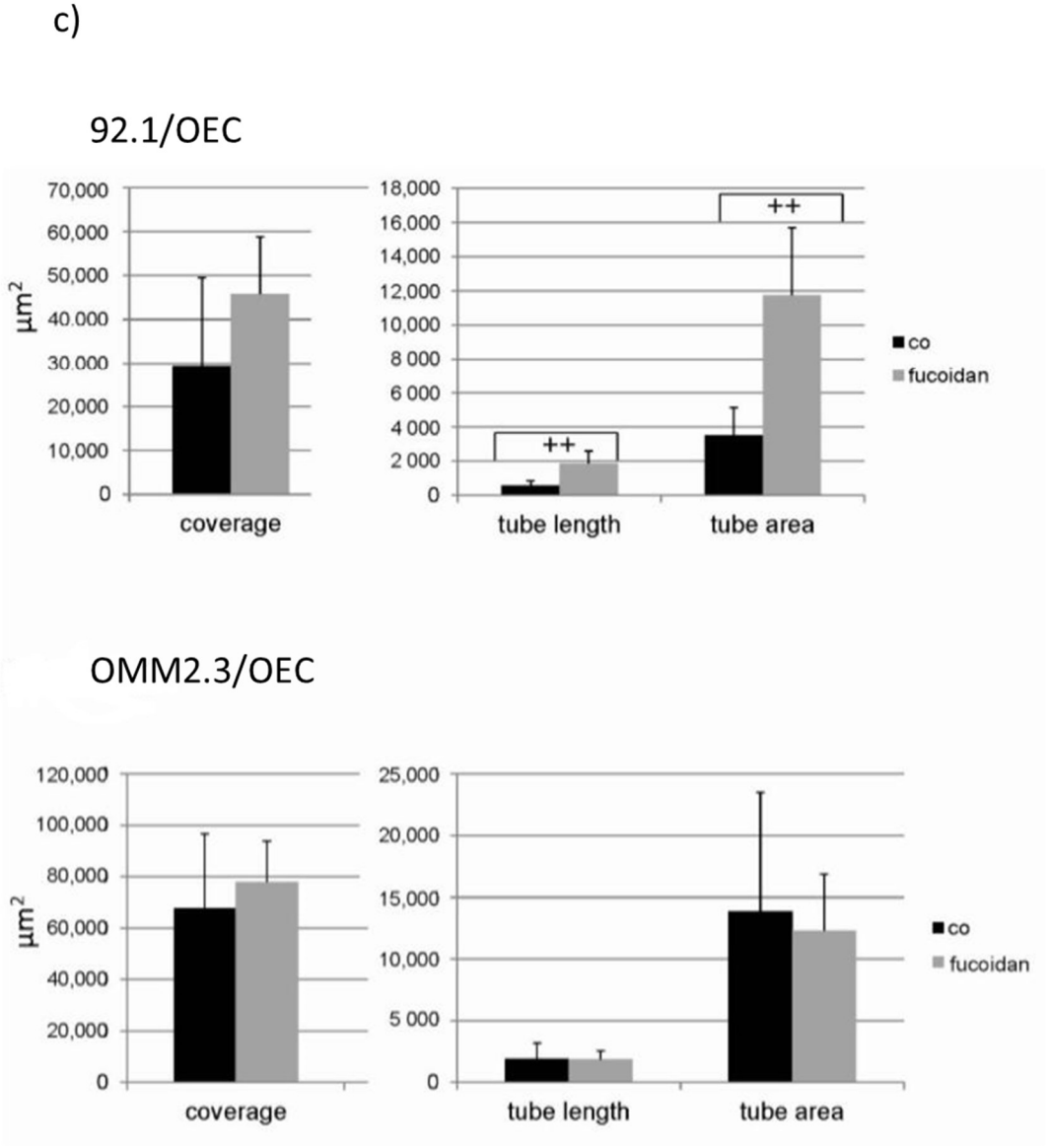

Figure 3.9 The immunostained co-cultures of a) primary melanoma cell line 92.1/OEC and b) metastatic melanoma cell line OMM2.3/OEC visualized by confocal laser scanning microscopy on day 7. Green: endothelial marker CD31 and blue: nuclei staining with Hoechst. The scale bar represents 150 µm. c) Quantitative analysis of coverage of OECs, tubular area and tubular length of pro-angiogenic structures.

3.2 Vitamin D_3 and LPS in a bone regenerative model

The bio-functional molecule Vitamin D_3 (VD_3) which has been well known for its significant roles in bone physiological processes was recently shown the anti-inflammatory effect in infections [200]. To investigate the impact of VD_3 at the cellular and molecular levels on bone regeneration and infection, the MSC/OEC co-culture was stimulated by the endotoxin Lipopolysaccharide (LPS) and the cell activities, pro-inflammatory cytokines and modulators in immune response were examined with or without VD_3 treatment. Cells involved in the experiments are listed in Table 3.2.

Cell type	Age	Gender	Passage
MSC1 (#15-1)	49	f	3
MSC2 (#15-2)	57	f	3
MSC3 (#15-4)	70	f	3
MSC4 (#16-2)	57	f	3
MSC5 (#22)	n/a	n/a	3
OEC1 (BC74)	37	m	10
OEC2 (BC167)	19	m	9
OEC3 (BC67)	36	m	10
OEC4 (BC147)	25	f	9
OEC5 (BC01)	59	f	7

Table 3.2 List of cells and donor information in the experiments. Female (f); male (m). n/a: the donor information was not available.

3.2.1 OEC morphology and angiogenic networks in MSC/OEC co-cultures with Vitamin D_3 and LPS treatment

The MSC/OEC co-cultures were fixed and immunostained with the endothelial marker VE-Cadherin (green), antimicrobial peptides LL-37 (red) and nuclei (blue) on day 7 (as shown in Figure 3.10 a). At this time point, OECs in all groups were found to form the capillary-like pro-angiogenic structures. In control and LPS group, some OEC mono-layers still existed; While in VD_3 treated conditions, OECs tended to aggregate in thin elongated enclosures of loops. However, there was no significant immunostain of LL-37 observed.

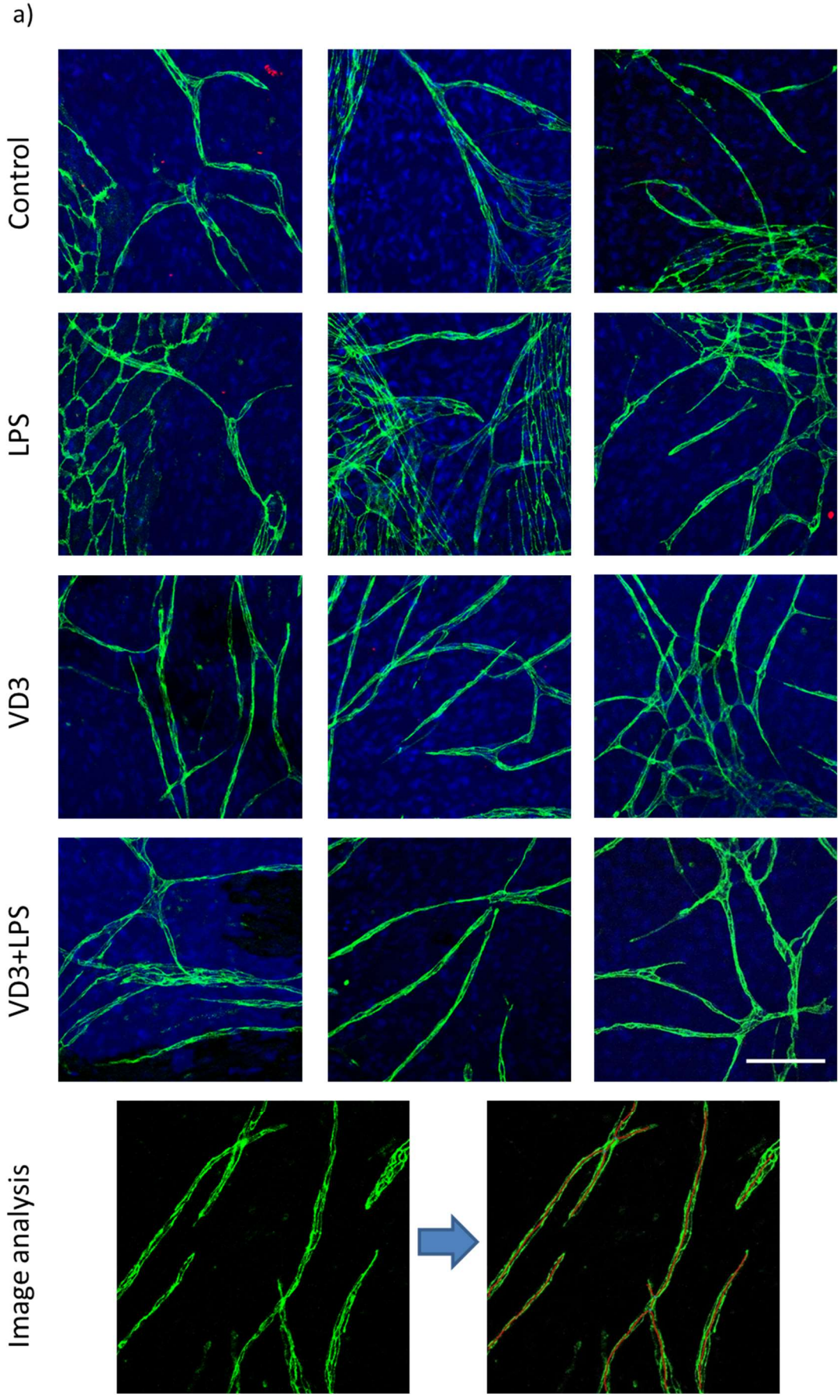
a)
Control
LPS
VD3
VD3+LPS
Image analysis

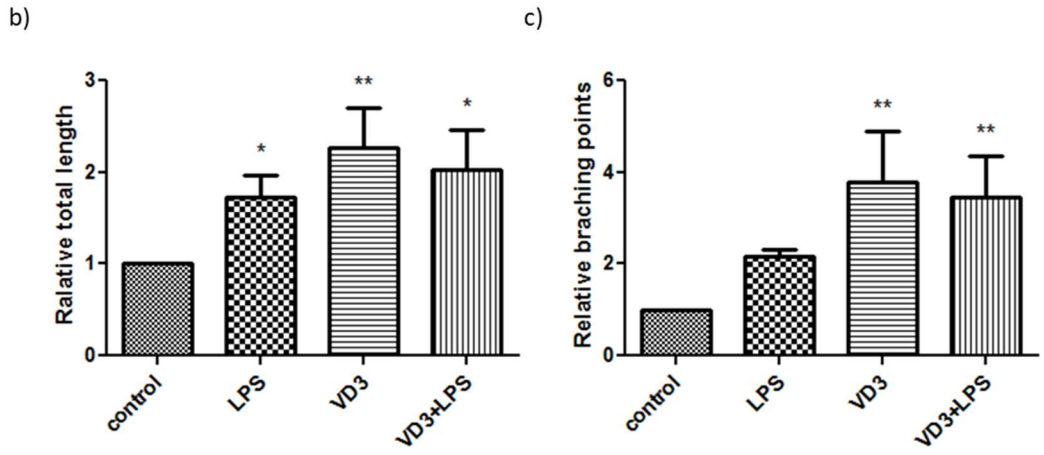

Figure 3.10 a) MSC/OEC co-cultures on day 7 with VD_3 treatment/ LPS stimulation visualized by confocal laser scanning microscopy. VE-Cadherin is depicted in green; LL-37 in red and nuclei are stained with Hoechst in blue. The scale bar represents 150 µm. The relative total length of angiogenic networks and number of branching points (control as 1) were quantified and presented in b) and c). The significant differences were calculated with Graph Pad Prism using 1-way ANOVA with Newman-Keuls Multiple Comparison Test. p < 0.05 and p** < 0.01. n=3.*

The total length of tube-like networks and number of branching points (junctions of the angiogenic networks) were analyzed by AnigoTool to characterize the angiogenic structures in each condition depicting the pro-angiogenic effect of LPS stimulation and VD_3 treatment. As it is shown in figure 3.10 b and c, VD_3 treatment led to a significant increase in length and number of junctions of angiogenic networks; LPS stimulation significantly improved the angiogenesis in terms of total length of the networks and doubled the number of junctions without statistical significance.

3.2.2 Quantitative assessment of gene expression

To further study the cell response to VD_3 treatment and LPS stimulation, the relative gene expression of endothelial markers, molecules associated with bone formation and osteogenic differentiation, regulators in control of angiogenesis, as well as inflammatory molecules and modulators in immune response was determined for MSC/OEC co-cultures (Figure 3.11 a), OEC mono-cultures (b) and MSC mono-cultures (c) by real time PCR at day 7.

LPS significantly enhanced the expression level of endothelial marker CD31 only in co-cultures, whilst the level of vwf showed no distinct change in response to the treatment. Neither VD_3 treatment nor LPS stimulation showed any influence on the expression of the osteogenic markers ALP and collagen type I. In contrast, the expression level of the late osteogenic marker osteocalcin in MSCs was actively improved by VD_3 treatment. The application of LPS resulted in an upregulation of VEGF, the major angiogenic regulator, with significant difference for co-cultures and a significant upregulation of VEGF in MSC mono-cultures in the presence of VD_3. In addition, LPS significantly improved the expression level of angiopoietin-1 (ANGPT-1) in MSC mono-cultures, while ANGPT-2 in OECs showed a tentatively increase in response to LPS without significant difference.

The LPS treatment activated acute inflammatory response in OECs. The expression level of toll-like receptor-4 (TLR4) which recognizes LPS and mediates the production of inflammatory cytokine, IL-6 for instance, was significantly upregulated by LPS in the presence of VD_3 in co-cultures. However, no significant difference was seen in TLR4 expression for OEC mono-cultures. For both OEC mono- and co-cultures, a tremendous upregulation of IL-6, the pro-inflammatory cytokine, was detected in response to LPS stimulation. In addition, adding LPS promoted the expression level of the macrophage lineage markers, of which CD68 was significantly upregulated, CD163 and CD206 were slightly increased in co-cultures. Tartrate-resistant acid phosphatase 5 (TRACP5) expressed by osteoclast for resorbing bones and inflammatory macrophages [201] responded to LPS stimulation showing a significant increase in co-cultures.

The intercellular adhesion molecule (ICAM) and vascular cell adhesion molecule (VCAM) expressed in OECs were demonstrated to regulate the adhesion of monocytes to endothelial cells in inflammatory response [202]. The expression level of ICAM was significantly enhanced by LPS stimulation in both mono- and co-cultures. In contrast, VCAM was significantly upregulated by LPS only in OEC mono-cultures when no VD_3 treatment was applied. In addition, LPS stimulation led to a significant upregulation of

complement 3 (C3), a molecule of the immune system, in OEC mono-cultures.

a)

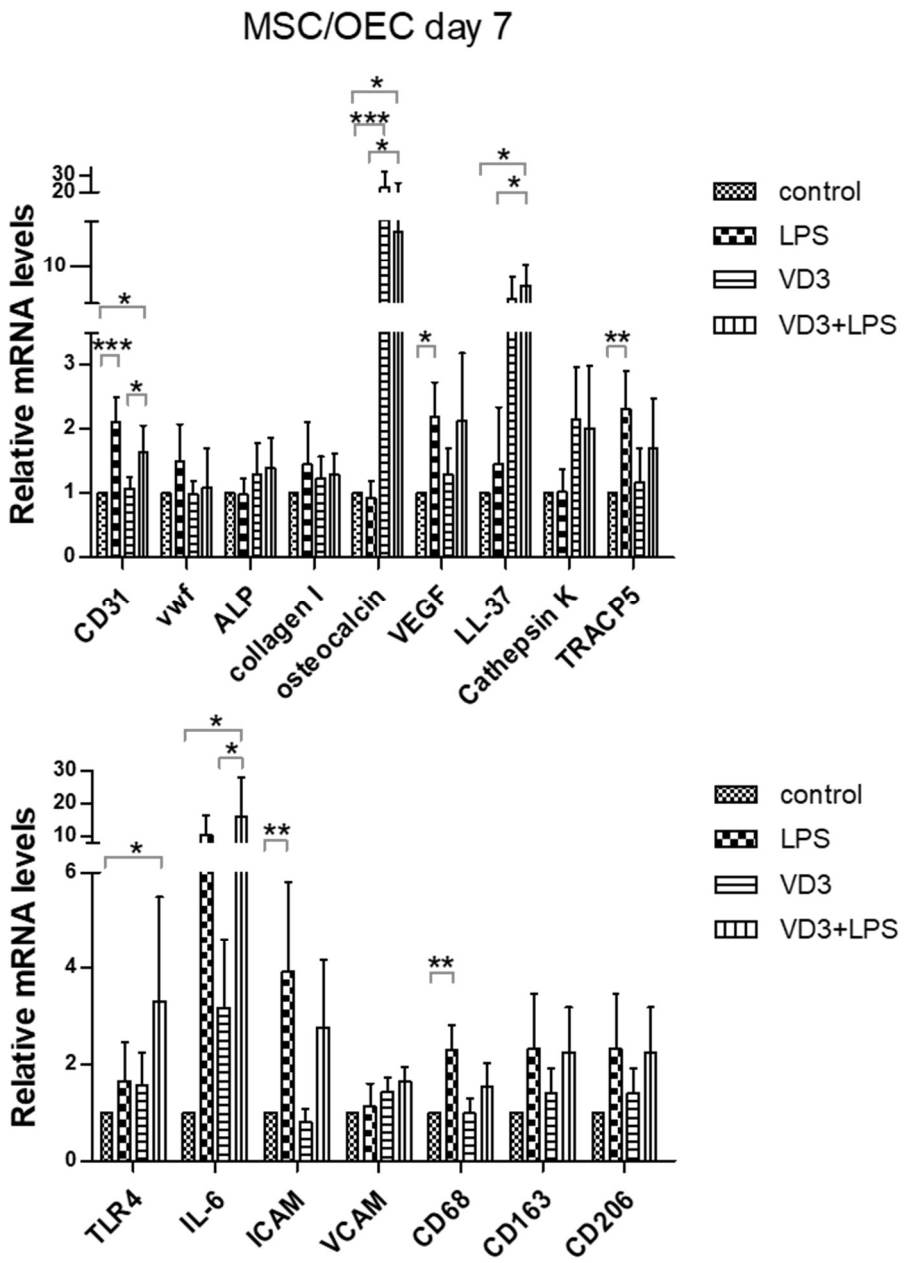

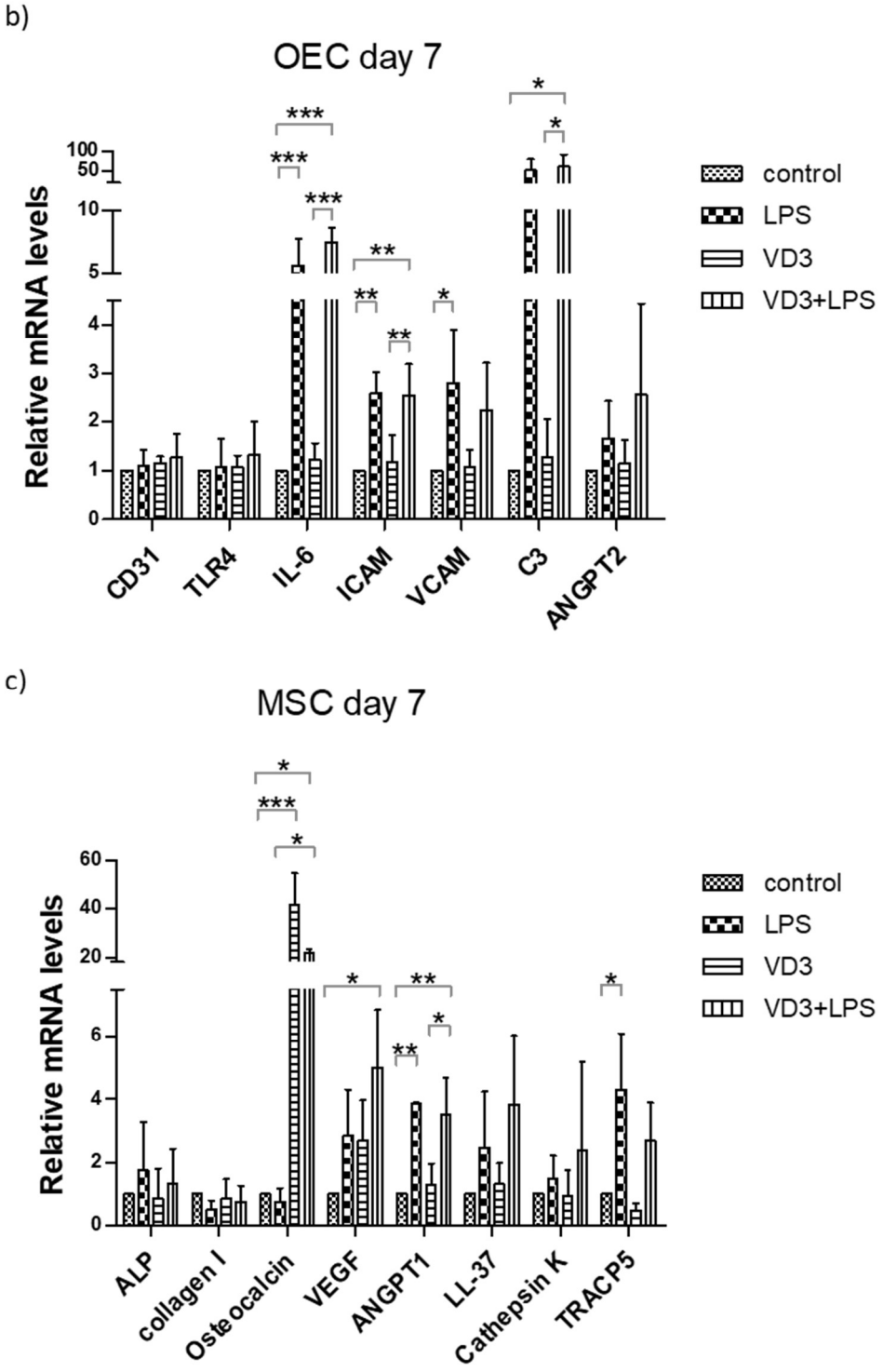

*Figure 3.11 Relative gene expression for endothelial markers (CD31, vwf), osteogenic markers (ALP, collagen I, osteocalcin), angiogenic factors (VEGF, Angiopoietin-1,2), inflammatory relevant molecules (IL-6, CD68, CD163, CD206, VCAM, ICAM, C3) and others (LL-37, Cathepsin K, TRACP5) evaluated by semi-quantitative RT-PCR for a) MSC/OEC co-cultures, b) OEC mono-cultures and c) MSC mono-cultures on day 7. 1-way ANOVA. *p < 0.05, **p < 0.01 and ***p <0.001. n ≥ 3.*

Vitamin D_3 significantly increased the expression level of cathelicidin (LL-37), the anti-microbial peptide, in OEC/MSC co-cultures. However, the upregulation of LL-37 by VD_3 treatment in MSC mono-cultures was not significant. In MSC mono-cultures, VD_3 did not show a significant effect on the expression level of Cathepsin K, the tissue resorbing enzyme activated by immune reaction, but the Cathepsin K level was tentatively improved by VD_3 in co-cultures.

3.2.3 Determination of different proteins by ELISA and Western blot

The pro-inflammatory cytokine interleukin-6 (IL-6), angiogenic regulator VEGF, soluble ICAM-1 and anti-microbial peptide cathelicidin (LL-37) in the presence of VD_3 were quantitatively detected in the culture supernatants by ELISA (Figure 3.12 a b c) and Figure supplement 1 for LL-37) to further examine the effect of VD_3 on inflammatory response at protein level.

In accordance with the result of expression level in OECs from the PCR result, the protein level of IL-6 was highly improved by LPS stimulation. ICAM-1, the immune response molecule mainly expressed in the LPS-activated OECs was also detected a significant increase in the supernatant of both mono- and co-cultures, which was consistent to the result at gene expression level. However, no significant effect of VD_3 treatment was seen on the protein levels for both molecules.

The relative VEGF level in supernatant showed a significant increase in response to Vitamin D_3 treatment for MSC mono-cultures, but no distinct change was found for co-cultures. In contrast, the significant upregulation of VEGF on gene expression level appeared only in response to LPS stimulation for co-cultures and LPS in the presence of VD_3 for MSC mono-cultures. Nevertheless, the angiogenic activity of OECs in co-cultures with MSCs was improved in terms of angiogenic structure parameters to both LPS stimulation and VD_3 treatment.

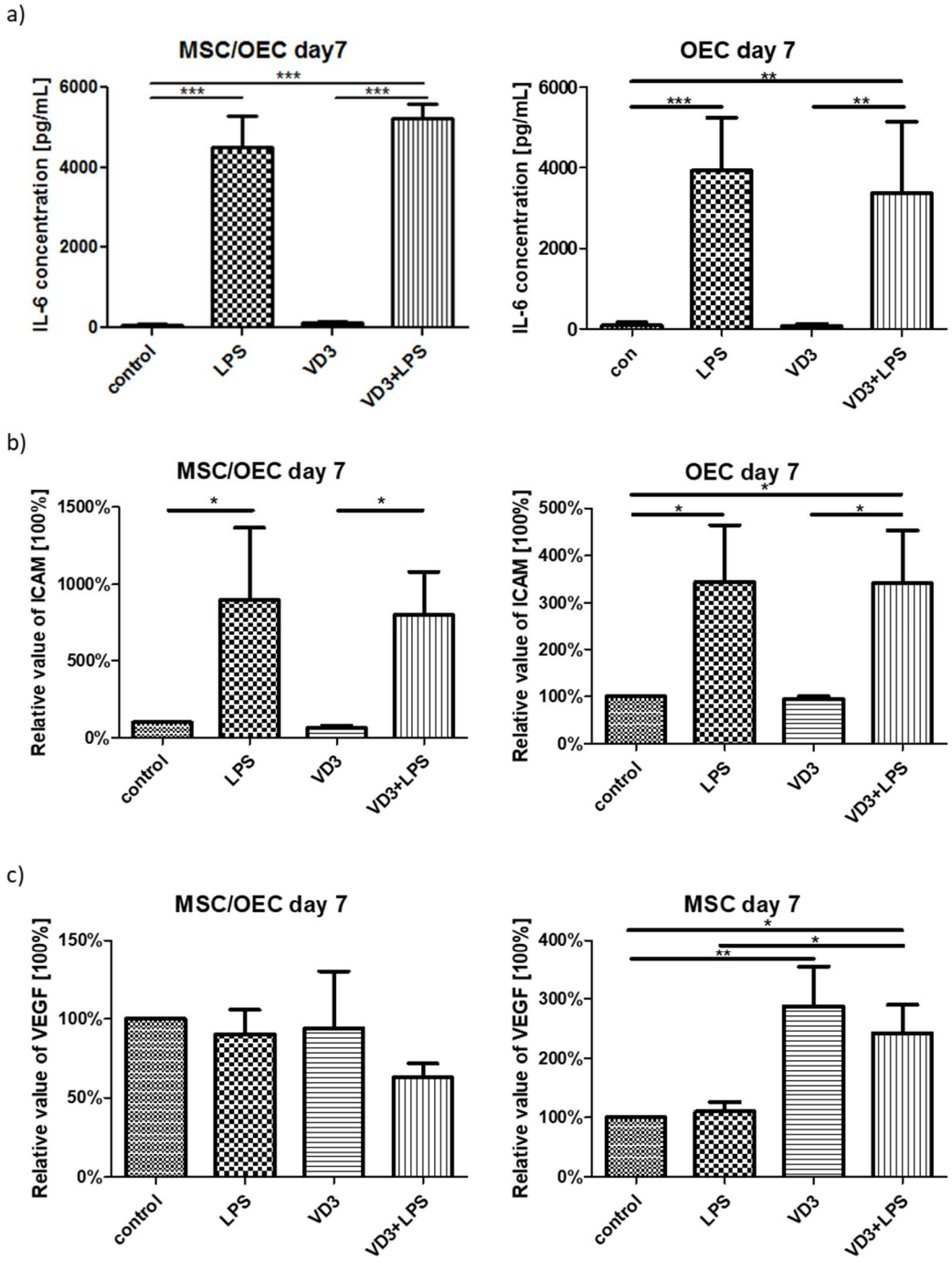

*Figure 3.12 Enzyme-linked immunosorbent assay for a) IL-6, b) ICAM (relative value) and c) VEGF (relative value) in the supernatant of mono-/co-cultures on day 7, paired t-test. *p < 0.05, **p < 0.01 and ***p < 0.001. n ≥ 3.*

The level of cathelicidin (LL-37) peptide in the supernatant of MSC/OEC co-cultures was measured with the Human LL-37 ELISA kit available in the market at present. It seems that the concentration of the samples was much lower than the working

concentration of the kit, which on the other hand explains the difficulty in visualizing immunostained peptides in co-cultures. To gain a further examination of this peptide in MSC mono-cultures, cells and 7-day VD_3 treated cells were respectively lysed for western blot. The LL-37 peptide with molecular weight around 19 kDa was used as positive control and showed a very weak band around 20 kDa; However, the samples showed nothing according to the positive control at the site around 20 kDa when 30 µg of total protein from cell lysis was loaded (result see Figure supplement 2).

3.2.4 Quantitative analysis of osteogenesis by detecting the calcification levels

The calcification levels were characterized on day 14 for the MSC co-/mono-cultures. In MSC/OEC co-cultures, the calcification levels displayed varying degrees of increase in response to Vitamin D_3 treatment. Therefore, overall, statistics presented a tentative increase of calcification without significant difference (Figure 3.13 a). In contrast, the MSC mono-cultures showed the opposite trend of calcification level to VD_3 treatment (Figure 3.13 b).

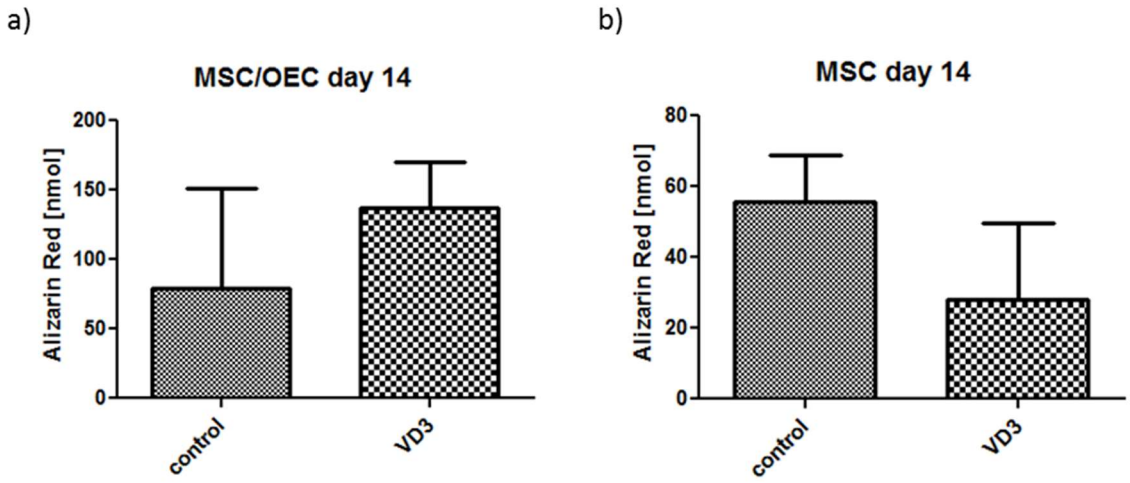

Figure 3.13 Quantification of Calcification based on Alizarin Red staining in response to VD_3 treatment for a) MSC/OEC co-cultures and b) MSC mono-cultures at day 14, paired t-test. n = 3.

In this part, Vitamin D_3 - a bone physiological compound, was investigated for its potential to modulate the inflammatory response induced by LPS in a bone regeneration co-culture model. In MSC/OEC co-cultures, Vitamin D_3 enhanced angiogenesis and tentatively promoted osteogenesis. Although no significant effect of VD_3 was detected on the inflammatory response at the protein level in this model, Vitamin D_3 significantly upregulated the gene expression level of the LL-37 gene, a gene coding for an anti-microbial peptide, in co-cultures indicating a potential beneficial influence of VD_3 in bone infection for further study.

The co-cultures of OEC/MSC and OEC/tumor cell lines provide a practical tool to investigate the functions of bioactive molecules of interest, for instance, fucoidan in bone regeneration and tumor progression, as well as Vitamin D_3 in bone inflammatory response. Nevertheless, the bioactive compounds and cells often need to be loaded to a 3D scaffold, which is compatible to the *in vivo* environment as a delivery system in medical applications. In the next part of this thesis, bio-functionalized hydrogels loaded with OECs and osteogenic differentiated MSCs were studied for their potential in pre-vascularization and their osteogenic properties.

Part II. 3D scaffolds for vascularization and bone regeneration

3.3 Angiogenesis in collagen hydrogels modified with bioactive peptide

Hydrogels, as a type of polymer biomaterial, play an important role in delivery systems for local application of bio-functional compounds and cells. Collagen, a component of ECM, possesses excellent biocompatible and biodegradable properties. Collagen hydrogels are often used as scaffolds to support cell growth and vascularization in tissue engineering. Here, the collagen was processed with IKVAV peptide which promotes OECs attachment and angiogenesis. The modified collagen gels were loaded with outgrowth endothelial cells (OECs) and the angiogenic activities were examined with fluorescent staining, DNA quantification and real time PCR. Information of cells and collagen hydrogels used in this part is listed in Table 3.3.

Cell type	Age	Gender	Passage	Gel (mg/mL)
OEC1 (BC73)	65	f	7	2.12
OEC2 (BC147)	25	f	12	1.84
OEC3 (BC152)	34	f	6	2.12

Table 3.3 Donor information of OECs and gels used in the experiments. Female (f); male (m).

3.3.1 Angiogenic networks of OECs encapsulated in collagen hydrogels and quantitative analysis

Three different groups of collagen hydrogels were prepared in the same concentration to encapsulate OECs. The IKVAV modified collagen was obtained from the lyophilized product of collagen incorporated with IKVAV peptide in the presence of DMSO as described in the method part 2.2.6.1. To assess the side effect of DMSO oxidation on collagen molecules, the modified collagen was produced in the same way without adding peptide. And the collagen without any processing was used as control condition for the experiment.

The OECs encapsulated in collagen hydrogels were pre-labeled with CellTracker (in green) and fixed for nuclei staining (Hoechst, in blue) after 3- and 7-days culture in EGM-2 supplemented with 50 ng/mL VEGF. Samples were visualized under confocal

microscopy affiliated with AIM Meta software.

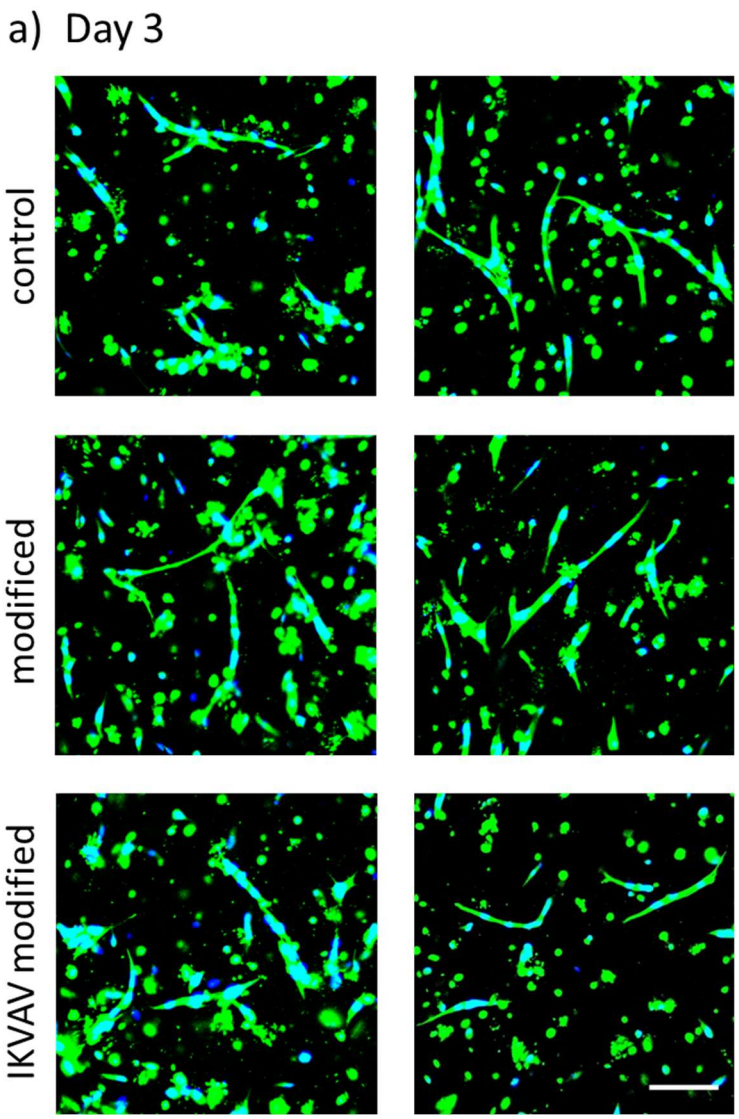

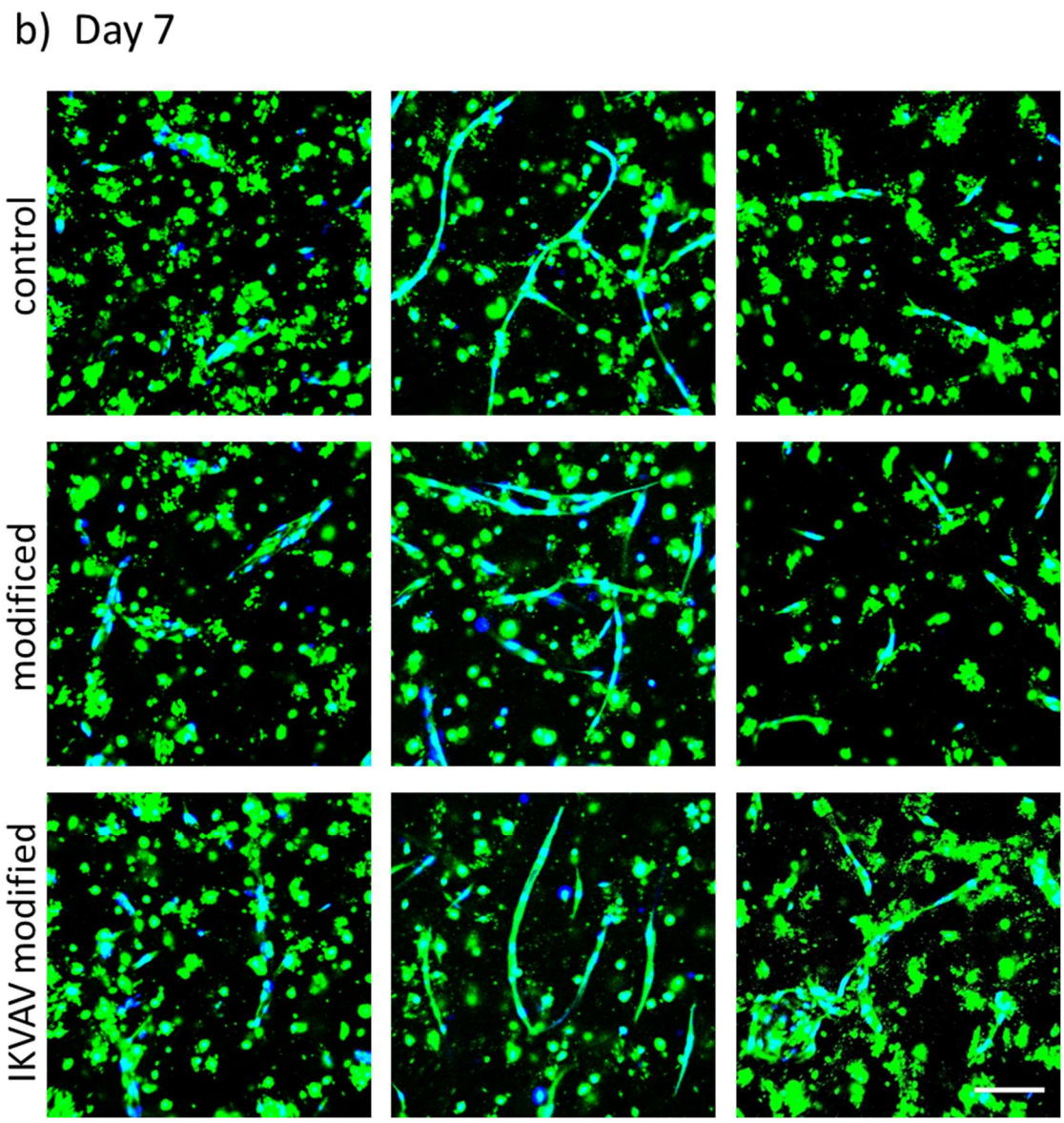

Figure 3.14 OECs prelabeled with CellTracker (green) and stained with Hoechst (blue) in control, modified and IKVAV modified collagen hydrogels on a) day 3 and b) day 7. Scale bars =200 μm.

As it is shown in Figure 3.14, the tube-like pro-angiogenic networks formed by OECs were observed on day 3 and 7. These pro-angiogenic structures appeared within 24 h in collagen hydrogels. The number and area of the structures varied from donor to donor. Unlike co-cultures in cell culture plates where pro-angiogenic networks formed among cell monolayers, the OECs encapsulated in 3D hydrogel stretched and aggregated to build up long and branched capillary like structures in diverse spatial orientations. On day 7, there were more dead cells observed than on day 3 (in Figure 3.14 b).

Accordingly, the DNA content on day 7 showed a 56% (±14.7%), 64% (±10%) and 68% (±10.6%) decrease compared to DNA content of cells on day 3 in average respectively for control, modified and IKVAV condition (shown in Figure 3.16 b).

The angiogenic structures were quantified with ImageJ by selecting contours of the structures with ROI manager and summing up the area of the regions. Results are depicted as relative values to controls in Figure 3.15. No significant effect of collagen modification was detected on pro-angiogenesis of OECs encapsulated in the gels in terms of area of angiogenic networks. Overall, the largest area of the structures appeared in modified collagen hydrogel on day 3 and in IKVAV modified collagen hydrogel on day 7 with no significant statistical difference to other groups.

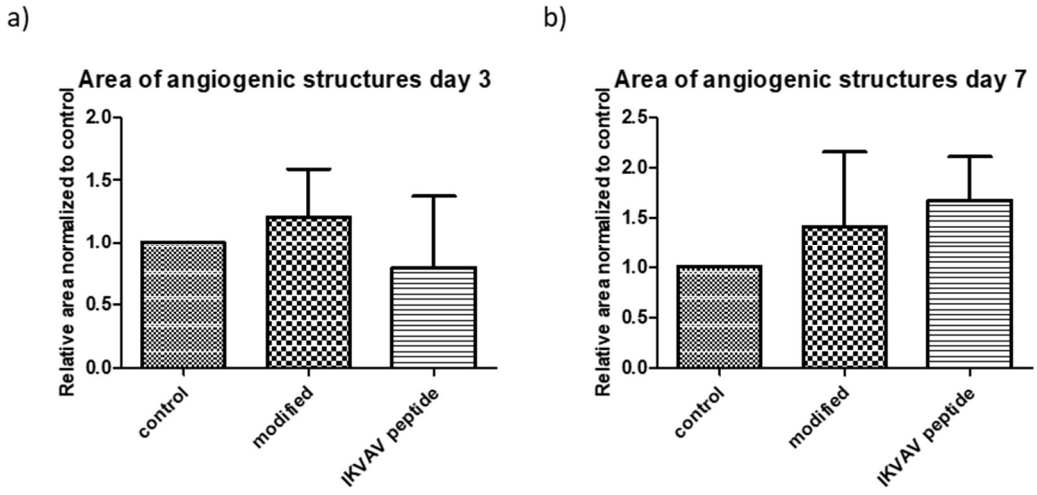

Figure 3.15 Quantitative analysis of angiogenesis structures of OECs on a) day 3 and b) day 7 in different collagen hydrogels normalized to control. $n \geq 2$.

3.3.2 DNA quantification of OECs in collagen hydrogels

To assess the viability and growth of the encapsulated OECs, the cell laden collagen hydrogels were melted at 60°C for DNA quantification. To eliminate the variation due to different donors and gel batches, the results in Figure 3.16 c and d are presented in relation to control in percentage. No significant difference of DNA amount was observed on day 3 and a slight decrease of DNA amount in IKVAV modified group was shown on day 7. When comparing DNA amount between two time points, the result (in

Figure 3.16 a) indicated a decrease of cell number in all three gels from day 3 to day 7 (DNA amount on day 7/DNA amount on day 3＜100%), which corresponds to what had been observed in the fluorescent stained samples.

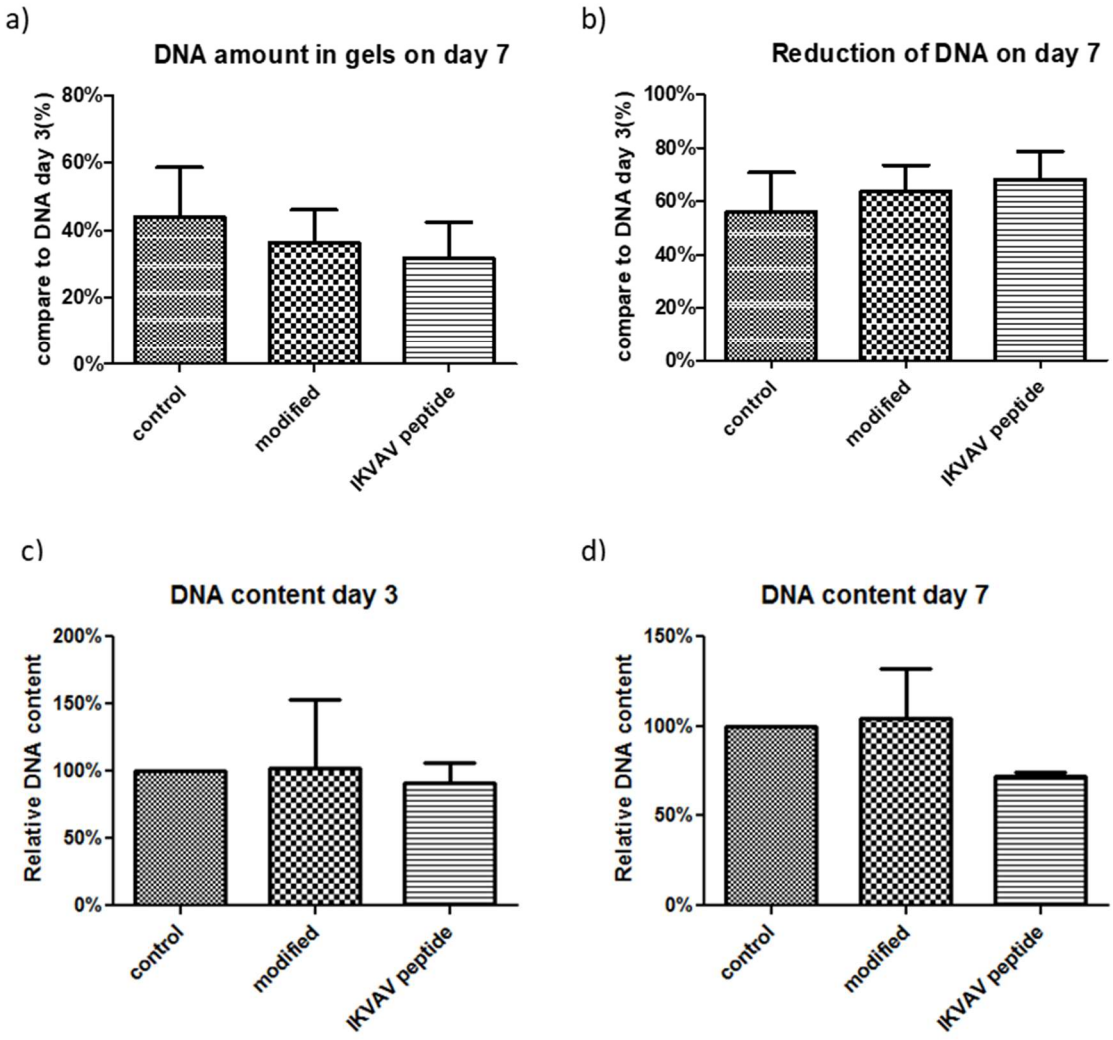

Figure 3.16 a) The DNA amount of cells in each gels on day 7 compared to DNA amount on day 3 in average, and b) the proportion of DNA reduction on day 7 to day 3. And the relative % DNA content of OECs in unmodified (as control), modified and IKVAV modified collagen gels on c) day 3 and d) day 7, 1-way ANOVA. n=3.

3.3.3 Quantitative assessment of gene expression on early time point

The relative gene expression levels of endothelial markers and angiogenesis relevant molecules were determined by real time PCR (Figure 3.17) on day 3. The results indicated a significant downregulation of the endothelial markers CD31, vwf and VE-

Cadherin for OECs in modified and IKVAV modified collagen hydrogels in comparison with the control. Integrin (β1), which is relevant to cell attachment, showed a significant decrease in both modified hydrogels as well.

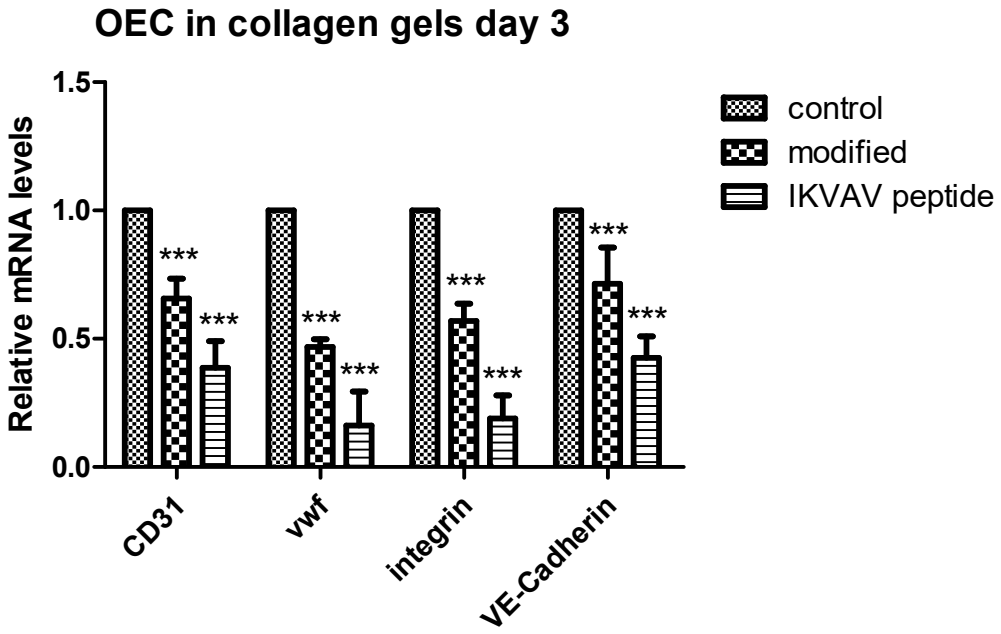

*Figure 3.17 Relative gene expression levels of endothelial markers and angiogenesis relevant molecules evaluated by semi-quantitative RT-PCR for OECs encapsulated in control, modified and IKVAV modified collagen hydrogels on day 3, 2-way ANOVA. ***p <0.001. n = 3.*

In this part, the collagen hydrogels showed excellent properties to serve as scaffolds for angiogenic activities of OECs. The tubular structures formed in the gels developed and sustained for 7 days in the experiment. However, via this modification approach, IKVAV peptide was not found a significant effect on the angiogenic activities of OECs in collagen hydrogel.

3.4 Osteogenic properties of silk fibroin composite hydrogels

Silk fibroin (SF), a type of natural protein derived from cocoon silk has been widely applied in bone tissue engineering for its excellent biocompatible, mechanical and biodegradable properties [203]. In this part, micro silk fibroin fibers (mSF) and mineralized micro silk fibroin fibers (mmSF) were combined in hydrogels to create biocompatible composite scaffolds for potential applications in bone regeneration. Bone marrow derived mesenchymal stem cells were seeded to the composite scaffolds to examine the cell attachment, morphological appearance and osteogenic activities at gene expression level.

Cell type	Age	Gender	Passage
MSC1 (#16-5)	53	f	3
MSC2 (#18-1)	47	m	3
MSC3 (#18-3)	69	m	3
MSC4 (#17-4)	n/a	n/a	3

Table 3.4 List of MSCs and donor information in the experiments. Female (f); male (m). n/a: the donor information was not available.

3.4.1 Cell morphology and attachment of MSCs in collagen-SF composite hydrogels

The mineralized silk fibroin fibers were coated with a complete hydroxyapatite layer on the surface prepared by the method in previous report [204]. Provided by Group Prof. D. A. Ossipov (Uppsala Uni.), the fibers (of 200-300 μm length) were homogeneously dispersed in 2 mg/mL collagen pre-gelation solutions and physically entrapped in the cured gels laden with cells. After 14 days culture, MSCs in the composite constructs were fixed and fluorescent stained against F-Actins and nuclei with Phalloidin-TRITC and Hoechst for visualization with fluorescent and confocal microscopy (figure 3.18 a and b). The gene expression levels of osteogenic markers were examined with rt-PCR (figure 3.18 c).

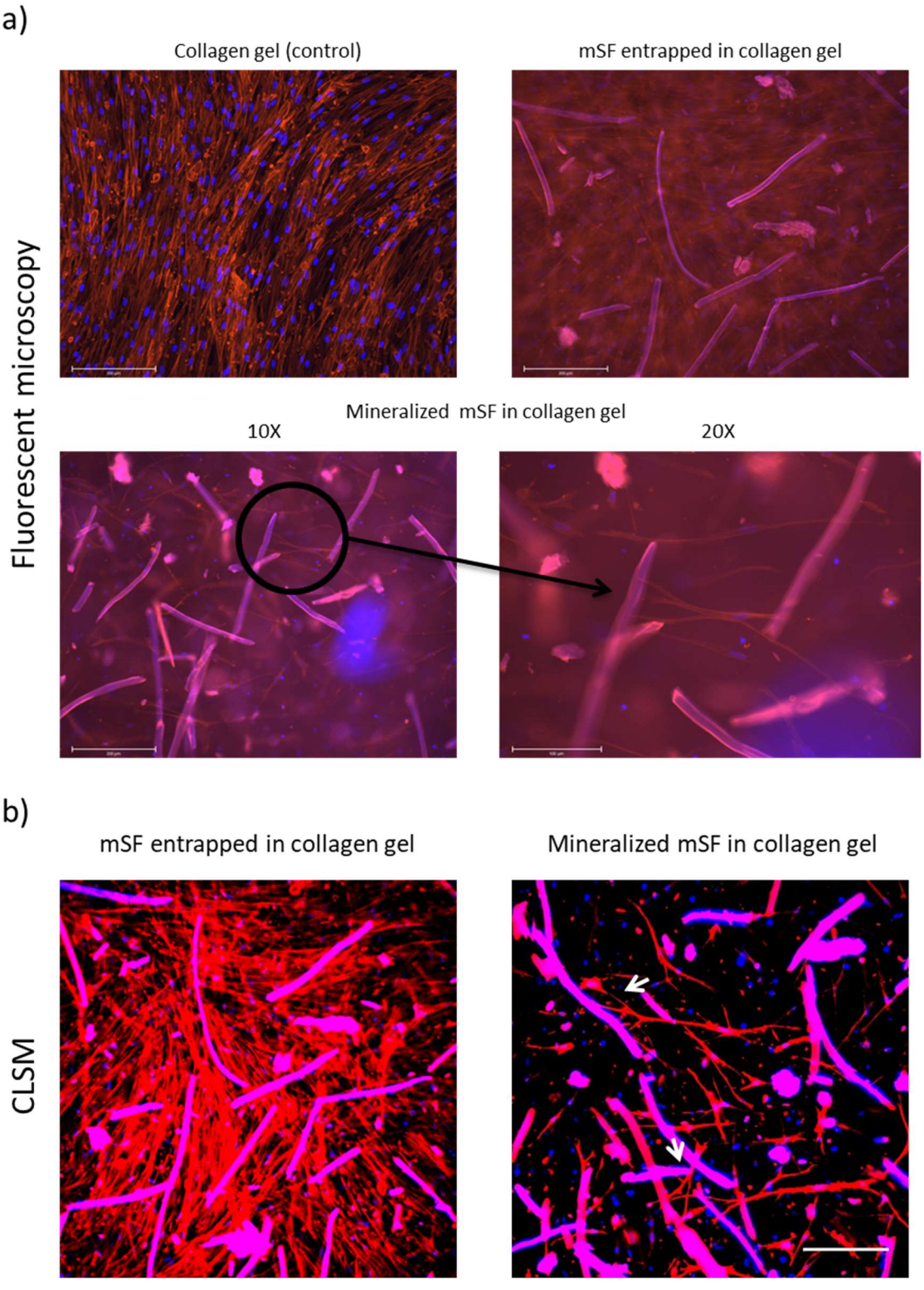
a)
Collagen gel (control)
mSF entrapped in collagen gel
Fluorescent microscopy
Mineralized mSF in collagen gel
10X
20X
b)
mSF entrapped in collagen gel
Mineralized mSF in collagen gel
CLSM

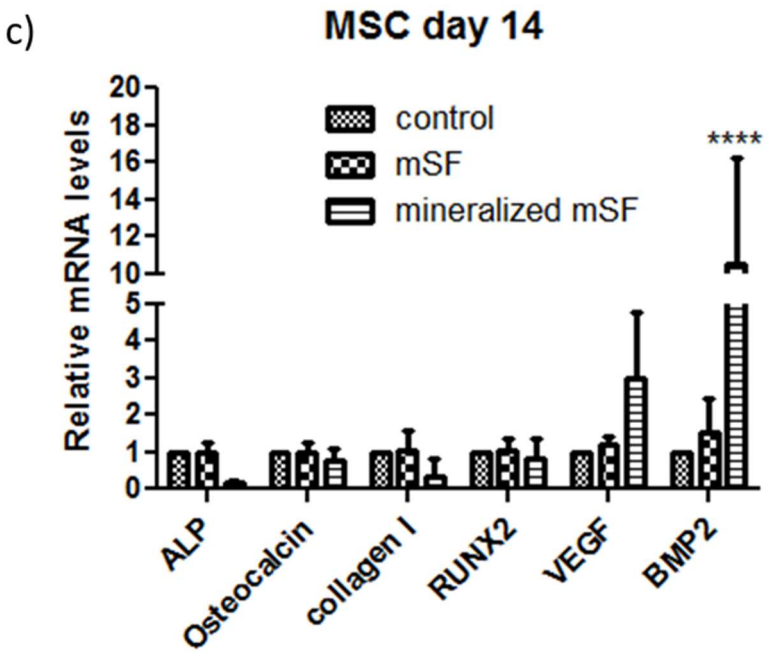

*Figure 3.18 MSCs were fluorescent stained with phalloidin-TRITC (red) and Hoechst (blue) on day 14. a) Cells were visualized with fluorescent microscope (EVOS) and b) confocal laser scanning microscope; the scale bar in a) 20×=100 µm, others=200 µm). c) Relative gene expression of hMSCs in collagen-SF gels for osteogenic markers (ALP, Osteocalcin, collagen I, RUNX2 and BMP-2) and growth factor VEGF on day 14, 2-way ANOVA. ****p<0.0001. n=3.*

The auto-fluorescence of silk fibers under both microscopes assists to locate the fibers in the gels. In comparison to the cells which orientated along the fibers in mSF-collagen gel, MSCs in mmSF-collagen scaffold reached to the biomineralized layer of mmSF with their protrusions (arrows in figure 3.18 a b). The PCR results indicated the gene expression level of several osteogenic differentiation markers, ALP (alkaline phosphatase), Col I (collagen type I), osteocalcin, RUNX2 (Runt-related transcription factor 2) and BMP-2 (bone morphogenetic factor-2) for the MSCs seeded in the silk fibroin composite collagen hydrogels in comparison to MSCs in collagen gels as control. The expression of osteogenic differentiate marker BMP-2 was significantly upregulated in mmSF-collagen gel. In contrast, the early osteogenic marker ALP, and collagen type I levels were tentatively decreased in this gel. VEGF, the angiogenic regulator was observed a slight increase in mmSF-collagen gel than other gels without significant

difference.

3.4.2 Cell morphology and attachment of MSCs on hyaluronic acid hydrogel-based SF composite scaffolds

The silk fibroin composite scaffolds based on hyaluronic acid hydrogel were prepared by Liyang Shi (in Group Prof. D. A. Ossipov, Division of Polymer Chemistry, Uppsala University). The mineralized micro silk fibroin fibers (mmSF or CaP@mSF) were chemically immobilized in the modified hyaluronic acid (HA) gel via the binding affinity of bisphosphonate (BP) on hyaluronan polymer to calcium ion on the surface of mmSF. In control group, micro silk fibroin fibers (mSF) without hydroxyapatite layer were physically entrapped in the same gel without chemical coordination. Both gels were thereafter stabilized through the photocrosslinking between acrylamide (Am) groups on the HA molecules to construct Am-HA-BP•CaP@mSF and Am-HA-BP•mSF scaffolds with better mechanical properties. The osteogenic differentiated MSCs were seeded on both Am-HA-BP•CaP@mSF and Am-HA-BP•mSF and visualized on day 14 with Calcein AM live cell staining and phalloidin-TRITC after fixation under confocal microscopy (Figure 3.19 a b).

Under fluorescent microscopy, the silk fibers were found intensive light reflection property which aids to locate the fibers especially in the blue channel. Cells aligned and orientated along the fibers (arrows) which indicated the favored attachment of MSCs on the fibers. The confluence of MSCs on Am-HA-BP•mSF seemed higher than the other group where cells formed more colonies with the CaP@mSF as the cores.

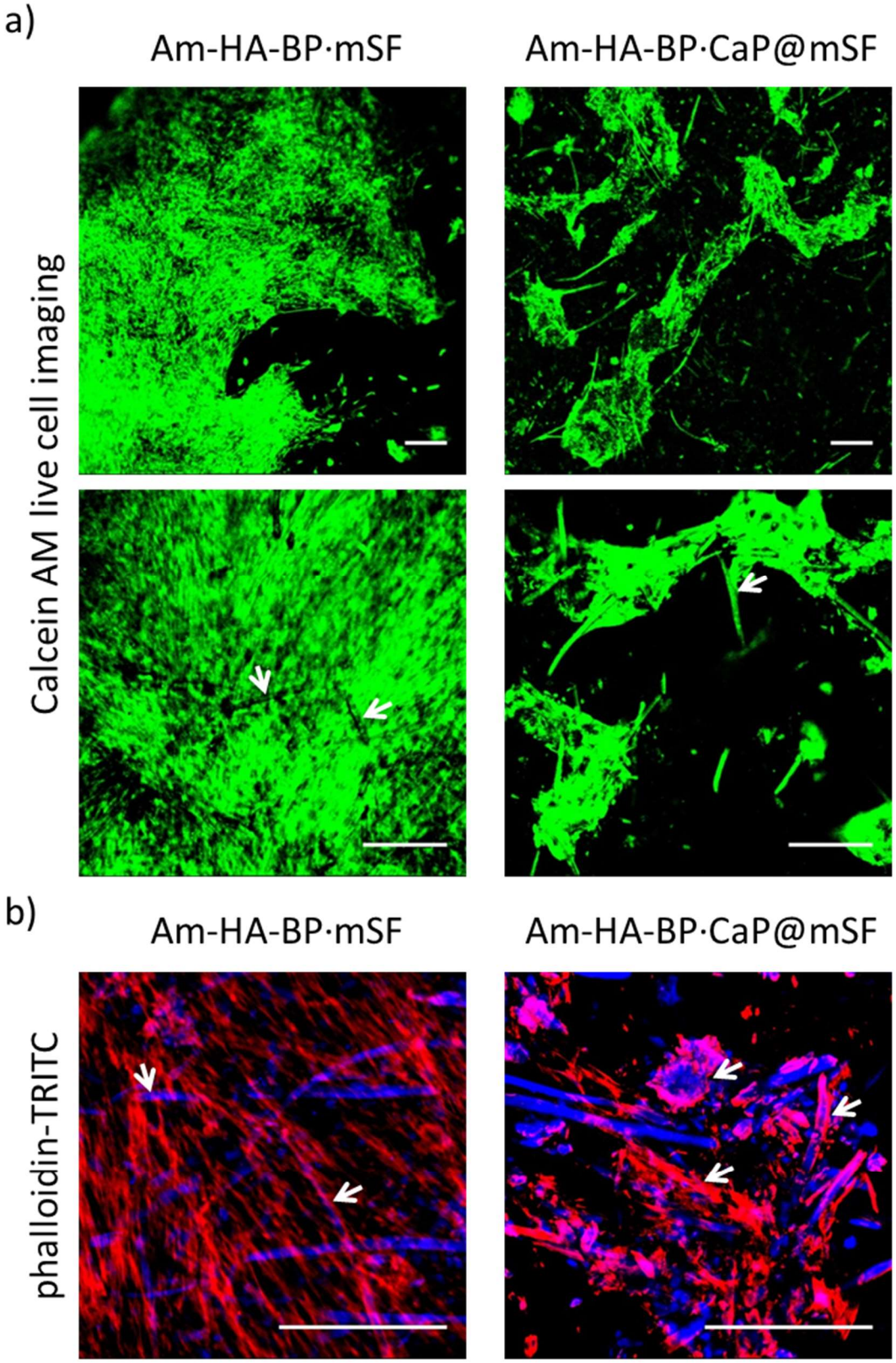
a)
Am-HA-BP·mSF
Am-HA-BP·CaP@mSF
Calcein AM live cell imaging
b)
Am-HA-BP·mSF
Am-HA-BP·CaP@mSF
phalloidin-TRITC

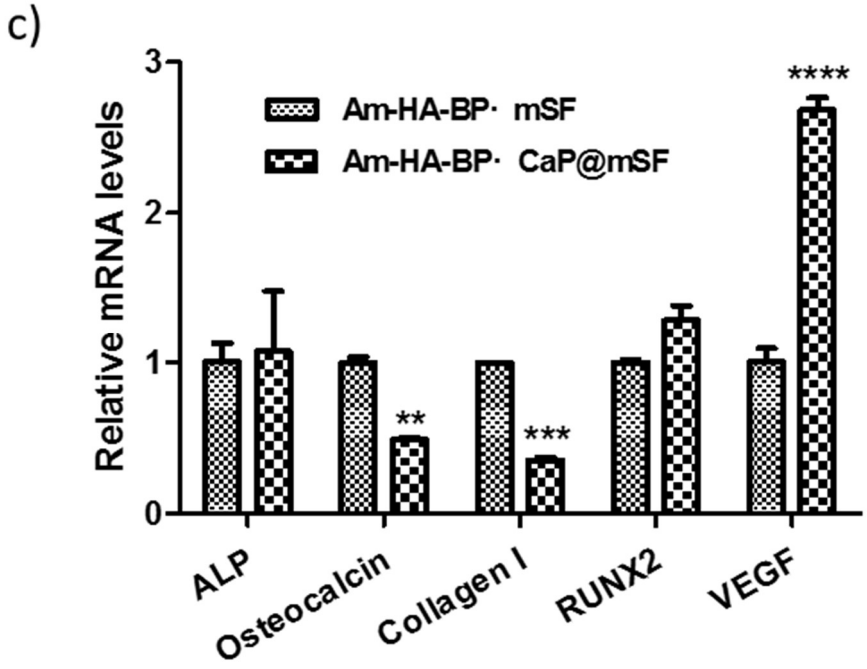

*Figure 3.19 a) Calcein AM staining of living cells (green) on day 14; b) Fluorescent stained cells with phalloidin-TRITC (red) and Hoechst (blue) on day 14. Cells were visualized with confocal laser scanning microscope and the scale bars represent 200 µm. c) Relative gene expression of hMSCs on hydrogels for osteogenic markers (ALP, Osteocalcin, collagen I and RUNX2) and growth factor VEGF on day 14, 2-way ANOVA. **p<0.01, ***p<0.001, ****p<0.0001. n=3.*

3.4.3 Gene expression of osteogenic markers of MSCs on HA based composite scaffolds

The gene expression level of multiple osteogenic differentiation markers was evaluated by real time PCR. Initial results indicated expression of ALP, collagen type I, osteocalcin, RUNX2, and VEGF in MSCs on both Am-HA-BP•CaP@mSF and Am-HA-BP•mSF hydrogels at different levels (Figure 3.19 c). The result showed a significant lower expression of osteocalcin and Col I on Am-HA-BP•CaP@mSF compared to Am-HA-BP•mSF hydrogel. ALP and the osteogenic differentiation related transcription factor RUNX2 [205] in contrast showed no significant difference in the tested samples. However, a significant increase was observed in the expression of VEGF which is tightly associated with the vascularization process during bone repair and in the context of silk fibroin based materials [7, 23, 90].

4. Discussion

In this thesis, bioactive molecules and hydrogels incorporated with bio-functional components were closely studied in the context of bone tissue engineering and regenerative medicine. First, fucoidan - a marine origin bioactive compound, was investigated for its effect on angiogenic and osteogenic activities in mono- and co-culture models relevant for bone repair and osteosarcoma. Next, the potential influence of the physiological molecule vitamin D_3 in inflammatory response in a bone regenerative co-culture model was examined. Moreover, functionalized collagen hydrogel and a novel hyaluronic acid based composite biomaterial were assessed for angiogenesis and bone tissue engineering respectively.

4.1 Study of fucoidan in bone and melanoma models

The crude fucoidan extract which was assessed in this part was obtained from brown algae *fucus vesiculosus*. As a potential candidate compound to be applied in clinical and pharmaceutical treatment, fucoidan was evaluated for cytotoxicity and endotoxicity. Endotoxins, also defined as pyrogens, are the residues of bacteria membrane which can lead to acute immune response and inflammatory reactions. OECs are highly sensitive to endotoxins and show a distinct immune response. The level of endotoxin in 100 µg/mL fucoidan solution was detected to be 0.06 EU/mL with LAL assay and 0.003 EU/mL by the EndoLISA® kit which excludes the interference of matrix substances in the crude extract. This result is acceptable as endotoxin free in terms of safety standards.

To study the cytotoxicity of fucoidan, MTS test on MSCs, MG63 and OECs was performed with a series of concentrations ranging from 50 to 500 µg/mL. The results indicated a tolerance curve of fucoidan treatment associated with cell type. MG63 showed the highest tolerance of fucoidan as indicated before and OECs are the most sensitive cell type among the cells which were assessed here. Hence, fucoidan was applied at a concentration of 100 µg/mL to characterize its bioactive functions, which did not show toxic side effects on the viability of the relevant cell types.

The DNA quantification for mono-/co-cultures of MSCs, MG63 and OECs was carried out to examine the impact of fucoidan on cell growth. The results indicated that fucoidan suppressed the growth of MSC mono- and co-cultures whereas on MG63, no significant effect was observed. In contrast, fucoidan significantly promoted the proliferation of OEC mono-cultures. A recent study demonstrated a similar effect of fucoidan on proliferation of OECs, in which fucoidan was found to improve the survival, proliferation and endothelial differentiation of senescent OECs [206].

In accordance with the literature fucoidan is discussed to modulate the angiogenic process being either applied to enhance angiogenesis for applications in tissue engineering or to restrict the angiogenic process in tumors [207, 208]. This pro- or anti-angiogenic effect of fucoidan is dependent on a variety of factors, such as the structural composition and molecular weight [209]. In addition, the effect of fucoidan depends on what manner the extract is delivered and introduced to the application system. In this study, the impact of free fucoidan was assessed on the cellular and molecular processes in angiogenesis and osteogenesis taking into account the effects of fucoidan on the individual key cell types and their interaction in co-cultures mediated by growth factors and chemokines.

The pro-angiogenic structures appeared in MSC/OEC co-cultures at an earlier time point, on day 7 whereas in MG63 co-cultures, tube-like structures were hardly found at this time point. However, the pro-angiogenic structures had been completely developed by day 10 in controls for both co-culture models. Fucoidan was observed to significantly reduce the angiogenic structures in both MSC/OEC and MG63/OEC co-cultures without cellular toxicity. Correspondingly, the quantitative analysis of the angiogenic structures in terms of length and area showed a significant decrease in fucoidan treated groups relative to controls. The reduced level of angiogenic structures found in the fucoidan treated co-cultures might be attributed to its effect on the angiogenic markers secreted by different cell types.

There was a tremendous decrease in the level of free VEGF detected in the supernatant

of the fucoidan treated co-cultures. In addition to VEGF, SDF-1 protein concentrations, as well as its receptor CXCR4 on relative gene expression level, were significantly lowered in response to fucoidan specifically for MG63/OEC co-cultures. In a recent study, MSCs have been shown as the main producer of SDF-1 [210] in the same co-cultures, whereas OECs show an expression of the corresponding receptor CXCR4. Thus, fucoidan has the potential to modulate this pathway of cellular crosstalk in normal bone physiology. In the context of osteosarcoma, several studies have reported that VEGF and SDF-1 are associated with poor prognosis in osteosarcoma [211-213], thus resulting in approaches to counteract this growth factor and chemokine as a therapeutic option for osteosarcoma treatment [214].

Besides VEGF and SDF-1, elevated Angpt-2 levels produced by tumor vessels are also considered as a critical factor in the tumor microenvironment. As an antagonist of Tie-2 receptor, Angpt-2 plays a role in angiogenesis to simulate the migration of endothelial cells and the formation of tube-like structures. It competitively impairs the binding of Angpt-1, which contributes to vessel stabilization and restricts new vessel formation, to the receptor [215, 216]. With fucoidan treatment, the Angpt-2 level in both co-culture models and their corresponding mono-cultures was much lower than that in the controls whereas the Angpt-1, especially in MG63 co-cultures was detected an increased level in response to fucoidan treatment. Beyond its direct effect on new blood vessel formation by endothelial cells, Angpt-2 also activates proangiogenic properties of circulating mononuclear cells [217, 218] which serve as supporting cells in blood vessel formation especially in the context of a tumor environment. Accordingly, Angpt-2 is also associated with increased inflammation and metastasis in a variety of tumors [219].

The calcification level of co-cultures was promoted in comparison with the corresponding mono-cultures for both MSCs and MG63 which might be associated with the osteogenic regulators expressed by OECs [220]. Treatment with fucoidan hindered the calcification level in both mono- and co-cultures. A significant decrease occurred in MSC mono-/co-cultures and a slight reduction for MG63 cultures. Alkaline

phosphatase (ALP), which is closely related to the mineralization of osteoblast-like cells as an early osteogenic marker, was significantly down-regulated in response to fucoidan treatment for MSC mono-cultures. Collagen type I, the matrix component secreted by osteoblast-like cells as a late osteogenic marker was also significantly decreased in both mono- and co-cultures of bone sarcoma cell line. However, the other late marker osteocalcin which is coded by the BGLAP gene and plays a role in the bone mineralization and formation process [221] did not show a significant change in response to fucoidan treatment.

The study of fucoidan (*f. vesiculosus*) crude extract in the vascularization of bone showed an impact on angiogenesis and osteogenesis for both physiological and pathological bone models via modulating the relevant factors. The control of factors such as VEGF, Angiopoitin-2 and SDF-1 in the tumor mircroenvironment for instance by fucoidan as a natural sulfated polysaccharide should provide a clinical value for osteosarcoma. Nevertheless, the specific action of fucoidan subfractions and the mode of application need further evaluation. According to the literature other groups also reported effects of fucoidan and in particular of fucoidan with low molecular weight on VEGF levels in tumor models [208, 222], as well as effects of fucoidan on SDF-1 levels [223]. Nevertheless, contradictory reports on the effect of fucoidan on angiogenesis exist [209]. The bio-functions of fucoidan extracts are highly dependent on the chemical and structural properties such as molecular weight, sulfation degree and side chain branching which vary with algae species, treatment, isolation methods and harvest seasons [112]. Hence the specific bio-functional structures need to be further clarified for greater efficacy prior to clinical application. In addition, the standard procedures of harvesting, purification, fractionation and in-depth understanding of bio-functional mechanism remain to be developed and investigated to define correlated bioactive features of fucoidan extracts for therapeutic purposes. Using a hydrogel drug delivery approach for medium molecular weight fractions of fucoidan, a recent study reported proangiogenic effects probably associated with locally higher VEGF concentration and

a more continuous release profile mediated by fucoidan. These observations were probably due to the binding capacity of fucoidan for VEGF in the hydrogel [224], thus resulting in a locally higher VEGF concentration and enhanced vascularization. This study nicely highlights an application dependent action of fucoidan and together with other studies of fucoidan on endothelial progenitor cells [225]. These studies might serve as a basis for using fucoidan for pro-angiogenic therapies related to tissue engineering and regenerative medicine. In contrast, in this thesis the fucoidan was added to the culture medium thus lowering the freely accessible VEGF for the cells in culture and ultimately leading to the reduction of vascular structures.

Overall, the heparin-like structure [226] and ability of fucoidan to bind VEGF [227] enable wide applications of these compounds to modulate angiogenesis but has to be evaluated in a context and application dependent manner. In the present study the available free VEGF and SDF-1 protein levels were reduced resulting in reduction of angiogenesis in response to low dose of fucoidans, whereas the cytotoxic effects were limited. These results showed the anti-angiogenic capacity of fucoidan to inhibit free angiogenic factors for bone tumor treatment. In addition, fucoidan, as a binding agent of VEGF for a local delivery system, could be used to deliver VEGF aiming at a pro-angiogenic effect in terms of bone regeneration. For clinical use and a better understanding of fucoidan, the precise definition of the relationship between the bio-functions and the structural features of fucoidan requires further investigation in future research.

Since the effect of fucoidan could vary with the mode of application and biological models, as well as due to its suggested anti-tumor potential, fucoidan was applied to the uveal melanoma cell lines to study its impact on angiogenesis in ophthalmological tumor models at a dose of 100 µg/mL. In contrast to the bone regenerative and sarcoma models above, where fucoidan impaired angiogenic activity of OEC via reducing VEGF and SDF-1, fucoidan treatment did not show any significant influence on the angiogenesis of the melanoma cell line co-cultures or the VEGF level. In addition, the

primary cell line 92.1 showed poor support of OECs in the co-culture most likely due to the nature of this cell type. Nevertheless, the length and area of OEC mono-layers on 92.1 was significantly improved in response to fucoidan, which correlated to the promotive effect of fucoidan on cell proliferation and viability for 92.1. Overall, the effect of fucoidan can vary with the manner of application, cell types and models, thus the exact impact should be closely examined case by case.

4.2 Study of Vitamin D_3 in a bone infection model

Inflammation plays an essential role in bone regeneration and healing; therefore, it has drawn growing attention for orthopedic studies. Systematic inflammation was found to impair bone repair processes and lead to upregulated bone resorption [228]. Acute inflammation in bone caused by infections, implantation or trauma can develop towards chronic inflammatory diseases and result in bone loss [229]. Nevertheless, as inflammation is involved in the early stage of the physiological bone healing process, the initial inflammatory response is believed to support bone repair and regeneration. Therefore, a comprehensive understanding of the underlying mechanisms of inflammation in the process of bone formation and interactions at cellular and molecular levels is vital for the treatment of bone destruction caused by disease and trauma in clinical practice. In this part, the osteogenic differentiated MSCs were co-cultured with OECs which contribute to vascularization and inflammatory response to study the bio-function of vitamin D_3 in a bone infectious model.

Lipopolysaccharide (LPS), the component in the membrane of Gram-negative bacteria could be recognized by the immune cells resulting in a subsequent inflammatory response. OECs and endothelial cells in previous studies were shown to reveal a severe inflammatory response mediated by LPS [230]. In this work, OECs showed active immune response with an upregulation of TLR4 and the inflammatory cytokine IL-6 after being subjected to LPS at a concentration of 100 ng/mL.

Besides the inflammatory response of OECs in mono- or co-cultures with MSCs induced by the exogenous stimuli, Vitamin D_3, well known for its biological functions in bone mineralization and anti-inflammatory effect, was applied to the cultures at a concentration of 10 nM. This is equivalent to physiological serum levels of 10-50 nM [231]. Herein, prior to being examined, the OEC mono- and co-cultures with MSC were treated with VD_3 for 7 days and/or LPS stimulation for 48 hours.

Recently, OECs and endothelial cells have been shown to increase angiogenesis in response to LPS stimulation via activation of TLR4 [230, 232]. In MSCs/OECs co-cultures, angiogenesis was promoted by VD_3 and/or LPS treatment compared to the control with regard to the length and number of branching points of the capillary-like networks composed of OECs. The gene expression level of TLR4 in OECs mono-cultures was not influenced by LPS stimulation according to the rt-PCR result. However, LPS in the presence of VD_3 significantly upregulated the expression of TLR4 in MSC/OEC co-cultures. TLR4 is expressed in a variety of cells, such as monocytes, macrophages, outgrowth endothelial cells (as what was shown in rt-PCR) and the bone marrow derived MSCs as well [233]. It recognizes pathogen associated molecular patterns, thus TLR4 can be activated when exposed to LPS and lead to the elevated production of pro-inflammatory cytokines, IL-6 for instance, resulting in endothelial inflammation which contributes to defend against infectious diseases and tissue injury. It has been reported that the TLR4-mediated production of pro-inflammatory cytokines can be activated through NF-κB signaling pathway in endothelial cells [234]. In OEC mono-cultures and co-cultures with MSC, the expression level of IL-6 was significantly promoted when exposed to LPS. Accordingly, LPS stimulation markedly enhanced the IL-6 level in the supernatant detected by Elisa.

In addition to the pro-inflammatory cytokine, LPS also promoted the mRNA expression level of monocyte/macrophage lineage cell markers, significantly for CD68 and tentatively for CD163 and CD206 in MSC/OEC co-cultures. Endothelial cells have been reported to express CD68 but on a relatively lower level when compared to

monocytes/ macrophages [235]. The expression of CD163 was reported in endothelial progenitor cells (EPCs) [236] which co-exist with our OECs derived from them as a minor sub-population. Notably, CD163 expression was also shown to be associated with endothelial differentiation and angiogenesis in recent studies [237]. The upregulated expression of the mannose receptor (CD206) which can recognize microorganisms and regulate inflammation also verified the inflammatory response to LPS simulation in the co-cultures.

Furthermore, other molecules which are involved in the immune response also showed a significant increase following LPS stimulation. The intercellular adhesion molecule (ICAM) and vascular cell adhesion molecule (VCAM) were both significantly upregulated in OEC mono-cultures in response to LPS treatment whereas the effect only occurred in co-cultures for ICAM. In addition, the protein level of ICAM in the supernatant of OEC mono- and co-cultures was significantly increased in response to LPS stimulation. The expression of these adhesion molecules can be upregulated during endothelial activation in response to stimuli, such as the pro-inflammatory cytokines [238]. ICAM and VCAM have been shown to facilitate the recruitment of leukocytes in endothelium *in vivo* [239] and play a role in endothelial junction maturation and vascular permeability [240]. The roles of ICAM in mediating EPC recruitment thus promoting angiogenesis, and VCAM as a surrogate angiogenic marker have been demonstrated in previous reports [241, 242]. Moreover, LPS showed a promotive effect on the expression of complement factor Complement 3 (C3) in OEC mono-cultures.

Besides the upregulated expression of inflammatory modulators, LPS significantly promoted the expression level of VEGF in MSCs. However, the protein level of VEGF in the supernatant did not show any change in response to LPS. The expression level of angiogenic regulator, angiopointin-1 in MSCs was significantly upregulated and anigopointin-2 in OECs was slightly upregulated by LPS stimulation. Furthermore, the endothelial marker CD31 examined in the co-cultures with MSCs after LPS stimulation showed a significant increase in its expression level. From above, it indicated that LPS

induced the inflammatory response and endothelial activation resulting in the improved expression of angiogenic factors which promote the angiogenic activity. Besides the effect of LPS on inflammatory response and angiogenesis, the osteoclast marker TRACP5 in MSCs was significantly promoted by LPS. The elevated expression of TRACP5, known as a bone resorption marker [243], implied the potential impact of LPS on osteoclastogenesis in MSC/OEC model as the result of an immune response.

VD_3 at a dose of 10 nM in this study was not observed to have a significant anti-inflammatory effect in the co-culture model. Nevertheless, the anti-microbial peptide cathelicidin (LL-37) was activated in MSCs with VD_3 treatment (the result of LL-37 expression by rt-PCR see Figure 3.11). The expression of LL-37 has been demonstrated to be promoted by VD_3 in a variety of cell types, such as monocytes, epithelial cells and macrophages, showing the role of VD_3 as an immune regulator [136, 244-246]. However, the LL-37 peptide was not detected in the supernatant by Elisa or in the protein lysate of MSC mono-cultures with western blot despite the significant elevation induced by VD_3 shown on the mRNA level. The discrepancy between expression level at gene level and protein production of cathelicidin stays yet unclear. This result might relate to the production of trace amounts of LL-37, which can hardly be detected by our technical approach and assays.

A tentative increase in the mineralization level in the co-cultures after 14 days treatment with VD_3 was shown. The expression level of late osteogenic marker osteocalcin was significantly upregulated by VD_3 independent of LPS. The stimulation of osteocalcin by VD_3 has also been reported in osteoblasts [122]. In contrast, another late osteogenic marker collagen type I and early marker ALP did not show much difference in expression level after being subjected to VD_3. No effect on the production of collagen I was observed in the osteoblastic cells in some *in vitro* studies [247], nevertheless positive effect of VD_3 on collagen I production was reported in other publications [122, 248]. The results from different research groups still remain varied and inconsistent for the cellular and molecular effects of VD_3 on bone formation, which are associated with

culture conditions, experimental models, state of cell differentiation, treatment manner and several other factors. Bone formation is a complex dynamic physiological process, and bone repair and regeneration could be enhanced by various factors with an overall effect of them. It is certain that a simple *in vitro* co-culture model can not reproduce such a complex *in vivo* environment, but it is more conducive to an in-depth study of the effects of molecules that are of interest on specific bone healing phases.

Overall, the LPS at a relatively low dose of 100 ng/mL induced endothelial activation and inflammatory response via the signaling pathway mediated by TLR4 activation in the OEC/osteogenic differentiated MSC co-cultures resulting in the promotion of angiogenic activities and upregulation of angiogenic modulating factors on the gene expression level. Vitamin D_3 significantly improved angiogenesis via regulating the VEGF level of MSCs. The activation of LL-37 in MSCs at the gene expression level by VD_3 suggested its potential effect on modulating the immune defense against LPS. Nevertheless, there is still an absence of significant evidence on the protein level to support the protective function of VD_3 in the inflammatory response. It is clear that a deeper insight into the details of the beneficial functions of VD_3 and the mechanisms behind them with a refined inflammatory model is still needed to evaluate the potential future clinical applications of VD_3 against bone infections.

4.3 IKVAV incorporated collagen hydrogels for pro-angiogenesis

IKVAV incorporated collagen hydrogels were fabricated to create an injectable hydrogel system with the purpose of efficient pre-vascularization for tissue regeneration. Collagen, the major organic component of extracellular matrix in bone tissue, has been investigated and widely applied as biomaterial for bone tissue engineering in the past decades. IKVAV peptide is the functional amino acid sequence mediating cell attachment on laminin, another important component of the extracellular matrix [249].

Previous assessment depicted the influence of protein concentration and matrix stiffness on angiogenic activity of endothelial cells *in vitro* [250]. The study of angiogenesis within a collagen I hydrogel indicated an optimal matrix concentration of 2 mg/mL [251]. Therefore, in this study an optimal concentration of collagen in control and modified gels for angiogenesis was vital to examine the impact of modification and peptide on angiogenesis independent of other impact factors. However, the mass loss of collagen cannot be excluded throughout the entire modification process including reaction, dialysis and lyophilization. Thus, collagen concentration after modification and incorporation of IKVAV was examined.

Collagen is composed of aggregates of fibrils which can be structurally divided into three polypeptides strands [252]. The complexity of collagen brings difficulties to its dissolution and characterization, hence the conventional protein concentration measurement methods, such as NANO drop and the BCA kit did not work for the collagen solution. To quantify the collagen samples, Sirius Red dyes, which bind to collagen in a QuickZyme Soluble Collagen Assay kit were used. The concentration result determined by the kit showed a yielding rate ranging between 70% and 87% after modification. The control collagen solution and modified collagen were adjusted to the optimal concentration for angiogenesis for the subsequent OEC encapsulation and assessment.

Cultured in EGM-2 supplemented with 50 ng/mL VEGF, the OECs encapsulated in collagen hydrogels elongated and aggregated to form capillary-like angiogenic structures on both day 3 and 7 in all groups. Furthermore, the modification and incorporation of IKVAV in the collagen hydrogels did not display any significant effect on the angiogenic structures of OECs in terms of the angiogenic coverage determined by quantitative analysis.

In the modification design, the IKVAV peptides were hypothesized to conjugate to cysteines on collagen via disulfide bonds by the mild oxidation agent DMSO. However, the expected chemical crosslinking between the peptide and collagen I could not be

detected by mass spectrometry. The cysteines are located on the terminals of the polypeptide chains to aid the synthesis and stability of collagen I macromolecules [253]. However, with a limited availability of free cysteines on collagen I for the intended modification, the IKVAV peptides might have linked to one another forming a disulfide-linked-double-peptide (IKVAV-S-S-IKVAV) rather than being conjugated to collagen. OECs can bind to and respond to active peptides, which may correlate to the significant decrease of endothelial markers on mRNA expression. However, binding peptides that are not conjugated to the cell microenvironment cannot anchor the cells to assist their migration, proliferation and angiogenic activities. Therefore, no promotive effect on angiogenic structures was observed or detected in a quantitative manner for the group cultured in the hydrogels modified with the IKVAV peptides.

Overall, collagen hydrogels support angiogenesis of OECs with the addition of VEGF, regardless of the incorporation of IKVAV peptides in our modification design. To better assess and use the IKVAV peptide, a bio-functional component of ECM, in an injectable hydrogel construct, a firm conjugation and matrix molecules with more available active binding sites could be employed in future design in the context of tissue regeneration. Due to the structural complexity of collagen and the lack of available modifiable groups, it is difficult to effectively conjugate IKVAV peptides to collagen molecules. Therefore, other macromolecules, such as gelatin or synthetic polymers modified with cell adhesive ligands, could be considered in future design.

4.4 Composite hydrogels with silk fibroin fiber for osteogenesis

Silk fibroin, due to its excellent biocompatibility and non-immunogenicity, has been fabricated into various forms like porous scaffolds, silk fibroin hydrogels and silk-based screws and plates for different medical and clinical applications [23, 254]. In this part, the osteogenic potential of composite biomaterials with silk fibroin fibers was studied. The micro silk fibroin fibers (mSF) of 200-300 μm long were first acquired from macro silk fibers by hydrolysis. Immersed in stimulated body fluid, the mSFs were found to be completely covered with a mineralized layer composed of aggregates of

hydroxyapatite microspheres. The osteogenic differentiated MSCs were applied to the composite hydrogels with biomineralized mSF to investigate the cell attachment and response and the potential of the constructs for bone regeneration.

The MSCs encapsulated in the collagen hydrogel with mSF showed good adhesion and growth within 14 days to the collagen matrix which can provide excellent support to MSCs for their attachment, migration, proliferation and significantly promote the osteogenic differentiation of MSC *in vitro* [255]. Compared to mSF which are more elastic and flexible, the presence of mineralized mSF coated with hydroxyapatite strengthened the gel. At the mRNA level, the bone differentiation marker BMP-2 was significantly upregulated whereas some of the osteogenic markers were slightly decreased by the presence of mineralized mSF which introduced the hydroxyapatite layer in the gel and changed the compliance of the construct at the same time. The tentative upregulation of angiogenic factor VEGF indicated the potential of mineralized mSF in bone regenerative application.

Next, the novel silk fibroin composite scaffolds, based on hyaluronic acid hydrogel, were evaluated for their osteogenic properties. Compared to the collagen hydrogel where the mSF and mineralized mSF were physically entrapped, the modified hyaluronic acid (HA) hydrogel immobilized the mineralized mSF via the CaP-BP bond by which the mineralized mSF were firmly and homogenously distributed. The control scaffolds were prepared by photocrosslinking the HA under UV with mSF physically entrapped (Am-HA-BP•mSF). MSCs were loaded on both composite scaffolds (Am-HA-BP•CaP@mSF) and controls. The cell morphology and patterns were visualized 14 days after seeding and osteogenic markers were examined on the mRNA expression level. The present *in vitro* results showed no restrictions in terms of the biocompatibility or bio-functionality of the Am-HA-BP•CaP@mSF hydrogel and showed a favored affinity and arrangement of MSCs towards mineralized fibers as indicated in the arrowed area in Figure 3.19. However, the PCR result showed a decrease of Col I and osteocalcin gene expression in osteogenic differentiated MSCs grown for 14 days on

the Am-HA-BP•CaP@mSF scaffolds when compared to the mSF scaffolds. The decrease in the expression level of these osteogenic markers might relate to the mineralized coatings on the fibers where cells aligned to. The decreased expression level of ALP and osteocalcin was also reported for the osteogenic induced MSCs with the treatment of nano-sized hydroxyapatite [256], indicating the response of osteogenic cells to a primary structural component of the skeleton. These data together with the morphological data might be considered as a motivation to analyze the impact of the self-healing silk-based hydrogels on the differentiation of MSCs in detail in future studies. Moreover, the current crosslinking between HA molecules to stabilize the hydrogel was initiated by a strong UV light, which is harmful to the cells. In our *in vitro* system, MSCs were loaded after stabilization for the characterization. In order to optimize the design of the construct, a new crosslinking strategy between HA molecules with no harm to the loaded cells could be employed, thus osteogenic cells or co-implantation of both osteogenic and endothelial cells could be encapsulated in the constructs before stabilization to achieve more effective tissue regeneration in bone defect.

5. Summary

In this thesis, bioactive molecules and bio-functionalized hydrogel scaffolds were studied with bone vascularization models to characterize their bioactive functions and potential applications in bone repair or tumor treatment. In this model, the primary outgrowth endothelial cells, which contribute to angiogenesis and form the capillary-like structures, were applied or co-cultured with osteogenic cells to examine the angiogenic and osteogenic processes *in vitro*.

The first bioactive substance of interest was crude fucoidan extract from *f. vesiculosus*. Addition of fucoidan to the bone regeneration and tumor models showed an impairing effect on angiogenesis via binding free VEGF and SDF-1 in the system, thereby decreasing the readily available amount for the cells. The inhibitory effect of fucoidan can be attributed to its heparin-like structure. On the other hand, fucoidan extract did not show a significant effect on angiogenesis or VEGF levels in the uveal melanoma co-culture model. It rather enhanced the attachment of OEC to the primary melanoma cell lines. The results indicate that the effect of fucoidan not only varies based on seaweed species and molecular weight of the compounds within the extract, but also depends on the cell type and method of application. Fucoidan is a promising bioactive agent for modulating vascularization in bone regeneration and tumor treatment. Nevertheless, standardization of its extraction procedure and a better understanding of the structural dependent biological features would be the challenges for future application.

In addition, the study of vascularization in the bone regenerative model showed LPS induced inflammation and promoted angiogenesis via the activation of TLR4. Inflammation plays an important role in bone healing and occurs in bone implantation, thus to fully understand the roles of the inflammatory response and immune factors is beneficial for a fast and efficient integration of implants in the context of bone tissue engineering. Vitamin D_3, however, did not show any significant anti-inflammatory effect in the model, contrary to expectations. Nevertheless, vitamin D_3 promoted

angiogenesis via elevating the VEGF level of MSCs, as well as the osteogenic activity in co-cultures.

To examine the bio-functionalized hydrogels with mono-culture models, the angiogenesis of OECs was supported in injectable 3D collagen hydrogels; however, no significant proangiogenic effect was observed following the incorporation of IKVAV peptide. An effective conjugation of IKVAV peptide to the matrix molecule is required to utilize its promotive effect on angiogenesis in a tissue regenerative construct. The composite biomaterials based on hyaluronic acid with mineralized silk fibroin fibers demonstrated *in vitro* biocompatibility with MSCs seeding and attachment implying the potential utilization of these biomaterials for bone regeneration.

To put it in a nutshell, investigated bioactive molecules and bio-functional scaffolds have potential applications to modulate angiogenesis and osteogenesis. Their biomimetic properties allow them to act on the cellular and molecular level to guide the performance of stem/progenitor cells. Employing the aforementioned approaches in a clinical setting requires further research.

6. Reference

1. Clarke, B., *Normal bone anatomy and physiology.* Clin J Am Soc Nephrol, 2008. **3 Suppl 3**: p. S131-9.
2. Dick, H.M. and R.J. Strauch, *Infection of massive bone allografts.* Clin Orthop Relat Res, 1994(306): p. 46-53.
3. Bauer, T.W. and G.F. Muschler, *Bone graft materials. An overview of the basic science.* Clin Orthop Relat Res, 2000(371): p. 10-27.
4. Tatara, A.M. and A.G. Mikos, *Tissue Engineering in Orthopaedics.* J Bone Joint Surg Am, 2016. **98**(13): p. 1132-9.
5. Brandi, M.L. and P. Collin-Osdoby, *Vascular biology and the skeleton.* J Bone Miner Res, 2006. **21**(2): p. 183-92.
6. Maes, C., et al., *Osteoblast precursors, but not mature osteoblasts, move into developing and fractured bones along with invading blood vessels.* Dev Cell, 2010. **19**(2): p. 329-44.
7. Fuchs, S., et al., *Contribution of outgrowth endothelial cells from human peripheral blood on in vivo vascularization of bone tissue engineered constructs based on starch polycaprolactone scaffolds.* Biomaterials, 2009. **30**(4): p. 526-34.
8. Unger, R.E., et al., *Tissue-like self-assembly in cocultures of endothelial cells and osteoblasts and the formation of microcapillary-like structures on three-dimensional porous biomaterials.* Biomaterials, 2007. **28**(27): p. 3965-76.
9. Dithmer, M., et al., *Fucoidan reduces secretion and expression of vascular endothelial growth factor in the retinal pigment epithelium and reduces angiogenesis in vitro.* PLoS One, 2014. **9**(2): p. e89150.
10. Velasco, M.A., C.A. Narvaez-Tovar, and D.A. Garzon-Alvarado, *Design, materials, and mechanobiology of biodegradable scaffolds for bone tissue engineering.* Biomed Res Int, 2015. **2015**: p. 729076.
11. Datta, H.K., et al., *The cell biology of bone metabolism.* J Clin Pathol, 2008. **61**(5): p. 577-87.
12. Florencio-Silva, R., et al., *Biology of Bone Tissue: Structure, Function, and Factors That Influence Bone Cells.* Biomed Res Int, 2015. **2015**: p. 421746.
13. Athanasiou, K.A., et al., *Fundamentals of biomechanics in tissue engineering of bone.* Tissue Eng, 2000. **6**(4): p. 361-81.
14. Marzona, L. and B. Pavolini, *Play and players in bone fracture healing match.* Clin Cases Miner Bone Metab, 2009. **6**(2): p. 159-62.
15. Berendsen, A.D. and B.R. Olsen, *Bone development.* Bone, 2015. **80**: p. 14-18.
16. Ai-Aql, Z.S., et al., *Molecular mechanisms controlling bone formation during fracture healing and distraction osteogenesis.* J Dent Res, 2008. **87**(2): p. 107-18.
17. Martin, T.J., *Bone biology and anabolic therapies for bone: current status and future prospects.* J Bone Metab, 2014. **21**(1): p. 8-20.
18. Athanasiou, V.T., et al., *Histological comparison of autograft, allograft-DBM, xenograft, and synthetic grafts in a trabecular bone defect: an experimental study in rabbits.* Med Sci Monit, 2010. **16**(1): p. BR24-31.
19. Tomford, W.W., *Transmission of disease through transplantation of musculoskeletal allografts.* J Bone Joint Surg Am, 1995. **77**(11): p. 1742-54.
20. Langer, R. and J.P. Vacanti, *Tissue engineering.* Science, 1993. **260**(5110): p. 920-6.
21. Choi, J., et al., *Controlled drug release from multilayered phospholipid polymer hydrogel on titanium alloy surface.* Biomaterials, 2009. **30**(28): p. 5201-8.
22. Shi, Z., et al., *Titanium with surface-grafted dextran and immobilized bone morphogenetic protein-2 for inhibition of bacterial adhesion and enhancement of osteoblast functions.* Tissue Eng Part A, 2009. **15**(2): p. 417-26.
23. Sun, W., et al., *Co-culture of outgrowth endothelial cells with human mesenchymal stem cells in silk fibroin hydrogels promotes angiogenesis.* Biomed Mater, 2016. **11**(3): p. 035009.

24. Robey, P., *"Mesenchymal stem cells": fact or fiction, and implications in their therapeutic use.* F1000Res, 2017. **6**.
25. Friedenstein, A.J., R.K. Chailakhjan, and K.S. Lalykina, *The development of fibroblast colonies in monolayer cultures of guinea-pig bone marrow and spleen cells.* Cell Tissue Kinet, 1970. **3**(4): p. 393-403.
26. Caplan, A.I., *Mesenchymal stem cells.* J Orthop Res, 1991. **9**(5): p. 641-50.
27. Gronthos, S., et al., *Surface protein characterization of human adipose tissue-derived stromal cells.* J Cell Physiol, 2001. **189**(1): p. 54-63.
28. Zvaifler, N.J., et al., *Mesenchymal precursor cells in the blood of normal individuals.* Arthritis Res, 2000. **2**(6): p. 477-88.
29. Crisan, M., et al., *A perivascular origin for mesenchymal stem cells in multiple human organs.* Cell Stem Cell, 2008. **3**(3): p. 301-13.
30. Dominici, M., et al., *Minimal criteria for defining multipotent mesenchymal stromal cells. The International Society for Cellular Therapy position statement.* Cytotherapy, 2006. **8**(4): p. 315-7.
31. Lv, F.J., et al., *Concise review: the surface markers and identity of human mesenchymal stem cells.* Stem Cells, 2014. **32**(6): p. 1408-19.
32. Arvidson, K., et al., *Bone regeneration and stem cells.* J Cell Mol Med, 2011. **15**(4): p. 718-46.
33. Amini, A.R., C.T. Laurencin, and S.P. Nukavarapu, *Bone tissue engineering: recent advances and challenges.* Crit Rev Biomed Eng, 2012. **40**(5): p. 363-408.
34. Risau, W., *Mechanisms of angiogenesis.* Nature, 1997. **386**(6626): p. 671-4.
35. Tongers, J., J.G. Roncalli, and D.W. Losordo, *Role of endothelial progenitor cells during ischemia-induced vasculogenesis and collateral formation.* Microvasc Res, 2010. **79**(3): p. 200-6.
36. Tang, H.S., Y.J. Feng, and L.Q. Yao, *Angiogenesis, vasculogenesis, and vasculogenic mimicry in ovarian cancer.* Int J Gynecol Cancer, 2009. **19**(4): p. 605-10.
37. Karamysheva, A.F., *Mechanisms of angiogenesis.* Biochemistry (Mosc), 2008. **73**(7): p. 751-62.
38. Patan, S., *Vasculogenesis and angiogenesis as mechanisms of vascular network formation, growth and remodeling.* J Neurooncol, 2000. **50**(1-2): p. 1-15.
39. Risau, W., et al., *Vasculogenesis and angiogenesis in embryonic-stem-cell-derived embryoid bodies.* Development, 1988. **102**(3): p. 471-8.
40. Jain, R.K., *Molecular regulation of vessel maturation.* Nat Med, 2003. **9**(6): p. 685-93.
41. Ferrara, N., *VEGF-A: a critical regulator of blood vessel growth.* Eur Cytokine Netw, 2009. **20**(4): p. 158-63.
42. Ferrara, N., *Vascular endothelial growth factor: molecular and biological aspects.* Curr Top Microbiol Immunol, 1999. **237**: p. 1-30.
43. Hoeben, A., et al., *Vascular endothelial growth factor and angiogenesis.* Pharmacol Rev, 2004. **56**(4): p. 549-80.
44. Ferrara, N., *VEGF: an update on biological and therapeutic aspects.* Curr Opin Biotechnol, 2000. **11**(6): p. 617-24.
45. Beamer, B., C. Hettrich, and J. Lane, *Vascular endothelial growth factor: an essential component of angiogenesis and fracture healing.* HSS J, 2010. **6**(1): p. 85-94.
46. Kalka, C., et al., *Transplantation of ex vivo expanded endothelial progenitor cells for therapeutic neovascularization.* Proc Natl Acad Sci U S A, 2000. **97**(7): p. 3422-7.
47. Tao, Z., et al., *Coexpression of VEGF and angiopoietin-1 promotes angiogenesis and cardiomyocyte proliferation reduces apoptosis in porcine myocardial infarction (MI) heart.* Proc Natl Acad Sci U S A, 2011. **108**(5): p. 2064-9.
48. Thurston, G., et al., *Leakage-resistant blood vessels in mice transgenically overexpressing angiopoietin-1.* Science, 1999. **286**(5449): p. 2511-4.
49. Hu, B. and S.Y. Cheng, *Angiopoietin-2: development of inhibitors for cancer therapy.* Curr

Oncol Rep, 2009. **11**(2): p. 111-6.
50. Papetti, M. and I.M. Herman, *Mechanisms of normal and tumor-derived angiogenesis.* Am J Physiol Cell Physiol, 2002. **282**(5): p. C947-70.
51. Folkman, J., *Tumor angiogenesis: therapeutic implications.* N Engl J Med, 1971. **285**(21): p. 1182-6.
52. Meadows, K.L. and H.I. Hurwitz, *Anti-VEGF therapies in the clinic.* Cold Spring Harb Perspect Med, 2012. **2**(10).
53. Asahara, T., et al., *Isolation of putative progenitor endothelial cells for angiogenesis.* Science, 1997. **275**(5302): p. 964-7.
54. Peichev, M., et al., *Expression of VEGFR-2 and AC133 by circulating human CD34(+) cells identifies a population of functional endothelial precursors.* Blood, 2000. **95**(3): p. 952-8.
55. Shi, Q., et al., *Evidence for circulating bone marrow-derived endothelial cells.* Blood, 1998. **92**(2): p. 362-7.
56. Basile, D.P. and M.C. Yoder, *Circulating and tissue resident endothelial progenitor cells.* J Cell Physiol, 2014. **229**(1): p. 10-6.
57. Reyes, M., et al., *Purification and ex vivo expansion of postnatal human marrow mesodermal progenitor cells.* Blood, 2001. **98**(9): p. 2615-25.
58. Gunsilius, E., et al., *Evidence from a leukaemia model for maintenance of vascular endothelium by bone-marrow-derived endothelial cells.* Lancet, 2000. **355**(9216): p. 1688-91.
59. Kalka, C., et al., *Vascular endothelial growth factor(165) gene transfer augments circulating endothelial progenitor cells in human subjects.* Circ Res, 2000. **86**(12): p. 1198-202.
60. Hattori, K., et al., *Vascular endothelial growth factor and angiopoietin-1 stimulate postnatal hematopoiesis by recruitment of vasculogenic and hematopoietic stem cells.* J Exp Med, 2001. **193**(9): p. 1005-14.
61. Pillarisetti, K. and S.K. Gupta, *Cloning and relative expression analysis of rat stromal cell derived factor-1 (SDF-1)1: SDF-1 alpha mRNA is selectively induced in rat model of myocardial infarction.* Inflammation, 2001. **25**(5): p. 293-300.
62. Yamaguchi, J., et al., *Stromal cell-derived factor-1 effects on ex vivo expanded endothelial progenitor cell recruitment for ischemic neovascularization.* Circulation, 2003. **107**(9): p. 1322-8.
63. Chong, M.S., W.K. Ng, and J.K. Chan, *Concise Review: Endothelial Progenitor Cells in Regenerative Medicine: Applications and Challenges.* Stem Cells Transl Med, 2016. **5**(4): p. 530-8.
64. Zaccone, V., et al., *Focus on biological identity of endothelial progenitors cells.* Eur Rev Med Pharmacol Sci, 2015. **19**(21): p. 4047-63.
65. Gulati, R., et al., *Diverse origin and function of cells with endothelial phenotype obtained from adult human blood.* Circ Res, 2003. **93**(11): p. 1023-5.
66. Ingram, D.A., et al., *Identification of a novel hierarchy of endothelial progenitor cells using human peripheral and umbilical cord blood.* Blood, 2004. **104**(9): p. 2752-60.
67. Case, J., et al., *Human CD34+AC133+VEGFR-2+ cells are not endothelial progenitor cells but distinct, primitive hematopoietic progenitors.* Exp Hematol, 2007. **35**(7): p. 1109-18.
68. Timmermans, F., et al., *Endothelial progenitor cells: identity defined?* J Cell Mol Med, 2009. **13**(1): p. 87-102.
69. Kaushal, S., et al., *Functional small-diameter neovessels created using endothelial progenitor cells expanded ex vivo.* Nat Med, 2001. **7**(9): p. 1035-40.
70. Shi, Y., et al., *Early endothelial progenitor cells as a source of myeloid cells to improve the pre-vascularisation of bone constructs.* Eur Cell Mater, 2014. **27**: p. 64-79; discussion 79-80.
71. Sales, K.M., et al., *Advancing vascular tissue engineering: the role of stem cell technology.* Trends Biotechnol, 2005. **23**(9): p. 461-7.
72. Melero-Martin, J.M., et al., *In vivo vasculogenic potential of human blood-derived endothelial progenitor cells.* Blood, 2007. **109**(11): p. 4761-8.

73. Yoder, M.C., et al., *Redefining endothelial progenitor cells via clonal analysis and hematopoietic stem/progenitor cell principals.* Blood, 2007. **109**(5): p. 1801-9.
74. Yoon, C.H., et al., *Synergistic neovascularization by mixed transplantation of early endothelial progenitor cells and late outgrowth endothelial cells: the role of angiogenic cytokines and matrix metalloproteinases.* Circulation, 2005. **112**(11): p. 1618-27.
75. Strehlow, K., et al., *Estrogen increases bone marrow-derived endothelial progenitor cell production and diminishes neointima formation.* Circulation, 2003. **107**(24): p. 3059-65.
76. Adams, V., et al., *Increase of circulating endothelial progenitor cells in patients with coronary artery disease after exercise-induced ischemia.* Arterioscler Thromb Vasc Biol, 2004. **24**(4): p. 684-90.
77. Kolbe, M., et al., *Enrichment of outgrowth endothelial cells in high and low colony-forming cultures from peripheral blood progenitors.* Tissue Eng Part C Methods, 2010. **16**(5): p. 877-86.
78. Fuchs, S., et al., *Outgrowth endothelial cells: sources, characteristics and potential applications in tissue engineering and regenerative medicine.* Adv Biochem Eng Biotechnol, 2010. **123**: p. 201-17.
79. Timmermans, F., et al., *Endothelial outgrowth cells are not derived from CD133+ cells or CD45+ hematopoietic precursors.* Arterioscler Thromb Vasc Biol, 2007. **27**(7): p. 1572-9.
80. Lin, Y., et al., *Origins of circulating endothelial cells and endothelial outgrowth from blood.* J Clin Invest, 2000. **105**(1): p. 71-7.
81. Childs, S.G., *Osteonecrosis: death of bone cells.* Orthop Nurs, 2005. **24**(4): p. 295-301; quiz 302-3.
82. Findlay, D.M. and D.R. Haynes, *Mechanisms of bone loss in rheumatoid arthritis.* Mod Rheumatol, 2005. **15**(4): p. 232-40.
83. Shaffer, J.W., et al., *Fate of vascularized and nonvascularized autografts.* Clin Orthop Relat Res, 1985(197): p. 32-43.
84. Deckers, M.M., et al., *Bone morphogenetic proteins stimulate angiogenesis through osteoblast-derived vascular endothelial growth factor A.* Endocrinology, 2002. **143**(4): p. 1545-53.
85. Deckers, M.M., et al., *Expression of vascular endothelial growth factors and their receptors during osteoblast differentiation.* Endocrinology, 2000. **141**(5): p. 1667-74.
86. Street, J., et al., *Vascular endothelial growth factor stimulates bone repair by promoting angiogenesis and bone turnover.* Proc Natl Acad Sci U S A, 2002. **99**(15): p. 9656-61.
87. Yang, X.B., et al., *Human osteoprogenitor bone formation using encapsulated bone morphogenetic protein 2 in porous polymer scaffolds.* Tissue Eng, 2004. **10**(7-8): p. 1037-45.
88. Au, P., et al., *Bone marrow-derived mesenchymal stem cells facilitate engineering of long-lasting functional vasculature.* Blood, 2008. **111**(9): p. 4551-8.
89. Duttenhoefer, F., et al., *3D scaffolds co-seeded with human endothelial progenitor and mesenchymal stem cells: evidence of prevascularisation within 7 days.* Eur Cell Mater, 2013. **26**: p. 49-64; discussion 64-5.
90. Fuchs, S., et al., *Dynamic processes involved in the pre-vascularization of silk fibroin constructs for bone regeneration using outgrowth endothelial cells.* Biomaterials, 2009. **30**(7): p. 1329-38.
91. Mayer, H., et al., *Vascular endothelial growth factor (VEGF-A) expression in human mesenchymal stem cells: autocrine and paracrine role on osteoblastic and endothelial differentiation.* J Cell Biochem, 2005. **95**(4): p. 827-39.
92. Clarkin, C.E., et al., *Evaluation of VEGF-mediated signaling in primary human cells reveals a paracrine action for VEGF in osteoblast-mediated crosstalk to endothelial cells.* J Cell Physiol, 2008. **214**(2): p. 537-44.
93. Dohle, E., et al., *Sonic hedgehog promotes angiogenesis and osteogenesis in a coculture system consisting of primary osteoblasts and outgrowth endothelial cells.* Tissue Eng Part A,

2010. **16**(4): p. 1235-7.
94. Wenger, A., et al., *Modulation of in vitro angiogenesis in a three-dimensional spheroidal coculture model for bone tissue engineering.* Tissue Eng, 2004. **10**(9-10): p. 1536-47.
95. Rouwkema, J., J. de Boer, and C.A. Van Blitterswijk, *Endothelial cells assemble into a 3-dimensional prevascular network in a bone tissue engineering construct.* Tissue Eng, 2006. **12**(9): p. 2685-93.
96. Fuchs, S., A. Hofmann, and C. Kirkpatrick, *Microvessel-like structures from outgrowth endothelial cells from human peripheral blood in 2-dimensional and 3-dimensional co-cultures with osteoblastic lineage cells.* Tissue Eng, 2007. **13**(10): p. 2577-88.
97. Kolbe, M., et al., *Paracrine effects influenced by cell culture medium and consequences on microvessel-like structures in cocultures of mesenchymal stem cells and outgrowth endothelial cells.* Tissue Eng Part A, 2011. **17**(17-18): p. 2199-212.
98. Kaigler, D., et al., *Endothelial cell modulation of bone marrow stromal cell osteogenic potential.* FASEB J, 2005. **19**(6): p. 665-7.
99. Villars, F., et al., *Effect of human endothelial cells on human bone marrow stromal cell phenotype: role of VEGF?* J Cell Biochem, 2000. **79**(4): p. 672-85.
100. Grellier, M., L. Bordenave, and J. Amedee, *Cell-to-cell communication between osteogenic and endothelial lineages: implications for tissue engineering.* Trends Biotechnol, 2009. **27**(10): p. 562-71.
101. Yu, H., et al., *Promotion of osteogenesis in tissue-engineered bone by pre-seeding endothelial progenitor cells-derived endothelial cells.* J Orthop Res, 2008. **26**(8): p. 1147-52.
102. Silva, T.H., et al., *Marine algae sulfated polysaccharides for tissue engineering and drug delivery approaches.* Biomatter. **2**(4): p. 278-89.
103. Mori, N., et al., *Beneficial effects of fucoidan in patients with chronic hepatitis C virus infection.* World J Gastroenterol. **18**(18): p. 2225-30.
104. Prokofjeva, M.M., et al., *Fucoidans as potential inhibitors of HIV-1.* Mar Drugs. **11**(8): p. 3000-14.
105. Han, Y.S., J.H. Lee, and S.H. Lee, *Antitumor Effects of Fucoidan on Human Colon Cancer Cells via Activation of Akt Signaling.* Biomol Ther (Seoul). **23**(3): p. 225-32.
106. Hsu, H.Y., et al., *Fucoidan inhibition of lung cancer in vivo and in vitro : role of the Smurf2-dependent ubiquitin proteasome pathway in TGFbeta receptor degradation.* Oncotarget. **5**(17): p. 7870-85.
107. Ruperez, P., O. Ahrazem, and J.A. Leal, *Potential antioxidant capacity of sulfated polysaccharides from the edible marine brown seaweed Fucus vesiculosus.* J Agric Food Chem, 2002. **50**(4): p. 840-5.
108. Li, X.J. and Q.F. Ye, *Fucoidan reduces inflammatory response in a rat model of hepatic ischemia-reperfusion injury.* Can J Physiol Pharmacol. **93**(11): p. 999-1005.
109. Silva, T.M., et al., *Partial characterization and anticoagulant activity of a heterofucan from the brown seaweed Padina gymnospora.* Braz J Med Biol Res, 2005. **38**(4): p. 523-33.
110. Ale, M.T., J.D. Mikkelsen, and A.S. Meyer, *Important determinants for fucoidan bioactivity: a critical review of structure-function relations and extraction methods for fucose-containing sulfated polysaccharides from brown seaweeds.* Mar Drugs. **9**(10): p. 2106-30.
111. Li, B., et al., *Fucoidan: structure and bioactivity.* Molecules, 2008. **13**(8): p. 1671-95.
112. Fitton, J.H., D.N. Stringer, and S.S. Karpiniec, *Therapies from Fucoidan: An Update.* Mar Drugs. **13**(9): p. 5920-46.
113. Matsubara, K., et al., *Effects of middle molecular weight fucoidans on in vitro and ex vivo angiogenesis of endothelial cells.* Int J Mol Med, 2005. **15**(4): p. 695-9.
114. Patankar, M.S., et al., *A revised structure for fucoidan may explain some of its biological activities.* J Biol Chem, 1993. **268**(29): p. 21770-6.
115. Nishino, T., et al., *Isolation and partial characterization of a novel amino sugar-containing fucan sulfate from commercial Fucus vesiculosus fucoidan.* Carbohydr Res, 1994. **255**: p. 213-

24.
116. Dithmer, M., et al., *Fucoidan reduces secretion and expression of vascular endothelial growth factor in the retinal pigment epithelium and reduces angiogenesis in vitro.* PLoS One. **9**(2): p. e89150.
117. Reys, L.L., et al., *Fucoidan Hydrogels Photo-Cross-Linked with Visible Radiation As Matrices for Cell Culture.* Acs Biomaterials Science & Engineering, 2016. **2**(7): p. 1151-1161.
118. Dusso, A.S., A.J. Brown, and E. Slatopolsky, *Vitamin D.* Am J Physiol Renal Physiol, 2005. **289**(1): p. F8-28.
119. Holick, M.F., et al., *Photosynthesis of previtamin D3 in human skin and the physiologic consequences.* Science, 1980. **210**(4466): p. 203-5.
120. Ponchon, G., A.L. Kennan, and H.F. DeLuca, *"Activation" of vitamin D by the liver.* J Clin Invest, 1969. **48**(11): p. 2032-7.
121. Adams, J.S. and M. Hewison, *Update in vitamin D.* J Clin Endocrinol Metab, 2010. **95**(2): p. 471-8.
122. van Leeuwen, J.P., et al., *Vitamin D control of osteoblast function and bone extracellular matrix mineralization.* Crit Rev Eukaryot Gene Expr, 2001. **11**(1-3): p. 199-226.
123. Zhou, S., et al., *Clinical characteristics influence in vitro action of 1,25-dihydroxyvitamin D(3) in human marrow stromal cells.* J Bone Miner Res, 2012. **27**(9): p. 1992-2000.
124. Reynolds, J.J., M.F. Holick, and H.F. De Luca, *The role of vitamin D metabolites in bone resorption.* Calcif Tissue Res, 1973. **12**(4): p. 295-301.
125. Turk, S., et al., *Comparative effect of oral pulse and intravenous calcitriol treatment in hemodialysis patients: the effect on serum IL-1 and IL-6 levels and bone mineral density.* Nephron, 2002. **90**(2): p. 188-94.
126. Muller, K., M. Diamant, and K. Bendtzen, *Inhibition of production and function of interleukin-6 by 1,25-dihydroxyvitamin D3.* Immunol Lett, 1991. **28**(2): p. 115-20.
127. Tsoukas, C.D., et al., *Inhibition of interleukin-1 production by 1,25-dihydroxyvitamin D3.* J Clin Endocrinol Metab, 1989. **69**(1): p. 127-33.
128. Qi, D.Y., et al., *Divergent regulation of 1,25-dihydroxyvitamin D3 on human bone marrow osteoclastogenesis and myelopoiesis.* J Cell Biochem, 1999. **72**(3): p. 387-95.
129. Flanagan, A.M., et al., *The role of 1,25-dihydroxycholecalciferol and prostaglandin E2 in the regulation of human osteoclastic bone resorption in vitro.* Int J Exp Pathol, 1995. **76**(1): p. 37-42.
130. Wang, D.S., et al., *Increase of vascular endothelial growth factor mRNA expression by 1,25-dihydroxyvitamin D3 in human osteoblast-like cells.* J Bone Miner Res, 1996. **11**(4): p. 472-9.
131. Meller, Y., et al., *Parathormone, calcitonin, and vitamin D metabolites during normal fracture healing in geriatric patients.* Clin Orthop Relat Res, 1985(199): p. 272-9.
132. Lin, R., *Crosstalk between Vitamin D Metabolism, VDR Signalling, and Innate Immunity.* Biomed Res Int, 2016. **2016**: p. 1375858.
133. Guo, J., et al., *1, 25(OH)(2)D(3) inhibits hepatocellular carcinoma development through reducing secretion of inflammatory cytokines from immunocytes.* Curr Med Chem, 2013. **20**(33): p. 4131-41.
134. Erbas, O., et al., *Cholecalciferol (vitamin D 3) improves cognitive dysfunction and reduces inflammation in a rat fatty liver model of metabolic syndrome.* Life Sci, 2014. **103**(2): p. 68-72.
135. Di Rosa, M., et al., *Vitamin D3: a helpful immuno-modulator.* Immunology, 2011. **134**(2): p. 123-39.
136. Wang, T.T., et al., *Cutting edge: 1,25-dihydroxyvitamin D3 is a direct inducer of antimicrobial peptide gene expression.* J Immunol, 2004. **173**(5): p. 2909-12.
137. Takemoto, M., et al., *Mechanical properties and osteoconductivity of porous bioactive titanium.* Biomaterials, 2005. **26**(30): p. 6014-23.
138. Li, D., et al., *Tissue-engineered bone constructed in a bioreactor for repairing critical-sized bone defects in sheep.* Int Orthop, 2014. **38**(11): p. 2399-406.

139. Hench, L.L., *The story of Bioglass.* J Mater Sci Mater Med, 2006. **17**(11): p. 967-78.
140. Habibovic, P., et al., *Influence of octacalcium phosphate coating on osteoinductive properties of biomaterials.* J Mater Sci Mater Med, 2004. **15**(4): p. 373-80.
141. Yuan, H., et al., *Osteoinduction by calcium phosphate biomaterials.* J Mater Sci Mater Med, 1998. **9**(12): p. 723-6.
142. Yuan, H., et al., *Bone induction by porous glass ceramic made from Bioglass (45S5).* J Biomed Mater Res, 2001. **58**(3): p. 270-6.
143. Yan, J., et al., *Cross-linking characteristics and mechanical properties of an injectable biomaterial composed of polypropylene fumarate and polycaprolactone co-polymer.* J Biomater Sci Polym Ed, 2011. **22**(4-6): p. 489-504.
144. Miller, R.A., J.M. Brady, and D.E. Cutright, *Degradation rates of oral resorbable implants (polylactates and polyglycolates): rate modification with changes in PLA/PGA copolymer ratios.* J Biomed Mater Res, 1977. **11**(5): p. 711-9.
145. Chaya, A., et al., *Fracture healing using degradable magnesium fixation plates and screws.* J Oral Maxillofac Surg, 2015. **73**(2): p. 295-305.
146. Eglin, D. and M. Alini, *Degradable polymeric materials for osteosynthesis: tutorial.* Eur Cell Mater, 2008. **16**: p. 80-91.
147. Teitelbaum, S.L., *Bone resorption by osteoclasts.* Science, 2000. **289**(5484): p. 1504-8.
148. Williams, D.F., *On the mechanisms of biocompatibility.* Biomaterials, 2008. **29**(20): p. 2941-53.
149. Albrektsson, T. and C. Johansson, *Osteoinduction, osteoconduction and osseointegration.* Eur Spine J, 2001. **10 Suppl 2**: p. S96-101.
150. Barradas, A.M., et al., *Osteoinductive biomaterials: current knowledge of properties, experimental models and biological mechanisms.* Eur Cell Mater, 2011. **21**: p. 407-29; discussion 429.
151. Hallab, N.J., *A review of the biologic effects of spine implant debris: Fact from fiction.* SAS J, 2009. **3**(4): p. 143-60.
152. Visuri, T., et al., *Decreased cancer risk in patients who have been operated on with total hip and knee arthroplasty for primary osteoarthrosis - A meta-analysis of 6 Nordic cohorts with 73,000 patients.* Acta Orthopaedica Scandinavica, 2003. **74**(3): p. 351-360.
153. Anderson, J.M., *Inflammatory response to implants.* ASAIO Trans, 1988. **34**(2): p. 101-7.
154. Christo, S.N., et al., *Innate Immunity and Biomaterials at the Nexus: Friends or Foes.* Biomed Res Int, 2015. **2015**: p. 342304.
155. Misiek, D.J., J.N. Kent, and R.F. Carr, *Soft tissue responses to hydroxylapatite particles of different shapes.* J Oral Maxillofac Surg, 1984. **42**(3): p. 150-60.
156. Tang, L., A.H. Lucas, and J.W. Eaton, *Inflammatory responses to implanted polymeric biomaterials: role of surface-adsorbed immunoglobulin G.* J Lab Clin Med, 1993. **122**(3): p. 292-300.
157. Hench, L.L. and J. Wilson, *Surface-active biomaterials.* Science, 1984. **226**(4675): p. 630-6.
158. Bergsma, E.J., et al., *Foreign body reactions to resorbable poly(L-lactide) bone plates and screws used for the fixation of unstable zygomatic fractures.* J Oral Maxillofac Surg, 1993. **51**(6): p. 666-70.
159. Sabokbar, A., O. Kudo, and N.A. Athanasou, *Two distinct cellular mechanisms of osteoclast formation and bone resorption in periprosthetic osteolysis.* J Orthop Res, 2003. **21**(1): p. 73-80.
160. Sicchieri, L.G., et al., *Pore size regulates cell and tissue interactions with PLGA-CaP scaffolds used for bone engineering.* J Tissue Eng Regen Med, 2012. **6**(2): p. 155-62.
161. Roosa, S.M., et al., *The pore size of polycaprolactone scaffolds has limited influence on bone regeneration in an in vivo model.* J Biomed Mater Res A, 2010. **92**(1): p. 359-68.
162. Karageorgiou, V. and D. Kaplan, *Porosity of 3D biomaterial scaffolds and osteogenesis.* Biomaterials, 2005. **26**(27): p. 5474-91.

163. Murphy, C.M., M.G. Haugh, and F.J. O'Brien, *The effect of mean pore size on cell attachment, proliferation and migration in collagen-glycosaminoglycan scaffolds for bone tissue engineering.* Biomaterials, 2010. **31**(3): p. 461-6.
164. Ko, K.S. and C.A. McCulloch, *Intercellular mechanotransduction: cellular circuits that coordinate tissue responses to mechanical loading.* Biochem Biophys Res Commun, 2001. **285**(5): p. 1077-83.
165. Huang, H., R.D. Kamm, and R.T. Lee, *Cell mechanics and mechanotransduction: pathways, probes, and physiology.* Am J Physiol Cell Physiol, 2004. **287**(1): p. C1-11.
166. Engler, A.J., et al., *Matrix elasticity directs stem cell lineage specification.* Cell, 2006. **126**(4): p. 677-89.
167. Lee, P.F., et al., *Angiogenic responses are enhanced in mechanically and microscopically characterized, microbial transglutaminase crosslinked collagen matrices with increased stiffness.* Acta Biomater, 2013. **9**(7): p. 7178-90.
168. Zajac, A.L. and D.E. Discher, *Cell differentiation through tissue elasticity-coupled, myosin-driven remodeling.* Curr Opin Cell Biol, 2008. **20**(6): p. 609-15.
169. Murphy, C.M., et al., *Cell-scaffold interactions in the bone tissue engineering triad.* Eur Cell Mater, 2013. **26**: p. 120-32.
170. Girones Molera, J., J.A. Mendez, and J. San Roman, *Bioresorbable and nonresorbable polymers for bone tissue engineering.* Curr Pharm Des, 2012. **18**(18): p. 2536-57.
171. Biela, S.A., et al., *Different sensitivity of human endothelial cells, smooth muscle cells and fibroblasts to topography in the nano-micro range.* Acta Biomater, 2009. **5**(7): p. 2460-6.
172. Blache, U., et al., *Dual Role of Mesenchymal Stem Cells Allows for Microvascularized Bone Tissue-Like Environments in PEG Hydrogels.* Adv Healthc Mater, 2016. **5**(4): p. 489-98.
173. Shekaran, A., et al., *Bone regeneration using an alpha 2 beta 1 integrin-specific hydrogel as a BMP-2 delivery vehicle.* Biomaterials, 2014. **35**(21): p. 5453-61.
174. Noguchi, T., et al., *Poly(vinyl alcohol) hydrogel as an artificial articular cartilage: evaluation of biocompatibility.* J Appl Biomater, 1991. **2**(2): p. 101-7.
175. Burdick, J.A. and K.S. Anseth, *Photoencapsulation of osteoblasts in injectable RGD-modified PEG hydrogels for bone tissue engineering.* Biomaterials, 2002. **23**(22): p. 4315-23.
176. Seliktar, D., et al., *MMP-2 sensitive, VEGF-bearing bioactive hydrogels for promotion of vascular healing.* J Biomed Mater Res A, 2004. **68**(4): p. 704-16.
177. Nguyen, Q.T., et al., *Cartilage-like mechanical properties of poly (ethylene glycol)-diacrylate hydrogels.* Biomaterials, 2012. **33**(28): p. 6682-90.
178. Brinkman, W.T., et al., *Photo-cross-linking of type I collagen gels in the presence of smooth muscle cells: mechanical properties, cell viability, and function.* Biomacromolecules, 2003. **4**(4): p. 890-5.
179. Sargeant, T.D., et al., *An in situ forming collagen-PEG hydrogel for tissue regeneration.* Acta Biomater, 2012. **8**(1): p. 124-32.
180. Ferreira, A.M., et al., *Collagen for bone tissue regeneration.* Acta Biomater, 2012. **8**(9): p. 3191-200.
181. Ramshaw, J.A., et al., *Collagens as biomaterials.* J Mater Sci Mater Med, 2009. **20 Suppl 1**: p. S3-8.
182. Gelse, K., E. Poschl, and T. Aigner, *Collagens--structure, function, and biosynthesis.* Adv Drug Deliv Rev, 2003. **55**(12): p. 1531-46.
183. Shekaran, A. and A.J. Garcia, *Extracellular matrix-mimetic adhesive biomaterials for bone repair.* J Biomed Mater Res A, 2011. **96**(1): p. 261-72.
184. Kaemmerer, E., et al., *Gelatine methacrylamide-based hydrogels: an alternative three-dimensional cancer cell culture system.* Acta Biomater, 2014. **10**(6): p. 2551-62.
185. Nichol, J.W., et al., *Cell-laden microengineered gelatin methacrylate hydrogels.* Biomaterials, 2010. **31**(21): p. 5536-44.
186. Lin, R.Z., et al., *Transdermal regulation of vascular network bioengineering using a*

photopolymerizable methacrylated gelatin hydrogel. Biomaterials, 2013. **34**(28): p. 6785-96.
187. Daniele, M.A., et al., *Interpenetrating networks based on gelatin methacrylamide and PEG formed using concurrent thiol click chemistries for hydrogel tissue engineering scaffolds.* Biomaterials, 2014. **35**(6): p. 1845-56.
188. Parmar, P.A., et al., *Collagen-mimetic peptide-modifiable hydrogels for articular cartilage regeneration.* Biomaterials, 2015. **54**: p. 213-25.
189. Ruel-Gariepy, E. and J.C. Leroux, *In situ-forming hydrogels--review of temperature-sensitive systems.* Eur J Pharm Biopharm, 2004. **58**(2): p. 409-26.
190. Park, H., et al., *Injectable chitosan hyaluronic acid hydrogels for cartilage tissue engineering.* Acta Biomater, 2013. **9**(1): p. 4779-86.
191. Grant, D.S., et al., *Interaction of endothelial cells with a laminin A chain peptide (SIKVAV) in vitro and induction of angiogenic behavior in vivo.* J Cell Physiol, 1992. **153**(3): p. 614-25.
192. Nakamura, M., et al., *Construction of multi-functional extracellular matrix proteins that promote tube formation of endothelial cells.* Biomaterials, 2008. **29**(20): p. 2977-86.
193. Nakamura, M., et al., *Promotion of angiogenesis by an artificial extracellular matrix protein containing the laminin-1-derived IKVAV sequence.* Bioconjug Chem, 2009. **20**(9): p. 1759-64.
194. Tam, J.P., et al., *Disulfide bond formation in peptides by dimethyl sulfoxide. Scope and applications.* Journal of the American Chemical Society, 1991. **113**(17): p. 6657-6662.
195. Kobayashi, T., et al., *TGF-beta1 and serum both stimulate contraction but differentially affect apoptosis in 3D collagen gels.* Respir Res, 2005. **6**: p. 141.
196. Moens, S., et al., *The multifaceted activity of VEGF in angiogenesis - Implications for therapy responses.* Cytokine Growth Factor Rev, 2014. **25**(4): p. 473-82.
197. Herrmann, M., S. Verrier, and M. Alini, *Strategies to Stimulate Mobilization and Homing of Endogenous Stem and Progenitor Cells for Bone Tissue Repair.* Front Bioeng Biotechnol, 2015. **3**: p. 79.
198. Ho, C.Y., et al., *Mesenchymal stem cells with increased stromal cell-derived factor 1 expression enhanced fracture healing.* Tissue Eng Part A, 2015. **21**(3-4): p. 594-602.
199. Shinohara, K., et al., *Stromal cell-derived factor-1 and monocyte chemotactic protein-3 improve recruitment of osteogenic cells into sites of musculoskeletal repair.* J Orthop Res, 2011. **29**(7): p. 1064-9.
200. von Essen, M.R., et al., *Vitamin D controls T cell antigen receptor signaling and activation of human T cells.* Nat Immunol, 2010. **11**(4): p. 344-9.
201. Janckila, A.J., et al., *Tartrate-resistant acid phosphatase as an immunohistochemical marker for inflammatory macrophages.* Am J Clin Pathol, 2007. **127**(4): p. 556-66.
202. Kevil, C.G., R.P. Patel, and D.C. Bullard, *Essential role of ICAM-1 in mediating monocyte adhesion to aortic endothelial cells.* Am J Physiol Cell Physiol, 2001. **281**(5): p. C1442-7.
203. Omenetto, F.G. and D.L. Kaplan, *New opportunities for an ancient material.* Science, 2010. **329**(5991): p. 528-31.
204. Xu, Z.P., et al., *Formation of hierarchical bone-like apatites on silk microfiber templates via biomineralization.* Rsc Advances, 2016. **6**(80).
205. Almalki, S.G. and D.K. Agrawal, *Key transcription factors in the differentiation of mesenchymal stem cells.* Differentiation, 2016. **92**(1-2): p. 41-51.
206. Lee, J.H., et al., *The sulfated polysaccharide fucoidan rescues senescence of endothelial colony-forming cells for ischemic repair.* Stem Cells, 2015. **33**(6): p. 1939-51.
207. Kim, B.S., et al., *Fucoidan-induced osteogenic differentiation promotes angiogenesis by inducing vascular endothelial growth factor secretion and accelerates bone repair.* 2018. **12**(3): p. e1311-e1324.
208. Chen, M.C., et al., *Low Molecular Weight Fucoidan Inhibits Tumor Angiogenesis through Downregulation of HIF-1/VEGF Signaling under Hypoxia.* Mar Drugs, 2015. **13**(7): p. 4436-51.
209. Ustyuzhanina, N.E., et al., *Fucoidans: pro- or antiangiogenic agents?* Glycobiology, 2014. **24**(12): p. 1265-74.

210. Shi, Y., et al., *Role of myeloid early endothelial progenitor cells in bone formation and osteoclast differentiation in tissue construct based on hydroxyapatite poly(ester-urethane) scaffolds.* J Orthop Res, 2016. **34**(11): p. 1922-1932.
211. Yu, D., et al., *SDF-1 Expression is Associated with Poor Prognosis in Osteosarcoma.* Ann Clin Lab Sci, 2016. **46**(5): p. 508-14.
212. Jerez, S., et al., *Proteomic Analysis of Exosomes and Exosome-Free Conditioned Media From Human Osteosarcoma Cell Lines Reveals Secretion of Proteins Related to Tumor Progression.* J Cell Biochem, 2017. **118**(2): p. 351-360.
213. Benslimane-Ahmim, Z., et al., *Osteoprotegerin regulates cancer cell migration through SDF-1/CXCR4 axis and promotes tumour development by increasing neovascularization.* Cancer Lett, 2017. **395**: p. 11-19.
214. Zhao, J., et al., *VEGF Silencing Inhibits Human Osteosarcoma Angiogenesis and Promotes Cell Apoptosis via PI3K/AKT Signaling Pathway.* Cell Biochem Biophys, 2015. **73**(2): p. 519-525.
215. Mochizuki, Y., et al., *Angiopoietin 2 stimulates migration and tube-like structure formation of murine brain capillary endothelial cells through c-Fes and c-Fyn.* J Cell Sci, 2002. **115**(Pt 1): p. 175-83.
216. Maisonpierre, P.C., et al., *Angiopoietin-2, a natural antagonist for Tie2 that disrupts in vivo angiogenesis.* Science, 1997. **277**(5322): p. 55-60.
217. Lewis, C.E., M. De Palma, and L. Naldini, *Tie2-expressing monocytes and tumor angiogenesis: regulation by hypoxia and angiopoietin-2.* Cancer Res, 2007. **67**(18): p. 8429-32.
218. DuBois, S. and G. Demetri, *Markers of angiogenesis and clinical features in patients with sarcoma.* Cancer, 2007. **109**(5): p. 813-9.
219. Tait, C.R. and P.F. Jones, *Angiopoietins in tumours: the angiogenic switch.* J Pathol, 2004. **204**(1): p. 1-10.
220. Matsubara, H., et al., *Vascular tissues are a primary source of BMP2 expression during bone formation induced by distraction osteogenesis.* Bone, 2012. **51**(1): p. 168-80.
221. Wei, J. and G. Karsenty, *An overview of the metabolic functions of osteocalcin.* Rev Endocr Metab Disord, 2015. **16**(2): p. 93-8.
222. Huang, T.H., et al., *Prophylactic administration of fucoidan represses cancer metastasis by inhibiting vascular endothelial growth factor (VEGF) and matrix metalloproteinases (MMPs) in Lewis tumor-bearing mice.* Mar Drugs, 2015. **13**(4): p. 1882-900.
223. Schneider, T., et al., *Interference with the CXCL12/CXCR4 axis as potential antitumor strategy: superiority of a sulfated galactofucan from the brown alga Saccharina latissima and fucoidan over heparins.* Glycobiology, 2015. **25**(8): p. 812-24.
224. Purnama, A., et al., *Fucoidan in a 3D scaffold interacts with vascular endothelial growth factor and promotes neovascularization in mice.* Drug Deliv Transl Res, 2015. **5**(2): p. 187-97.
225. Boisson-Vidal, C., et al., *Neoangiogenesis induced by progenitor endothelial cells: effect of fucoidan from marine algae.* Cardiovasc Hematol Agents Med Chem, 2007. **5**(1): p. 67-77.
226. de Azevedo, T.C., et al., *Heparinoids algal and their anticoagulant, hemorrhagic activities and platelet aggregation.* Biomed Pharmacother, 2009. **63**(7): p. 477-83.
227. Lake, A.C., et al., *Low molecular weight fucoidan increases VEGF165-induced endothelial cell migration by enhancing VEGF165 binding to VEGFR-2 and NRP1.* J Biol Chem, 2006. **281**(49): p. 37844-52.
228. Claes, L., S. Recknagel, and A. Ignatius, *Fracture healing under healthy and inflammatory conditions.* Nat Rev Rheumatol, 2012. **8**(3): p. 133-43.
229. Loi, F., et al., *Inflammation, fracture and bone repair.* Bone, 2016. **86**: p. 119-30.
230. Ma, B., et al., *TLR4 stimulation by LPS enhances angiogenesis in a co-culture system consisting of primary human osteoblasts and outgrowth endothelial cells.* J Tissue Eng Regen Med, 2017. **11**(6): p. 1779-1791.
231. Lips, P., *Vitamin D deficiency and secondary hyperparathyroidism in the elderly: consequences for bone loss and fractures and therapeutic implications.* Endocr Rev, 2001.

22(4): p. 477-501.
232. Pollet, I., et al., *Bacterial lipopolysaccharide directly induces angiogenesis through TRAF6-mediated activation of NF-kappaB and c-Jun N-terminal kinase.* Blood, 2003. **102**(5): p. 1740-2.
233. Liotta, F., et al., *Toll-like receptors 3 and 4 are expressed by human bone marrow-derived mesenchymal stem cells and can inhibit their T-cell modulatory activity by impairing Notch signaling.* Stem Cells, 2008. **26**(1): p. 279-89.
234. Medzhitov, R., *Toll-like receptors and innate immunity.* Nat Rev Immunol, 2001. **1**(2): p. 135-45.
235. Gottfried, E., et al., *Expression of CD68 in non-myeloid cell types.* Scand J Immunol, 2008. **67**(5): p. 453-63.
236. Urbich, C., et al., *Proteomic characterization of human early pro-angiogenic cells.* J Mol Cell Cardiol, 2011. **50**(2): p. 333-6.
237. Koh, Y.W., et al., *CD163 expression was associated with angiogenesis and shortened survival in patients with uniformly treated classical Hodgkin lymphoma.* PLoS One, 2014. **9**(1): p. e87066.
238. Videm, V. and M. Albrigtsen, *Soluble ICAM-1 and VCAM-1 as markers of endothelial activation.* Scand J Immunol, 2008. **67**(5): p. 523-31.
239. Sans, M., et al., *VCAM-1 and ICAM-1 mediate leukocyte-endothelial cell adhesion in rat experimental colitis.* Gastroenterology, 1999. **116**(4): p. 874-83.
240. Amsellem, V., et al., *ICAM-2 regulates vascular permeability and N-cadherin localization through ezrin-radixin-moesin (ERM) proteins and Rac-1 signalling.* Cell Commun Signal, 2014. **12**: p. 12.
241. Wu, Y., et al., *Essential role of ICAM-1/CD18 in mediating EPC recruitment, angiogenesis, and repair to the infarcted myocardium.* Circ Res, 2006. **99**(3): p. 315-22.
242. Byrne, G.J., et al., *Serum soluble vascular cell adhesion molecule-1: role as a surrogate marker of angiogenesis.* J Natl Cancer Inst, 2000. **92**(16): p. 1329-36.
243. Halleen, J.M., et al., *Tartrate-resistant acid phosphatase 5b (TRACP 5b) as a marker of bone resorption.* Clin Lab, 2006. **52**(9-10): p. 499-509.
244. Schauber, J., et al., *Histone acetylation in keratinocytes enables control of the expression of cathelicidin and CD14 by 1,25-dihydroxyvitamin D3.* J Invest Dermatol, 2008. **128**(4): p. 816-24.
245. Gombart, A.F., N. Borregaard, and H.P. Koeffler, *Human cathelicidin antimicrobial peptide (CAMP) gene is a direct target of the vitamin D receptor and is strongly up-regulated in myeloid cells by 1,25-dihydroxyvitamin D3.* FASEB J, 2005. **19**(9): p. 1067-77.
246. Yim, S., et al., *Induction of cathelicidin in normal and CF bronchial epithelial cells by 1,25-dihydroxyvitamin D(3).* J Cyst Fibros, 2007. **6**(6): p. 403-10.
247. Fromigue, O., P.J. Marie, and A. Lomri, *Differential effects of transforming growth factor beta2, dexamethasone and 1,25-dihydroxyvitamin D on human bone marrow stromal cells.* Cytokine, 1997. **9**(8): p. 613-23.
248. van den Bemd, G.J., et al., *Differential effects of 1,25-dihydroxyvitamin D3-analogs on osteoblast-like cells and on in vitro bone resorption.* J Steroid Biochem Mol Biol, 1995. **55**(3-4): p. 337-46.
249. Tashiro, K., et al., *A synthetic peptide containing the IKVAV sequence from the A chain of laminin mediates cell attachment, migration, and neurite outgrowth.* J Biol Chem, 1989. **264**(27): p. 16174-82.
250. Rao, R.R., et al., *Matrix composition regulates three-dimensional network formation by endothelial cells and mesenchymal stem cells in collagen/fibrin materials.* Angiogenesis, 2012. **15**(2): p. 253-64.
251. Edgar, L.T., et al., *Extracellular matrix density regulates the rate of neovessel growth and branching in sprouting angiogenesis.* PLoS One, 2014. **9**(1): p. e85178.

252. Kadler, K.E., *Fell Muir Lecture: Collagen fibril formation in vitro and in vivo.* Int J Exp Pathol, 2017. **98**(1): p. 4-16.
253. Barth, D., et al., *The role of cystine knots in collagen folding and stability, part II. Conformational properties of (Pro-Hyp-Gly)n model trimers with N- and C-terminal collagen type III cystine knots.* Chemistry, 2003. **9**(15): p. 3703-14.
254. Perrone, G.S., et al., *The use of silk-based devices for fracture fixation.* Nat Commun, 2014. **5**: p. 3385.
255. Somaiah, C., et al., *Collagen Promotes Higher Adhesion, Survival and Proliferation of Mesenchymal Stem Cells.* PLoS One, 2015. **10**(12): p. e0145068.
256. Ha, S.-W., et al., *Nano-hydroxyapatite modulates osteoblast lineage commitment by stimulation of DNA methylation and regulation of gene expression.* Biomaterials, 2015. **65**: p. 32-42.

7. Supplements

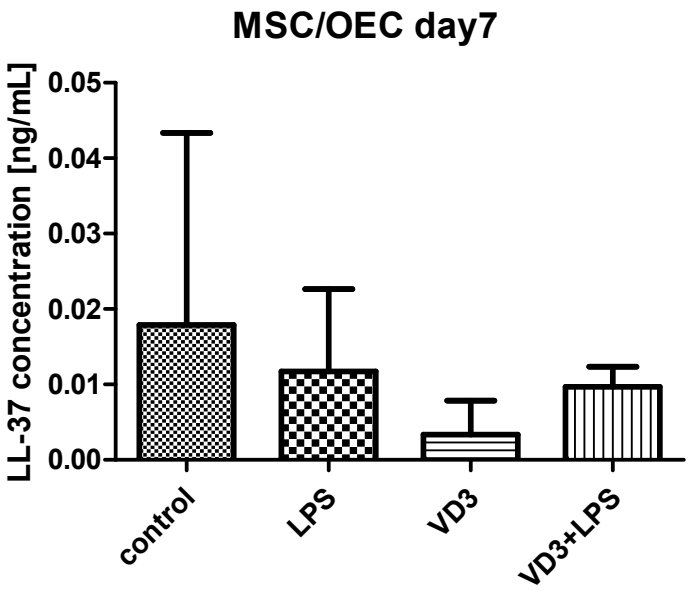

Supplement Figure 1 Enzyme-linked immunosorbent assay for LL-37 in the supernatant of co-cultures on day 7. n = 3.

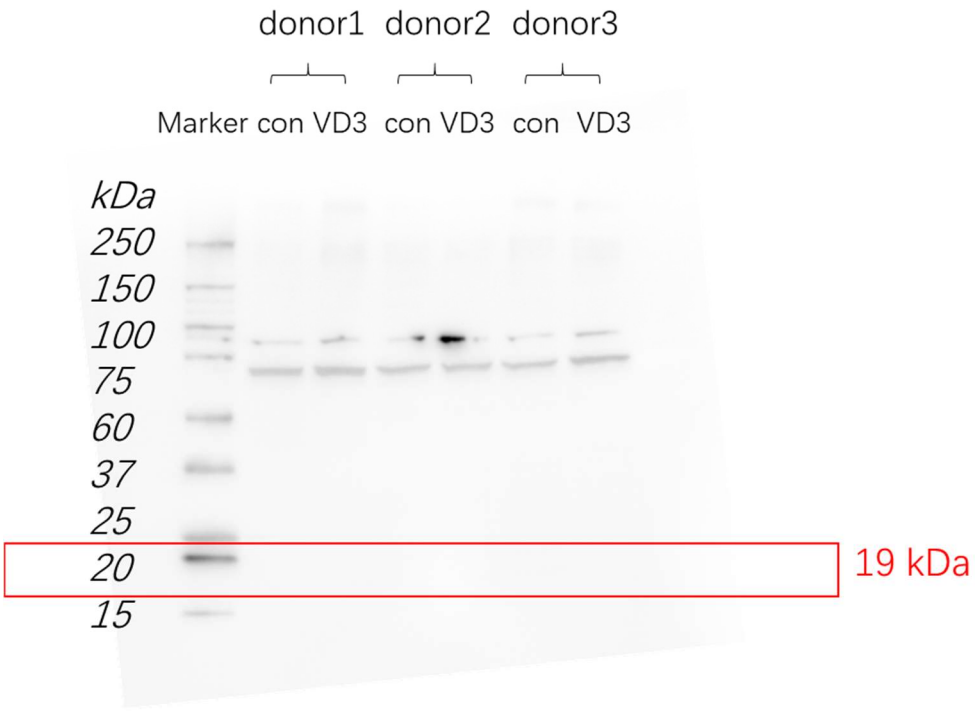

Supplement Figure 2 Western blot detection of cathelicidin in MSC mono-cultures control and Vitamin D3 treatment at day 7. n = 3.

8. Appendix

8.1 List of figures

8.2 List of Tables

8.3 List of publications and abstracts

Publications:

Shi Y, **Wang F**, Tiwari S, Yesilbas M, Steubesand N, Weitkamp JT, Klüter T, Lippross S, Eglin D, Seekamp A, Fuchs S. Role of myeloid early endothelial progenitor cells in bone formation and osteoclast differentiation in tissue construct based on hydroxyapatite poly(ester-urethane) scaffolds. J Orthop Res. 2016 Nov;34(11):1922-1932.

Wang F, Schmidt H, Pavleska D, Wermann T, Seekamp A, Fuchs S. Crude Fucoidan Extracts Impair Angiogenesis in Models Relevant for Bone Regeneration and Osteosarcoma via Reduction of VEGF and SDF-1. Mar Drugs. 2017 Jun 20;15(6).

Dithmer M, Kirsch AM, Richert E, Fuchs S, **Wang F**, Schmidt H, Coupland SE, Roider J, Klettner A. Fucoidan Does Not Exert Anti-Tumorigenic Effects on Uveal Melanoma Cell Lines. Mar Drugs. 2017 Jun 22;15(7).

Shi L, **Wang F**, Zhu W, Xu Z, Fuchs S, Hilborn J, Zhu L, Ma Q, Wang Y, Weng X, Ossipov D. Self-Healing Silk Fibroin-Based Hydrogel for Bone Regeneration: Dynamic Metal-Ligand Self-Assembly Approach. Adv. Funct. Mater. 2017, 1700591 August 2017.

Janga H, Cassidy L, **Wang F**, Spengler D, Oestern-Fitschen S, Krause MF, Seekamp A, Tholey A, Fuchs S. Site-specific and endothelial-mediated dysfunction of the alveolar-capillary barrier in response to lipopolysaccharides. J Cell Mol Med. 2018 Feb;22(2):982-998.

Rasch A, Naujokat H, **Wang F**, Seekamp A, Fuchs S, Klüter T. Evaluation of bone allograft processing methods: Impact on decellularization efficacy, biocompatibility and mesenchymal stem cell functionality. PLoS One. 2019 Jun 20;14(6):e0218404.

Klüter T, Hassan R, Rasch A, Naujokat H, **Wang F**, Behrendt P, Lippross S, Gerdesmeyer L, Eglin D, Seekamp A, Fuchs S. An Ex Vivo Bone Defect Model to Evaluate Bone Substitutes and Associated Bone Regeneration Processes. Tissue Eng Part C Methods.2020 Jan;26(1):56-65.

Abstracts in scientific practice

Posters

Wang F, Seekamp A, Fuchs S. The impact of fucoidan from fucus vesiculosus on angiogenesis in OEC and MSC co-culture system. TERMIS-EU Tissue Engineering and Regenerative Medicine International Society-EU, 28 June-01 July 2016, Uppsala, Sweden.

Wang F, Wermann T, Lange L, Seekamp A, Fuchs S. 3-D organoid systems based on human stem cells to monitor vascularization processes: From molecular mediators to therapeutical applications. International Symposium "Precision Medicine in Chronic Inflammation" of the Cluster of Excellence "Inflammation at Interfaces". 26 March 2018, Hamburg, Germany.

Presentation

Wang F, Schmidt H, Pavleska D, Wermann T, Seekamp A, Fuchs S. Fucoidan impairs angiogenesis in co-culture models relevant for bone regeneration and osteosarcoma. Deutsche Kongress für Orthopädie und Unfallchirurgie (DKOU), 26 Oct 2017, Berlin, Germany.

8.4 Acknowledgement

I would like to express my sincere gratitude to all the people who helped me during my Ph.D. study at University Medical Center Schleswig-Holstein Kiel, Experimental Trauma Surgery.

A special acknowledgement from me should be conveyed to Prof. Dr. Sabine Fuchs for her supervision, from which I greatly benefited and learned a lot. I am very grateful for all her valuable advices in the past 5 years and solutions for the technical problems and challenges I met in my experimental works. As a Master graduate student of biomaterials who was absolutely new in medical life science at the beginning of my doctoral study, I would like to thank Prof. Fuchs for giving me this opportunity to work under her guidance and leading me into this scientific field. Her instructions and suggestions on my presentations, manuscript and dissertation helped me to walk through every stage of my study.

I would like to thank Prof. Dr. Susanne Alban for her interest on my work and being the first referee for my dissertation. I also want to express my gratitude to Prof. Alban for her helpful advices on my dissertation.

I owe many thanks to my colleagues, collaborators and friends who supported, helped and accompanied me to spend an unforgettable time in Kiel. Sincere gratitude to Katrin Lange, Anne-Rose Nissen and Dijana Pavleska for their warm technical assistance. Many thanks to Dr. Harald Schmidt for his professional analysis of angiogenesis, Prof. Dmitri Ossipov and Dr. Liyang Shi for their novel composite hydrogels. All I could say is-thanks to my colleagues in the lab: Harshavardhan Janga, Junyu Xiong, Rywan Hassan, Alexander Rasch, Julia Ohmes, Yuejun Xiao, for the happy time we shared together and special thanks to Julia Ohmes for her kind help in translating and correcting my German abstract. In addition, I am truly grateful for the concerns and help of my friends in Kiel, Hayley Reid, Mohamed Moktar and Bo Li, as well as the visits from old friends, Iris Wu and Junli Xiang, who I have known for more than 20 years.

I would like to convey my gratitude to my beloved parents for their constant supports, considerations and confidence in me.

At last, I want to express my appreciation to the Interreg Project “FucoSan Gesundheit aus dem Meer” which provides us the financial support and chance to further study on Fucoidan.

8.5 Declaration

I, Fanlu Wang, hereby confirm that:

Apart from the supervisor's guidance, the content and design of this thesis is all my own work and only using the sources listed.

The thesis has not been submitted either partially or wholly as part of a doctoral examination procedure to another examining body. And the thesis has not been published or submitted for publication.

The thesis has been prepared subject to the Rules of Good Scientific Practice of the German Research Foundation.

And no academic degree has ever been withdrawn from me.

Kiel, (Date)

Signature: